

INVESTIGATION OF THE ROLE OF ARSENIC TRIOXIDE ON THE EXPRESSION OF
RBBP6 SPLICE VARIANTS AND THEIR SPECIFIC MICRORNAS (MIRS) DURING
CELL CYCLE PROGRESSION AND APOPTOSIS OF BREAST CANCER CELLS

BY

MAKGOO LILIAN

A DISSERTATION SUBMITTED IN FULFILMENT OF THE REQUIREMENTS FOR
THE DEGREE OF MASTER OF SCIENCE (BIOCHEMISTRY)

IN

THE DEPARTMENT OF BIOCHEMISTRY, MICROBIOLOGY AND BIOTECHNOLOGY

SCHOOL OF MOLECULAR AND LIFE SCIENCES

FACULTY OF SCIENCE AND AGRICULTURE,

UNIVERSITY OF LIMPOPO, SOUTH AFRICA.

SUPERVISOR: DR Z. MBITA

2019

Table of Contents

I.	Declaration	iv
II.	Dedication	v
III.	Acknowledgments	vi
IV.	Research Outputs	vii
V.	List of abbreviations	viii
VI.	List of figures	xiv
VII.	List of tables	xvi
VIII.	Abstract	xviii
CHAPTER ONE: INTRODUCTION.....		1
1.	Introduction	1
1.1.	Breast cancer	1
1.2.	<i>RBBP6</i> gene and its products.....	2
1.3.	Problem statement	4
1.4.	Rational and motivation	5
1.5.	Aim of the study.....	6
1.6.	Objectives of the study	6
1.7.	Dissertation structure	7
CHAPTER TWO: LITERATURE REVIEW.....		9
2.	Introduction	9
2.1.	Breast cancer risks.....	9
2.2.	Classification and prevalence of breast cancer.....	10
2.3.	Breast cancer subtypes	11
2.5.	Apoptosis	13
2.5.1.	Extrinsic pathway.....	13
2.5.2.	Intrinsic pathway.....	15
2.5.3.	Arsenic trioxide (As_2O_3) as an apoptotic inducer.....	16
2.5.4.	Apoptosis inhibition in breast cancer.....	17
2.6.	MicroRNAs	18
2.7.	Retinoblastoma Binding Protein 6	19
2.7.1.	Retinoblastoma binding protein 6 in carcinogenesis	22
2.7.2.	Involvement of <i>RBBP6</i> in nucleic acid metabolism and embryonic development..	24
2.8.	Cell cycle.....	24
2.8.1.	Regulation of the cell cycle	26
2.9.	Y-box binding protein 1 interaction with <i>RBBP6</i>	26

2.10. Regulation of RBBP6 by microRNAs	27
CHAPTER THREE: MATERIALS AND METHODS	28
3.1. Introduction	28
3.1.1. Cell lines	28
3.1.2. Chemicals and reagents.....	28
3.1.3. Antibodies.....	28
3.2. Cell culture maintenance and treatments	29
3.3. Cytotoxicity and cell viability analysis	29
3.4. Morphological assessment of apoptosis using fluorescence and light microscopy.....	30
3.5. Flow cytometry	31
3.5.1. Apoptosis analysis.....	31
3.5.2. Multi-caspase analysis	31
3.5.3. MitoPotential analysis.....	32
3.5.4. Cell cycle analysis.....	32
3.6. Total RNA extraction	33
3.6.1. RNA Gel electrophoresis	34
3.6.1.1. Preparation of RNA agarose gel.....	34
3.7. cDNA synthesis.....	34
3.8. Primer design.....	35
3.9. Polymerase chain reaction	37
3.9.1. Agarose gel electrophoresis of DNA	38
3.10. Quantification of RBBP6 variant 3 mRNA using Real-Time PCR.....	38
3.11. Immunocytochemistry.....	39
3.12. Prediction and validation of RBBP6 specific miRs	40
3.13. Statistical data analysis	40
CHAPTER FOUR: RESULTS	41
4. Introduction	41
4.1. <i>In vitro</i> reduction of the viability of MCF-7 cells by arsenic trioxide	41
4.1.1. Confirmation of arsenic trioxide-reduced cell viability in MCF-7 cells.....	45
4.2. Morphological changes of arsenic trioxide, cobalt chloride and curcumin-treated MCF-7 cells.....	48
4.3. Arsenic trioxide induces apoptosis in MCF-7 cells	51
4.4. Arsenic trioxide induces caspase-dependent apoptosis in MCF-7 cells.....	54
4.5. Arsenic trioxide induces the extrinsic apoptotic pathway in MCF-7 cells.....	57

4.6.	Arsenic trioxide induces G2/M cell cycle arrest in MCF-7 cells	60
4.7.	The effect of arsenic trioxide on the expression of RBBP6 splice transcripts	63
4.8.	Quantitative Real-Time PCR analysis of RBBP6 variant 3 (DWNN) in MCF-7 and Hek-293 cells	69
4.9.	Immunocytochemistry analysis	71
4.10.	Predicted RBBP6 specific microRNAs analysis in MCF-7 breast cancer cells	74
CHAPTER FIVE: DISCUSSION AND CONCLUSION		76
5.0.	Introduction	76
5.1.	Arsenic trioxide inhibits MCF-7 cell growth	77
5.2.	Arsenic trioxide induces features of apoptosis in MCF-7 cells	77
5.2.1.	Arsenic trioxide induces apoptosis in MCF-7 cells	77
5.2.2.	Arsenic trioxide induces caspase-dependent apoptosis in MCF-7 cells	78
5.2.3.	Arsenic trioxide induces death receptor-mediated apoptotic pathway in MCF-7 cells ..	78
5.3.	Arsenic trioxide induces G2/M cell cycle arrest in MCF-7 cells	79
5.4.	Arsenic trioxide regulates the expression of RBBP6 variants during cell cycle arrest and apoptosis	79
5.4.1.	Quantitative analysis of the expression of RBBP6 variant 3	81
5.4.2.	Analysis of RBBP6 protein localization	81
5.5.	Analysis of predicted RBBP6 specific microRNAs in MCF-7 cells	81
5.6.	Conclusion	82
5.7.	Future work	82
CHAPTER SIX: REFERENCES		83
CHAPTER SEVEN: APPENDIX		101
Appendix A:	Stock solutions recipes	101
Appendix B:	PCR primer design guidelines	102
Appendix C:	GAPDH and RBBP6 variant 3 standard curves constructed with dilutions made from Hek 293 cDNA	108
Appendix D:	RBBP6 primary antibody	109
Appendix E:	RBBP6 secondary antibody	110

I. Declaration

I, Lilian Makgoo, hereby, declare that the work **“Investigation of the role of arsenic trioxide on the expression of RBBP6 splice variants and their specific microRNAs during cell cycle progression and apoptosis of breast cancer cells”** submitted in this dissertation to the University of Limpopo for the fulfilment of the Master of Science is my own work that has not been submitted for any degree or examination in any other university. Where contributions of others are involved, every effort have been indicated and acknowledged by complete references.

Signature: _____

Date: _____

II. Dedication

This work is dedicated to my late grandfather, Phogole Thobejane and my late grandmother, Matladi Thobejane who both passed on in 2018. It is also dedicated to all the orphans and families of those who died because of breast cancer.

III. Acknowledgments

I would like to express my special thanks of gratitude to the following people and organisations for their contribution towards the completion of this study:

- The almighty God for His constant strength and protection throughout my life.
- My supervisor, Dr Z Mbita, for his patience, constructive criticism, motivation, enthusiasm, and immense knowledge.
- Department of Biochemistry, Microbiology and Biotechnology staff members for assisting me in finalizing this project within the limited time frame.
- My mom, Botsetse Makgoo, for supporting me and for the prayers she offered.
- National Research Foundation for funding.
- Lastly, the University of Limpopo, for the opportunity and the resources for completing this project.

IV. Research Outputs

Oral and poster Presentations

- **L. Makgoo**, K. Laka and Z. Mbita. The effect of arsenic trioxide on the expression of RBBP6 splice variants in MCF-7 breast cancer cells. South African Society for Biochemistry and Molecular Biology Conference. North West University. 8-11 July 2018.
- **L. Makgoo**, K. Laka and Z. Mbita. The role of arsenic trioxide and curcumin in the regulation of RBBP6-related cell cycle arrest and apoptosis in MCF-7 breast cancer cells. Faculty of Science and Agriculture Research Day 2017. University of Limpopo. 28 November 2017.
- **L. Makgoo**, K. Laka and Z. Mbita. The regulation of RBBP6 variants in MCF-7 breast cancer cells by cobalt chloride and arsenic trioxide. 1st Ellisras Longitudinal Study International Conference 2017. University of Limpopo. 19 October 2017.

Publication

- **Makgoo, L.**, Laka, K., and Mbita, Z. (2018). The role of arsenic trioxide and curcumin in the regulation of RBBP6-related cell cycle arrest and apoptosis in MCF-7 breast cancer cells. *CardioVascular Journal of Africa*. Accepted for publication.
- Kagiso Laka, **Lilian Makgoo**, Zukile Mbita (2019) Survivin Splice Variants in Arsenic Trioxide (As₂O₃)-Induced Deactivation of PI3K and MAPK Cell Signalling Pathways in MCF-7 Cells. *Genes* Vol. 10 (1), 41.

V. List of abbreviations

μM	Micromolar
3' UTR	3' untranslated region
AIF	Apoptosis-inducing factor
A–P	Anterior–posterior
Apaf-1	Apoptosis protease activating factor-1
As ₂ O ₃	Arsenic trioxide
ATCC	American Type Culture Collection
ATM	Ataxia telangiectasia Mutated
Bax	Bcl-2 associated X protein
Bcl-2	B-cell lymphoma-2
BCL2L2	Bcl-2-like protein 2
Bcl-xL	B-cell lymphoma-extra large
BH	Bcl-2 Homology
Bid	Bcl-2 interacting domain death agonist Bromide
BTB	Broad-Complex, Tramtrack and Bric a brac
Caspase	Cysteine aspartic-specific proteases
CC	Coiled coil
Cdc2	Cell division cycle-2
CDK	Cyclin-dependent kinase
Cdki	Cyclin-dependent kinase inhibitor

cDNA	Complementary DNA
cFLIP	Cellular FLICE-like inhibitory protein
CoCl ₂	Cobalt chloride
C ₂₁ H ₂₀ O ₆	Curcumin
CstF64	Cleavage stimulation factor 64
Cyt c	Cytochrome c
DAPI	4',6-diamidino-2-phenylindole
dATP	deoxyadenosine triphosphate
DEPC	Diethyl pyrocarbonate
DGCR8	DiGeorge syndrome critical region protein 8
DISC	Death-inducing signalling complex
DMEM	Dulbecco's Modified Eagle's Medium
DMSO	Dimethyl sulphoxide
DNA	Deoxyribonucleic acid
DNase	Deoxyribonuclease
DWNN	Domain with No Name
EDTA	Ethylene diamine tetra acetic acid
ER	Oestrogen receptor
ER-	Oestrogen Receptor negative
FADD	Fas-associated death domain
Fas	Fibroblast-associated
FasL	Fas Ligand

FBS	Foetal bovine serum
FITC	Fluorescein isothiocyanate
FLICE	Fas-associated death domain-like interleukin-1 β -converting enzyme
G0	Gap 0
G1	Gap 1
G2	Gap 2
HDM2	Human double minute 2
HER2+	Human Epidermal growth factor Receptor 2+
HERG	<i>Human ether-a-go-go related gene</i>
HtrA2	High temperature requirement A2
IAP	Inhibitor of Apoptosis Protein
ICAD	Inhibitor of caspase activated DNase
INK4	Inhibitors of cdk4
M phase	Mitosis
MCF-7	Michigan Cancer Foundation-7
BRCA	BReast CAncer gene
BRCA 1	BReast CAncer gene one
BRCA 2	BReast CAncer gene two
RNA	Ribonucleic acid
MCM10	Minichromo- some maintenance 10
MDM2	Murine Double Minute 2

miRs	Micro RNA
MOPS	(3-(N-morpholino) propanesulfonic acid)
mRNA	Messenger RNA
MTT	3-(4,5-dimethylthiazol-2-yl)-2-5-diphenyltetrazolium
NADPH	Nicotinamide Adenine Dinucleotide Phosphate Hydrogen
NLS	Nuclear Localization Signal
P2P-R	Proliferation potential protein-related
p53	Protein 53 (tumour protein 53)
PACT	P53-associated cellular protein testis-derived
Paz	Piwi Argonaute Zwillie
PBS	Phosphate buffered saline
PCR	Polymerase chain reaction
PIWI	<i>P-element-induced wimpy testis</i>
PR	Proline Rich domain
PR+	Progesterone-receptor positive
pRB	Retinoblastoma protein
qPCR	Quantitative polymerase chain reaction
RBBP6	Retinoblastoma binding protein 6
RING	Really interesting new gene
RNA	Ribonucleic acid

RNAi	RNA interference
ROS	Reactive Oxygen Species
RS	Serine-arginine
S phase	DNA synthesis phase
Smac	Second Mitochondria-Derived Activator of Caspases
SNAMA	Something that sticks like glue
tBid	Truncated Bcl-2 inhibitor of death
TNBC	Triple negative breast cancers
TNF	Tumour necrosis factor
TNF-R	Tumour necrosis factor R
TNF- α	<i>Tumour necrosis factor-alpha</i>
TNF- α L	Tumour necrosis factor-alphaL
TRADD	TNF-R1-associated death domain protein
TRAIL	TNF-related apoptosis-inducing ligand
Tris	Trihydroxymethylaminomethane
TRPC6	Transient receptor potential cation 6
UV	Ultra violet radiation
USA	United States of America
WHO	World health organization
XIAP	X-linked inhibitor of apoptosis protein
YB-1	Y-box-binding protein 1

ZBTB38

BTB domain containing-38

ZnF

Zinc finger

VI. List of figures

Chapter 2	Page
Figure 2.1: Death-receptor mediated apoptosis pathway.....	14
Figure 2.2: Mitochondrial mediated apoptosis pathway.....	16
Figure 2.3: RBBP6 proven and hypothetical isoforms.....	21
Figure 2.4: The role played by p53 in cell cycle regulation.....	22
Figure 2.5: Regulation of pRB in coordination with the cell cycle.....	23
Figure 2.6: Typical eukaryotic cell division cycle and CDKs that regulate each phase in the cycle.....	25
Chapter 4	
Figure 4.1A: Effect of arsenic trioxide on the viability of MCF-7 cells.....	42
Figure 4.1B: Effect of cobalt chloride on the viability of MCF-7 cells.....	43
Figure 4.1C: Effect of curcumin on the viability of MCF-7 cells.....	44
Figure 4.2: Analysis of % cell viability in MCF-7 cells using the Muse™ Count & Viability Kit	46
Figure 4.3: Confirmation of percentage viability of MCF-7 cells in response to arsenic trioxide, cobalt chloride and curcumin.....	47
Figure 4.4: Light microscopic analysis of the effect of arsenic trioxide, cobalt chloride and curcumin on the morphology of MCF-7 cells.....	49
Figure 4.5: Fluorescence microscopic analysis of the effect of arsenic trioxide, cobalt chloride and curcumin on the morphology of MCF-7 cells.....	50
Figure 4.6: Confirmation of arsenic trioxide induced apoptosis in MCF-7 cells.....	52
Figure 4.7: Average % apoptosis in arsenic trioxide treated MCF-7 cells.....	53
Figure 4.8: Confirmation of arsenic trioxide-induced caspase dependent apoptosis in MCF-7 cells.....	55
Figure 4.9: Average % of caspase positive cells in arsenic trioxide treated MCF-7 cells.....	56
Figure 4.10: Confirmation of arsenic trioxide-induced extrinsic apoptosis pathway in MCF-7 cells.....	58
Figure 4.11: Arsenic trioxide induced extrinsic apoptosis pathway in MCF-7 cells.....	59
Figure 4.12: Cell cycle analysis of arsenic trioxide treated MCF-7 cells.....	61

Figure 4.13: Analysis of arsenic trioxide-induced G2/M cell cycle arrest in MCF-7 breast cancer cells.....	62
Figure 4.14: Expression analysis of RBBP6 variant 1 and 2 in arsenic trioxide-treated MCF-7 cells and untreated Hek 293 cells.....	64
Figure 4.15: Analysis of RBBP6 variant 1 and variant 2 band densities in MCF-7 and Hek-293 cells.....	65
Figure 4.16: Expression analysis of RBBP6 variant 3 in untreated MCF-7 cells, Caski cells and Hek 293 cells.....	67
Figure 4.17: Analysis of RBBP6 variant 3 band densities in MCF-7, Caski and Hek-293 cells.....	68
Figure 4.18: Quantitative analysis of the expression of RBBP6 variant 3 in untreated MCF-7 and Hek-293 cells.....	70
Figure 4.19: Localization of RBBP6 isoform 1, 2 and 4 in MCF-7 cells.....	72
Figure 4.20: Analysis of fluorescence intensities for the detection of RBBP6 isoform 1,2 and 4 in MCF-7cells.....	73

VII. List of tables

Chapter 2	Page
Table 2.1: Gene expression profiles of breast cancer subtypes.....	11
Chapter 3	
Table 3.1: The cocktail for cDNA synthesis.....	35
Table 3.2: Different primer sets, sequences and product sizes.....	36
Table 3.3: The cocktail for Polymerase Chain Reaction.....	37
Table 3.4: Temperature profiles used for PCR.....	38
Table 3.5: Real-time PCR setup.....	39
Table 3.6: Typical real-time conditions.....	39
Chapter 4	
Table 4.1A: Cell viability average percentages \pm standard error of the mean (SEM) after the treatment of MCF-7 cells with various concentrations of arsenic trioxide (As_2O_3).....	42
Table 4.1B: Average percentages of cell viability \pm SEM after treating the MCF-7 cells with various concentrations of cobalt chloride (CoCl_2).....	43
Table 4.1C: Cell viability average percentages \pm SEM after treating MCF-7 cells with various concentrations of curcumin ($\text{C}_{21}\text{H}_{20}\text{O}_6$).....	44
Table 4.3: Cell viability average percentages \pm SEM after the treatment of MCF-7 cells with arsenic trioxide, cobalt chloride and curcumin.....	47
Table 4.7: Apoptosis average percentages \pm SEM after the treatment of MCF-7 cells with arsenic trioxide and curcumin.....	53
Table 4.9: Average percentages of caspase positive cells \pm SEM after treating the MCF-7 cells with various concentrations of arsenic trioxide and curcumin.....	56

Table 4.11: Extrinsic apoptosis average percentages \pm SEM after the treatment of MCF-7 cells with arsenic trioxide and curcumin.....	59
Table 4.13: Average percentages of cell populations \pm SEM after treating the MCF-7 cells with arsenic trioxide and cobalt chloride.....	62
Table 4.15: Average band densities of GAPDH and RBBP6 variant 1 and 2 \pm SEM for PCR analysis in MCF-7 and Hek 293 cells.....	65
Table 4.17: Average band densities of RBBP6 variant 3 and GAPDH \pm SEM for PCR analysis in MCF-7 cells, Caski and Hek-293 cells.....	68
Table 4.18A: Relative expression of RBBP6 variant 3 normalized using GAPDH.....	69
Table 4.18B: RBBP6 variant 3 relative expression average percentages \pm standard error of the mean (SEM) in MCF-7 and Hek-293 cells.....	70
Table 4.20: Average fluorescence intensities \pm standard error of the mean (SEM) in MCF-7 cells for ICC analysis.....	73
Table 4.21: RBBP6 specific microRNAs regulated in cancer.....	74
Table 4.22: Different bioinformatics tools predicting RBBP6 variant 1 specific miRNAs..	74
Table 4.23: The involvement of RBBP6 specific miRNAs in breast cancer.....	75

VIII. Abstract

Retinoblastoma binding protein 6 (RBBP6) is the protein encoded by the *Retinoblastoma Binding Protein 6 (RBBP6)* gene that is located in chromosome 16p12.2. There is a growing list of newly discovered RBBP6 hypothetical splice variants but there are only three RBBP6 splice variants that are well documented. RBBP6 has been previously implicated in the regulation of cell cycle and apoptosis but little is known about the expression and regulation of the human RBBP6 splice variants during cell cycle progression and breast cancer development. This study was aimed at determining the expression pattern of RBBP6 alternatively spliced variants during arsenic trioxide-induced cell cycle arrest and apoptosis in breast cancer MCF-7 cells. It was also aimed at determining RBBP6 specific microRNAs and how they are regulated in MCF-7 breast cancer cells.

MCF-7 cells were maintained and subjected to arsenic trioxide-induced cell cycle arrest and apoptosis. The MTT (3-(4, 5-dimethylthiazol-2-yl)-2, 5-diphenyltetrazolium bromide) and the Muse™ Count & Viability assays were used to evaluate the effect of arsenic trioxide on the viability of MCF-7 cells. Cell cycle arrest using 11 µM arsenic trioxide and apoptosis using 32 µM arsenic trioxide were analysed using the MUSE® Cell Analyzer, light and fluorescence microscopy. Arsenic trioxide-induced apoptosis was analysed using the Muse™ Annexin V & Dead Cell Kit, MultiCaspase and MitoPotential assays using the Muse™ MultiCaspase Kit and Muse™ MitoPotential Kit. Arsenic trioxide-induced cell cycle arrest was analysed using the Muse™ Cell Cycle Kit. Semi-quantitative analysis of RBBP6 variants was carried out using the conventional Polymerase Chain Reaction (PCR), while the quantitative analysis was done using the Real-Time Quantitative PCR. The localization of RBBP6 isoforms was done using Immunocytochemistry (ICC). Web based Bioinformatics tools were used to identify RBBP6-specific microRNAs.

The MTT results showed that arsenic trioxide decreased the viability of the MCF-7 cells in a dose-dependent manner. The Muse™ Cell Cycle analysis showed that 11 µM of arsenic trioxide induced G2/M cell cycle arrest in MCF-7 cells, while the Muse™ Annexin V & Dead Cell assay showed that 32 µM of arsenic trioxide induced the extrinsic apoptotic pathway in MCF-7 breast cancer cells. Using the conventional PCR, the MCF-7 cells were

found to express the RBBP6 variant 1 transcript but lacks the expression of variant 2 and 3 transcripts, contrary to the kidney embryonic Hek 293 cells that exhibited the expression of RBBP6 variant 1, 2 and 3. Additionally, arsenic trioxide downregulated RBBP6 variant 1 in breast cancer cells during cell cycle arrest and apoptosis. The Real-Time PCR confirmed that MCF-7 cells lowly express RBBP6 variant 3. On the other hand, the ICC analysis showed that RBBP6 isoform 1 is localized and highly expressed in MCF-7 breast cancer cells. The Web based Bioinformatics tools showed that RBBP6 variant 1 specific microRNAs are down regulated in MCF-7 breast cancer cells. These results together showed that As_2O_3 is effective against MCF-7 cells and also regulated the expression of RBBP6 variants, especially, variant 1.

This study showed that there are RBBP6 variants that are involved in breast cancer progression and there are those that may be involved in breast cancer suppression. Targeting these RBBP6 variants for therapeutic development is a promising strategy. In conjunction with RBBP6 expression, arsenic trioxide should be further explored as a breast cancer drug.

CHAPTER ONE: INTRODUCTION

1. Introduction

Cancer, a public health problem worldwide, refers to the uncontrollable cell growth leading to the formation of a tumour. Based on the updated incidences, new cancer cases, mortality and survival rate show that the major problem is in economically developing countries (low and medium resource countries) [Torre *et al.*, 2015]. This global shift is influenced by factors such as genetic instability (events capable of causing unscheduled alterations, either of a temporary or permanent nature, within the genome), chronic infections and entrenchment of modifiable risk factors, for example, being overweight or obese (Rock *et al.*, 2015; Torre *et al.*, 2012). Cancer develops in various organs as a consequence of a series of genetic changes, including nucleotide mutations and chromosomal rearrangements (Shalini *et al.*, 2011). These organs include brain, head and neck, mouth, lung, liver, breast, prostate, stomach, pancreas and kidney (Kourinou *et al.*, 2013; Young, 2013). The types of cancers that affect these organs are categorized as organ specific cancers (Shalini *et al.*, 2011). Cancer in South Africa has emerged as a health problem, with breast cancer being one of the prominent cancers affecting women. According to the South African National Cancer Registry, breast cancer is the most commonly diagnosed cancer among women with an age-standardised incidence rate of 27 per 100 000 women and a lifetime risk of 1 in 29 (Singh *et al.*, 2015).

1.1. Breast cancer

Breast cancer is a disease characterized by the uncontrollable growth of cells situated in the breast. The resultant type of breast cancer depends on the breast cells that are affected. Based on gene profiling, these include Basal-like, HER2-enriched, Normal breast-like, Luminal A, Luminal B and Claudin-low breast cancers (Gatza *et al.*, 2010). Age and stage at diagnosis differ considerably between the different races and populations living in South Africa (Walker *et al.*, 2004). Many different determinants such as socioeconomic, status geographic accessibility to medical centres with oncologic

services affect patients with breast cancer, especially rural black women. Late diagnosis contributes to difficulties associated with cancer treatment.

Different methods that are employed for the treatment of breast cancer include surgery, radiotherapy and chemotherapy (Goldhirsch *et al.*, 2013; Hortobagyi, 1998). Setbacks associated with the current treatment regimens include non-specificity of the chemo drugs and late diagnosis. Non-specificity is associated with the fact that chemo drugs tend to eliminate both cancerous and normal cells. Additionally, breast cancer cells have been shown to be resistant to apoptosis, which is a process that eliminates damaged cells and a process that is induced by chemotherapeutic drugs. This process is influenced by different genes that code for either oncoproteins or tumour suppressors. Unlike some genes, which are involved in either apoptosis or cell cycle regulation, RBBP6 is involved in both processes (Ntwasa, 2016; Mbita *et al.*, 2012).

1.2. RBBP6 gene and its products

Retinoblastoma binding protein 6 (RBBP6) is one of the genes that have shown a great potential as therapeutic targets (Mbita *et al.*, 2012; Motadi *et al.*, 2011; Li *et al.*, 2007). RBBP6 is a protein encoded by a *RBBP6* gene located in chromosome 16p12.2. This gene is transcribed into three splice variants due to alternative splicing (Mbita *et al.*, 2012). These alternatively spliced variants include a 6.1 kilobases (kb) mRNA transcript and a 1.1 kilobases mRNA transcript (variant 3). The 6.1 kilobases variant is alternatively spliced into two mRNA variants, one containing exon 16 (variant 1) while variant 2 lacks exon 16 and consequently resulting in three mRNA transcripts (Mbita *et al.*, 2012). Variant 3 is translated into RBBP6 isoform 3 (118 aa) while isoform 1 is translated into a 1792 amino acid protein, with isoform 2 made up of 1758 amino acids translated from variant 2 (Mbita *et al.*, 2012).

Recently, Ntwasa (2016) reported that there are four isoforms, but it is not clear how the fourth isoform is derived. According to Ensembl genome browser 93 database (http://www.ensembl.org/Human/Search/Results?q=rbbp6;facet_species=Human), isoform 4 has 952 amino acids. There is little or no information about this isoform, and there has been no mRNA sequence published on this variant. Little is known about the

expression and regulation of the human RBBP6 splice variants during cell cycle progression, apoptosis and breast cancer development. Previously, Gao and Scott (2002) had reported on the involvement of P2P-R (rat homologue) in mitotic apoptosis but Mbita *et al.* (2012) and Motadi *et al.* (2011) reported the involvement of human RBBP6 in cell cycle regulation. Recently, Ntwasa (2016) reviewed the role of RBBP6 in carcinogenesis, implicating RBBP6 as a key role player in both carcinogenesis and cell cycle regulation.

RBBP6 is made of different domains, which include the highly conserved RBBP6 N-terminal domain called Domain With No Name (DWNN) domain, followed by the Zinc finger (ZnF), Really Interesting New Gene (RING), Proline Rich (PR), Coiled coil (CC), Serine-arginine (RS), Rb-binding domain, p53-binding domains and Nuclear Localization Signal (NLS). The first three exons that encode DWNN are found in transcripts 1, 2 and 3. The DWNN domain is a novel ubiquitin-like motif, that makes up RBBP6 isoform 3, which shares 22% similarity with the ubiquitin. This suggests its involvement in the regulation of protein turn-over in the cell (Pugh *et al.*, 2006). Moreover, the presence of the RING finger in RBBP6 suggests a possible role in ubiquitin ligase-like activities (Pugh *et al.*, 2006). Indeed, RBBP6 was reported to have ubiquitin ligase-like activity through its RING finger domain resulting in the ubiquitination of YB-1 and proteasomal degradation through the proteasome pathway (Chibi *et al.*, 2008). Screening tests performed over a decade ago showed that RBBP6 interacts with both p53 and pRB through its pRb- and p53-binding domains (Simons *et al.*, 1997). Additionally, Mbita *et al.* (2012) showed the crucial role of RBBP6 isoform 3 in arsenic trioxide-induced G2/M arrest and p53 stabilization in normal kidney cells.

Anticancer drugs have been shown to induce apoptosis in cancer cells and arsenic trioxide is a known anticancer drug effective against leukaemia (Yedjou *et al.*, 2010; Mahieux *et al.*, 2001). Several mechanisms of action have been proposed for arsenic trioxide activity, including induction of apoptosis mediated by reactive oxygen species, promotion of cellular differentiation, and inhibition of angiogenesis (Lu *et al.*, 2007; Berenson and Yeh, 2006; Baj *et al.*, 2002; Miller *et al.*, 2002). Arsenic trioxide induces either the receptor-mediated apoptotic pathway or the mitochondrial-mediated pathway depending on the cell type (Yun *et al.*, 2016; Zhou *et al.*, 2008; Baj *et al.*, 2002). As₂O₃

has also been shown to reduce migration and invasion of cervical and ovarian cancer cells *in vitro* (Yu *et al.*, 2007; Zhang and Wang, 2006). Preclinical studies of arsenic trioxide have shown antitumor activity in murine solid tumour models, including breast, brain, liver, gastric, prostate, renal, and bladder cancer (Dilda and Hogg, 2007; Chen *et al.*, 2002). The emerging consensus is that the induction of cell cycle arrest and apoptosis are the principal modalities involved in the antitumor effect of arsenic trioxide. The exact mechanism on how arsenic trioxide induces cell cycle arrest and apoptosis is not fully understood.

Extensive research has identified various molecular routes that can be used for the treatment of breast cancer. Gene therapy is a type of cancers treatment that is still in the early stages of research. *RBBP6* is one of the genes that showed potential for the treatment of cancer by being regulated in majority of cancers such as colon (Chen *et al.*, 2013), lung (Motadi *et al.*, 2011) and prostate cancers (Singh *et al.*, 2006). So far, there is no report on the regulation of *RBBP6* splice variants by arsenic trioxide in MCF-7 breast cancer cells. Targeting these *RBBP6* variants for therapeutic development is a promising strategy.

1.3. Problem statement

Despite the progress made in the improvement of breast cancer treatment, it is still difficult to eliminate breast cancer cells without affecting the adjacent normal cells and to minimize the long and short-term side effects that are associated with the current breast cancer treatment (Di Leo *et al.*, 2015). The emergence of cancer gene therapy promises to be an innovative treatment strategy for the prevention of cancer related deaths. *Retinoblastoma binding protein 6 (RBBP6)* is one of the genes that have shown potential as therapeutic targets (Mbita *et al.*, 2012; Motadi *et al.*, 2011; Li *et al.*, 2007). It remains a puzzle how *RBBP6* is regulated during carcinogenesis and there is a growing interest in the role played by a novel group of regulatory biomarker, microRNAs (miRs), in cell homeostasis and during carcinogenesis (Bahrami *et al.*, 2018; Jiang *et al.*, 2005). This study will focus on deciphering the regulation of *RBBP6* splice variants by arsenic trioxide during cell cycle progression and apoptosis in breast cancer MCF-7 cells.

1.4. Rational and motivation

Previously, Gao and Scott (2002) had reported on the involvement of P2P-R (RBBP6 rat homologue) in mitotic apoptosis, suggesting that *P2P-R* gene products are pro-apoptotic. Others contradicted this report by suggesting that the expression of RBBP6 is upregulated in majority of cancer such as colon (Chen *et al.*, 2013), lung (Motadi *et al.*, 2011) and prostate (Singh *et al.*, 2006). This suggest that RBBP6 can either induce or inhibit apoptosis via the interaction with tumour suppressor genes such as pRB and p53, which mainly regulate apoptosis and cell cycle progression (Li *et al.*, 2007). It remains unclear how RBBP6 expression is regulated in human cancers and the emergence of miRs opens a new avenue for exploration.

MicroRNAs were discovered in 1993 describing small transcript produced by the *lin-4* gene in *Caenorhabditis elegans* (Lee *et al.*, 1993), it was later proven that miRs are non-coding ribonucleic acids (RNAs) ranging between 18 and 22 bases in length (Lee *et al.*, 1993). They have been reported to bind to the 3' untranslated region (UTR) of their target specific mRNAs (Bartel, 2004). Their main function has been reported to involve regulation of transcription and translation (Iorio *et al.*, 2005). Mature MiRs are located in the nucleus or cytoplasm depending on the role they intend to play (Calin *et al.*, 2004).

Specific miRs are either upregulated or downregulated in breast cancer. It has been reported that miR-125b, miR-10b, miR-145 are down-regulated in breast cancer suggesting that they play a role as tumour suppressor genes (Götte *et al.*, 2010; Iorio *et al.*, 2005; Lee *et al.*, 2005). MiR-21 and miR-155 have been implicated in tumour progression and have been shown to be upregulated in breast cancer (Shenouda and Alahari, 2009; Yan *et al.*, 2008; Iorio *et al.*, 2005) suggesting that they maybe oncogenes. Despite the extensive literature implicating miRs in breast cancer, there has been no study indicating their roles in the regulation of RBBP6 and its role in carcinogenesis. Therefore, a query that arises is, could these miRs play a role on the expression and regulation of RBBP6 variants in breast cancer? The expression of *RBBP6* gene products has not been fully elucidated in breast cancer but Mbita *et al.* (2012) indicated that tumour islands do lowly express RBBP6. As already mentioned, there has been no report linking the regulation of RBBP6 by miRs.

1.5. Aim of the study

This study was aimed at determining the expression patterns of RBBP6 alternatively spliced variants during arsenic trioxide-induced cell cycle arrest and apoptosis in breast cancer MCF-7 cells. It was also aimed at predicting and identifying RBBP6 specific miRs.

1.6. Objectives of the study

The objectives of the study were to:

- i. Determine inhibitory concentrations of arsenic trioxide and the positive controls (cobalt chloride and curcumin for cell cycle arrest and apoptosis, respectively), that could reduce cell viability by 50% using the 3-(4, 5-dimethylthiazol-2-yl)-2, 5-diphenyltetrazolium bromide (MTT) assay.
- ii. Determine the expression of RBBP6 splice variants including possible novel variants by conventional PCR and Real Time-PCR during arsenic trioxide-induced cell cycle arrest and apoptosis.
- iii. Determine the localization and expression of RBBP6 isoforms including possible novel isoforms by immunocytochemistry during arsenic trioxide-induced cell cycle arrest and apoptosis.
- iv. Predict RBBP6-specific MiRs using web-based bioinformatics tools.

1.7. Dissertation structure

The dissertation is organized into seven chapters and they are described as follows:

Chapter 1

This chapter covers the problem statement highlighting setbacks with the current breast cancer treatment and gene therapy as a possible route for treating breast cancer. It also includes questions to be answered, aims and objectives.

Chapter 2

This chapter covers the literature review addressing the status of this research and the gaps that exist in our understanding of the role of arsenic trioxide and microRNAs on the expression of RBBP6 splice variants, and the expression pattern of these variants in MCF-7 breast cancer cells.

Chapter 3

This chapter explains all the methods and materials used. Composition of buffer solutions used along with manufacturer's information are given in Appendix A, D and Appendix E, respectively.

Chapter 4

This section reports the findings of this study on the role of arsenic trioxide on the expression of RBBP6 splice variants during cell cycle progression and apoptosis in breast cancer MCF-7 cells. The effect of arsenic trioxide on the viability of MCF-7 breast cancer cells (Fig. 4.1A, 4.2 and 4.3) and their morphology (Fig. 4.4 and 4.5) was reported. The MUSE® Cell Analyzer (Fig. 4.6-4.13) results on the effect of arsenic trioxide on apoptosis and G2/M cell cycle arrest in MCF-7 breast cancer cells was also reported. This section further reports the conventional PCR (Fig. 4.14-4.17), Real-Time PCR (Fig. 4.18) and Immunocytochemistry (Fig. 4.19 and 20) results on the expression of RBBP6 variants in breast cancer MCF-7 cells. Identification and regulation of RBBP6 specific microRNAs in breast cancer MCF-7 cells was also covered (Table 4.22 and 4.23).

Chapter 5

Chapter 5 covers the general discussion by classifying and comparing the results to the most current information that is available, it also summarizes conclusions indicating possible future investigations.

Chapter 6

This section lists the sources that owns the ideas used in this dissertation to support the scientific arguments.

Chapter 7

Finally, chapter 7 covers the supplementary information that helps to clarify this dissertation.

CHAPTER TWO: LITERATURE REVIEW

2. Introduction

Cancer remains one of the leading causes of death in many countries including South Africa. Carcinogenesis is a complex process, consequently, finding effective therapies to treat different cancers such as breast cancer often depends on new discoveries about the underlying cellular mechanisms. Breast cancer is the most common cancer that is prevalent in women than in men in both developed and developing countries (Ly *et al.*, 2013). It is also the second leading cause of death worldwide following lung cancer (Wang *et al.*, 2009). Although breast cancer is thought to be a common cancer in the developed countries, the majority (69%) of all breast cancer deaths occurs in developing countries (Cheraghi *et al.*, 2012). According to the National Cancer Institute in 2013, 232,340 female breast cancer cases and 2,240 male breast cancer cases are reported in the USA, including 39,620 deaths caused by the disease (Abdollahi *et al.*, 2015). In South Africa, about 8000 new cases of breast cancer are reported each year (Baatjes *et al.*, 2016).

2.1. Breast cancer risks

The mechanism of how breast cancer develops is not fully understood, but some of the factors that cause and influence the risk of developing breast cancer are well documented. Breast cancer risk factors are divided into intrinsic and extrinsic factors (Kamińska *et al.*, 2015). Understanding the relative influence of intrinsic and extrinsic risk factors in breast cancer development is important for strategizing breast cancer prevention. Extrinsic risk factors include environmental risk factors such as smoking, ultraviolet exposure and high-fat diet, which account for at least 70–90% of lifetime cancer incidences (Wu *et al.*, 2016). Good lifestyle and engaging in regular physical activity have been shown to decrease the chances of getting breast cancer (Kamińska *et al.*, 2015). Obesity in woman after menopause is also one of the elevated risks of developing breast cancer because fat cells produce oestrogen; extra fat cells produce more oestrogen in the body, and oestrogen is a risk factor for hormone-receptor-positive breast cancer development (La Vecchia *et al.*, 2011).

Intrinsic risk factors are heritable or genetic factors that increase the risk of the developing breast cancer (Tomasetti and Vogelstein, 2015). These factors include race, sex, age and genetic makeup (Kamińska *et al.*, 2015). Gender is a risk factor of developing breast cancer where being a woman increases the chances of being diagnosed with breast cancer than being a man (Kamińska *et al.*, 2015). The main reason why woman develop breast cancer is because their breast cells are continuously exposed to the growth-promoting factors, which include the female hormones such as oestrogen and progesterone (Kamińska *et al.*, 2015). The oestrogen and progesterone imbalance are likely to result with Oestrogen Receptor-positive (ER+) cancers or Progesterone Receptor-positive (PR+) cancers.

Age is another factor that contributes to the risk of breast cancer development. The risk of getting breast cancer increases as a person ages because the longer the person live, the chances for genetic damage (mutations) in the body also increases, and as the person age our bodies are less capable of repairing genetic damages (McPherson *et al.*, 2000). Inheritance of mutated susceptibility genes is also a factor that increase the chances of getting breast cancer. Most inherited cases of breast cancer are linked to genetic mutations in the *BReast CAncer* gene one (*BRCA1*) and *BReast CAncer* gene two (*BRCA2*) [Francken *et al.*, 2013].

2.2. Classification and prevalence of breast cancer

Breast cancer regularly starts off in the inner lining of the milk ducts or the lobules that supply them with milk. The cancer cells can extend to other parts of the body through a process called metastasis and are therefore referred to as malignant tumours. Breast cancer that initiates in the lobules is identified as lobular carcinoma, while the ones that develop from the ducts are called ductal carcinomas (Bickel *et al.*, 2015). The majority of breast cancer cases affect women, but breast cancer does occur in men too. Breast cancer is the most common invasive cancer in females worldwide (Parkin and Fernández, 2006). According to Bickel *et al.* (2015), breast cancer can also be divided into invasive and non-invasive breast cancer. In the invasive breast cancers, cancer cells escape from inside the lobules or within the ducts and attack nearby tissues. Through the bloodstream, the abnormal cells can reach the lymph nodes, and later make their way to other organs,

such as the bones, liver and lungs. In non-invasive breast cancer, the cancer is localized to its starting point and does not spread to other parts of the body and these are often referred to as benign tumours. The major problem of non-invasive breast cancer is the fact that it is a direct precursor of most invasive breast cancers (Allred *et al.*, 2008). Breast cancer can also be classified into subtypes.

2.3. Breast cancer subtypes

Breast cancer is not a single disease, because it is composed of distinct biological subtypes. It is classified into three subtypes based on gene expressed, hormone receptor markers and their frequency of occurrence as tabulated on Table 2.1 (Anderson *et al.*, 2014). Biomarkers such as oestrogen receptor (ER), progesterone receptor (PR) and epidermal growth factor receptor 2 (HER2) are mainly used to differentiate between these subtypes. Basal-like breast cancers, which are often referred to as Triple-negative breast cancer (TNBC), are the most aggressive and show resistance to breast cancer treatment (Arpino *et al.*, 2015).

Table 2.1: Gene expression profiles of breast cancer subtypes.

Molecular subtype	Biomarker	Frequency (%)	References
Basal-like	ER- PR- HER2-	10-20	Gatza <i>et al.</i> , 2010
HER2-enriched	ER- PR- HER2+	10-15	Anderson <i>et al.</i> , 2014
Normal breast-like	ER-/+ HER2-	5-10	Eroles <i>et al.</i> , 2012
Luminal A	ER+ PR+ HER2-	50-60	Anderson <i>et al.</i> , 2014
Luminal B	ER+/- PR+/- HER2-/+	10-20	Gatza <i>et al.</i> , 2010
Claudin-low	ER- PR- HER2-	12-14	Eroles <i>et al.</i> , 2012

(-): Negative; (+): Positive; (-/+): Negative or positive and (+/-): Positive or negative

2.4. Breast cancer treatment

There are several strategies that are used for the treatment of breast cancer, and these include radiotherapy, chemotherapy and surgery (Hortobagyi, 1998). Radiotherapy uses high-energy X-rays to eliminate breast cancer cells. Radiotherapy targets both breast cancer cells and the normal cells but the normal cells can also repair themselves (Early

Breast Cancer Trialists' Collaborative Group, 2005). Radiation-related heart disease and skin reaction are the most common side effects of radiotherapy (Taylor and Kirby, 2015). Ectopic over-expression of genes such as *survivin* has been used to protect normal cells from radiation (Carruthers *et al.*, 2016). This suggests that genes such as *survivin* and *RBBP6* can be targeted for therapeutic strategies. Usually, radiotherapy is used after surgery to destroy any persistent cancer cells. Typically, radiotherapy is applied about a month after surgery or chemotherapy.

In chemotherapy, cytotoxic drugs are used to destroy the cancer cells (Wagland *et al.*, 2016). The goal of every breast cancer chemotherapy is to promote apoptosis in the breast cancer cells. The oncologist may recommend a chemotherapy called adjuvant chemotherapy, which is a therapy that is given in addition to the initial therapy to maximize its effectiveness, if the cancer cells are spreading to new areas of the body (Wagland *et al.*, 2016). If the tumours are large, chemotherapy may be used before surgery. This is done to shrink the tumour, making its removal easier. This is known as neo-adjuvant chemotherapy. Chemotherapy is associated with a range of side effects including hair loss, nausea and vomiting, fatigue, anaemia, and changes in taste and smell (Wagland *et al.*, 2016).

Most women with breast cancer, especially with late stage, have surgery as an initial treatment strategy. There are different types of breast cancer surgery and these include lumpectomy in which only the part of the breast containing the cancer is removed. The goal is to remove the cancer cells as well as some surrounding normal tissue. How much of the breast is removed depends on the size and location of the tumour (Tartter *et al.*, 2000). There is also a surgery in which the entire breast is removed, including all of the breast tissue or cells and sometimes other nearby tissues, and this surgery is called mastectomy (Rippy *et al.*, 2014). There is also a surgery in which an area of lymph nodes that may contain cancer cells is removed and this type of surgery is called lymph node dissection. This surgery is usually used for diagnostic and prognostic purposes (Bembenek and Schlag, 2000). Lymph nodes may be removed either as part of the surgery to remove the breast cancer or as a separate operation. Generally, both radiation and chemotherapy are expected to destroy breast cancer cells through apoptosis.

2.5. Apoptosis

Apoptosis is a programmed cell death as opposed to necrosis, and other forms of cell death, which include autophagy. During development, many cells are produced and some undergo programmed cell death and thereby, contribute to the shaping of many organs and tissues (Abud, 2004). Apoptosis is also important in the function of the immune system and in the elimination of microbial infected cells, thereby, maintaining cellular homeostasis. Defects in apoptosis can lead to cancer, autoimmune diseases and spreading of viral infections (Rathmell and Thompson, 2002). During apoptosis, initiator caspases are activated and engage in death inducing signalling complexes either in response to the ligation of cell surface death receptors (extrinsic pathways) or in response to signals initiated inside the cell (intrinsic pathways).

The cellular machinery involved in the execution of apoptosis in eukaryotic cells includes a family of cysteine proteases, termed caspases. Caspases are a group of cysteine proteases that cleave target proteins at specific aspartate residues (Shalini *et al.*, 2015). In general, three amino acid residues that lie upstream of the aspartate residue in the substrate determine the specificity of recognition by individual caspases. Caspases are synthesized as precursors (pro-caspases) and are converted into mature enzymes through dimerization and autocleavage (Shalini *et al.*, 2015). The apoptotic caspases can be divided into initiator and executioner caspases. The group of apoptotic initiator caspases consist of caspase-2, -8, -9 and -10, while the group of executioner caspases comprises of caspases-3, -6 and -7 (Zhou *et al.*, 2006). Induction of apoptosis via death receptors typically results in the activation of an initiator caspase-8 or caspase-10 and executioner caspase-3. On the other hand, the mitochondrial pathway of apoptosis leads to the activation of initiator caspase-9 and executioner caspase-3.

2.5.1. Extrinsic pathway

The extrinsic pathway involves the association of receptor-mediated transmembrane death receptor [Fas and Tumour Necrosis Factor- α (TNF- α)] and its extracellular ligand [Fas-Ligand (Fas-L) and TNF- α Ligand], other members includes the tumour necrosis factor-related apoptosis-inducing ligand (TRAIL) receptor (Chen and Goeddel, 2002; Wajant, 2002; Locksley *et al.*, 2001). In the cytoplasmic side of the cell, death receptors

comprise of death domains which recruit and bind to adaptor molecules required for the initiation of a caspase cascade (Fig. 2.1). Fas recruits Fas-associated death domain protein (FADD) while TNF-R recruits TNF-R1-associated death domain protein (TRADD) (Ashkenazi, 2002). Such association leads to the establishment of the death-inducing signalling complex (DISC) that is comprised of death receptor, its ligand and initiator procaspase-8 (or procaspase-10) [Yang *et al.*, 2005]. The complex enables the autoactivation of procaspase-8/10 giving rise to active caspases-8/10 (Ola *et al.*, 2011). The active caspase-8 then activates downstream executioner caspases that cleave cellular death substrates such as Inhibitor of Caspase-activated DNase (ICAD), resulting in morphological and biochemical changes that are often observed in apoptotic cells (Ghobrial *et al.*, 2005).

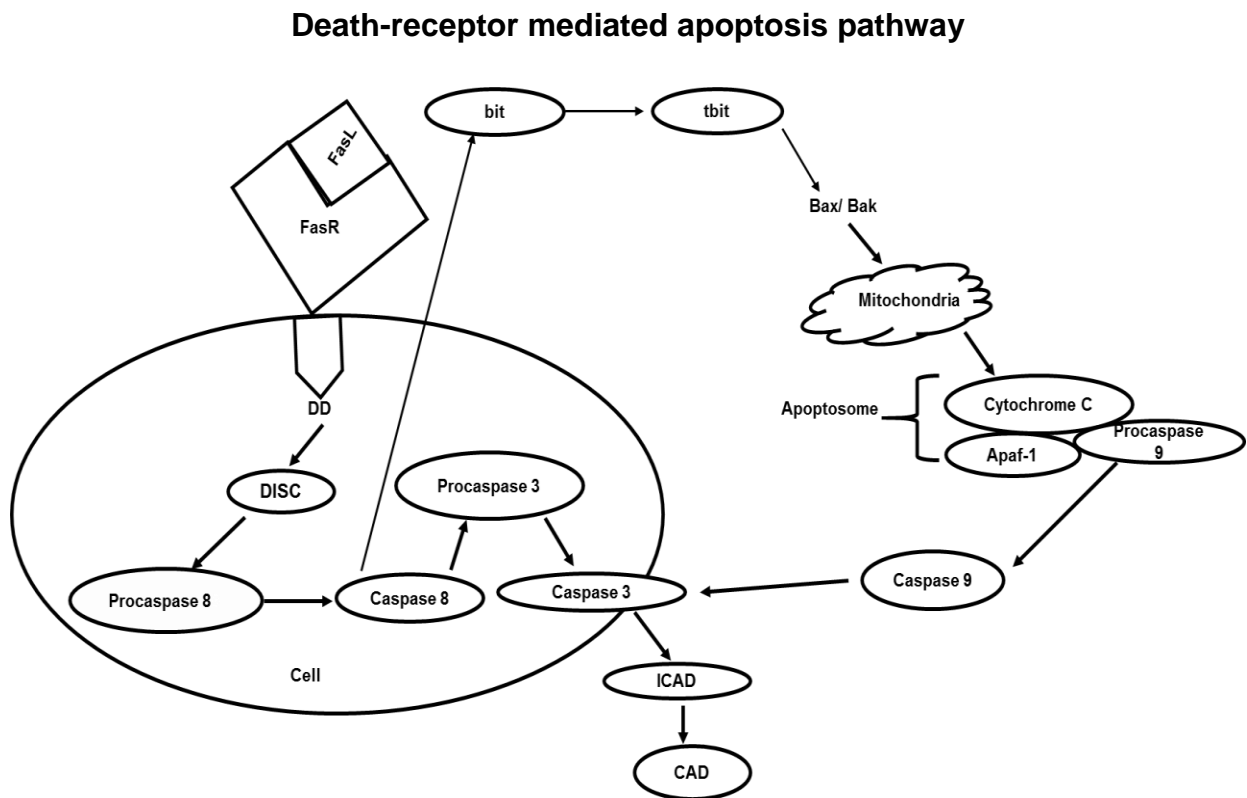


Figure 2.1: Death-receptor mediated apoptosis pathway (Ghobrial *et al.*, 2005).

2.5.2. Intrinsic pathway

Death stimuli including DNA damage, chemotherapeutic agents and UV radiation permeabilize the outer mitochondrial membrane. Permeabilization of the outer mitochondrial membrane permits the leakage of at least five apoptotic mediators (apoptotic proteins) from the mitochondrial intermembrane space and these include HtrA2, Cytochrome *c* (*cyt c*), Second Mitochondria-Derived Activator of Caspases (Smac), apoptosis-inducing factors (AIF) and endonuclease G (Germain and Shore, 2003; Hengartner and Horvitz, 1994). These proteins induce apoptosis in dissimilar ways. Smac and HtrA2 suppress the ability of IAPs (inhibitors of apoptosis proteins) to inhibit caspases. Endonuclease G and AIF are involved in DNA fragmentation, and AIF is similarly involved in chromatin condensation. The release of these apoptotic mediators from mitochondria is known to be regulated by the Bcl-2 family of proteins (Wang, 2001; Korsmeyer *et al.*, 2000).

The intrinsic apoptotic pathways also identified as mitochondrial pathways or stress pathways are activated by various array of death stresses, which include DNA damage, chemotherapeutic agents and UV radiation leading to permeabilization of the outer mitochondrial membrane and release of apoptotic proteins into the cytosol (Ola *et al.*, 2011). Cytochrome *c* is the most studied mitochondrial protein that is involved in the intrinsic pathway. Cytochrome *c* forms apoptosome with apoptotic protease activating factor 1 (Apaf1) and the inactive form of caspase-9 (Riedl and Salvesen, 2007; Li *et al.*, 1997). This complex hydrolyses adenosine triphosphate to cleave and activate caspase-9. The initiator caspase-9 then cleaves and activates the executioner caspases-3/6/7, resulting in cell apoptosis (Fig. 2.2). Caspase-8 also has a major role to play by activating the Bid that leads to the activation of truncated Bid (tBid), which translocate to mitochondria and facilitate the release of *cyt c*. The activated caspase-9 then cleaves procaspase-3, resulting in the activated caspase-3, an executioner caspase which cleaves multiple other substrate (ICAD) within the cells (Ghavami *et al.*, 2009; Fan *et al.*, 2005). Cleavage of substrates such as ICAD by caspase-3 release the Caspase-Activated DNase (CAD), which then cleaves DNA.

Mitochondrial mediated apoptosis pathway

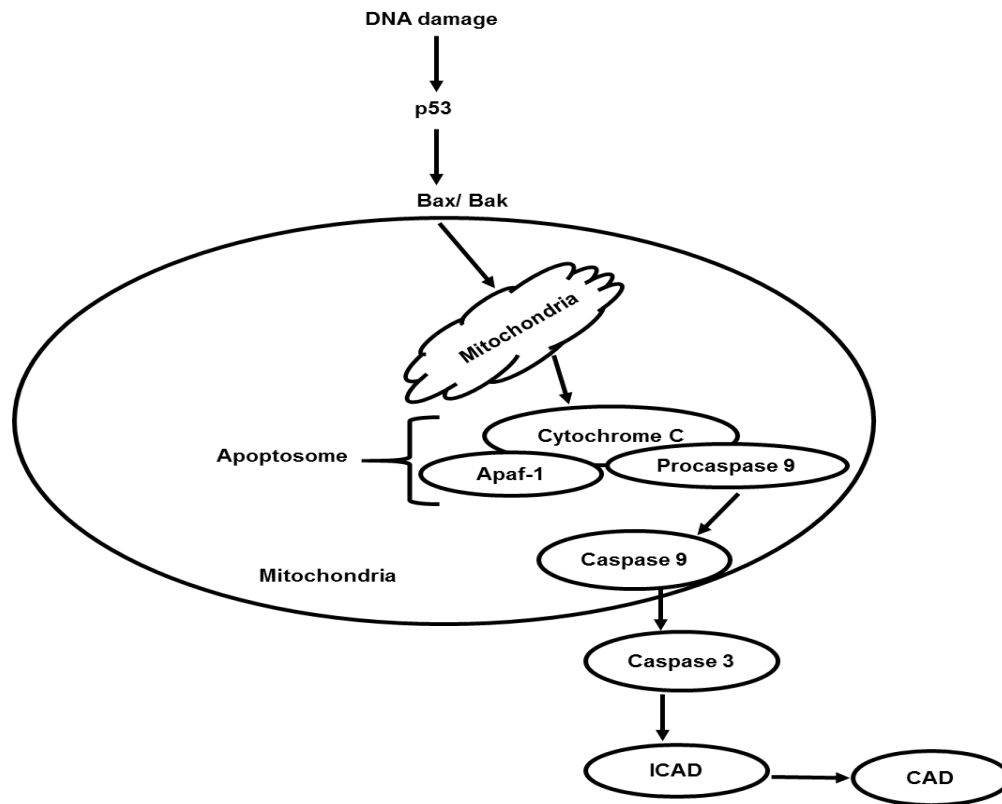


Figure 2.2: Mitochondrial mediated apoptosis pathway (Ghobrial *et al.*, 2005).

2.5.3. Arsenic trioxide (As_2O_3) as an apoptotic inducer

Previous studies have demonstrated that a wide range of anticancer agents, including chemotherapeutic agents induce apoptosis in malignant cells *in vitro*. Apoptosis inducers include cytarabine, 5-fluorouracil (5FU), fludarabine, doxorubicin, cyclophosphamide, cisplatin, etoposide, dactinomycin, camptothecin and arsenic trioxide (Kaufmann and Earnshaw, 2000). Arsenic trioxide (As_2O_3) is an inorganic compound, which promotes apoptosis and necrosis in a concentration and time-dependent manner. Whether a cell dies by necrosis or apoptosis rests on the cell death signal, the tissue type, and the developmental stage of the tissue. As_2O_3 has been shown to induce both cell cycle arrest and apoptosis associated with DNA fragmentation, changes in mitochondrial membrane potential and establishment of increased reactive oxygen species (ROS) [Zhang *et al.*, 2015]. As_2O_3 -induced apoptosis has been shown in MCF-7 cells through the activation of caspase-3 (Wang *et al.*, 2011). MicroRNA-328 (miR-328) which regulates the expression

of the *Human ether-a'-go-go related gene (HERG)* was found to enhance the As₂O₃-induced apoptosis (Wang *et al.*, 2011). This was also supported by Zhang *et al.* (2016) who indicated that arsenic trioxide suppresses cell growth by inhibiting miR-27a. Arsenic trioxide has also been shown to induce cell cycle arrest in myeloma (Liu *et al.*, 2003), chondrosarcoma cells (Jiao *et al.*, 2015) and colorectal cancer cells (Eyvani *et al.*, 2016).

2.5.4. Apoptosis inhibition in breast cancer

One of the hallmarks of cancer, including breast cancer, is resistance to apoptosis, a programmed cell death. It should be stressed that apoptosis is a well-defined and probably the most frequent form of programmed cell death, but non-apoptotic types of cell death may be of biological significance as they can serve to back up failed apoptosis or occur independent of apoptosis (Foghsgaard *et al.*, 2001). In breast cancer, the cancerous cells are resistant to apoptosis, and consequently, continue to divide without going through the normal cell homeostasis, which involves apoptosis. Additionally, they can even migrate to other parts of the breast. In breast cancer, the therapeutic goal is to trigger tumour-selective cell death. The mechanisms responsible for such death are of clear importance in determining the efficacy of specific treatments. Therefore, this study focused on deciphering arsenic trioxide triggered tumour-selective cell death in breast cancer cells and the regulation of RBBP6 splice variants by arsenic trioxide.

Breast cancer cells have been reported to be resistant to apoptosis due to the high expression of anti-apoptotic proteins, including RBBP6 (Moela *et al.*, 2014). RBBP6 has been reported to either inhibit or promote apoptosis in cancerous cells depending on how it interacts with pRB and p53 (Simons *et al.*, 1997). The RBBP6 isoform 1 protein is expressed extremely in most human tumours such as colon (Chen *et al.*, 2013), oesophagus (Mbita *et al.*, 2012) and prostate (Singh *et al.*, 2006). RBBP6 is also shown to be associated with proliferation in oesophageal cancer cells by negatively regulating p53 by acting as a scaffold to recruit MDM-2 to interact with p53 therefore leading to p53 depletion, thus facilitating cell proliferation (Li *et al.*, 2007). Some of the proteins involved in the regulation of apoptosis by regulating the activation of caspases are the Bcl-2 family of proteins. Bcl-2 inhibits the release of cytochrome c required in the intrinsic pathway (Czabotar *et al.*, 2014).

2.6. MicroRNAs

MicroRNAs (miRs) are a class of small noncoding RNAs that control gene expression by targeting their specific mRNAs and triggering either translation repression or RNA degradation (Vasudevan *et al.*, 2008). Their aberrant expression has been implicated in human diseases, including cancer (Garzon *et al.*, 2010). Mature miRs are 19 to 25-nucleotides long cleaved from 70 to 100 nucleotide hairpin pre-miRs precursors. The precursor is cleaved by cytoplasmic RNase III Dicer into 22-nucleotide miRs duplex where one strand of the short-lived duplex is degraded, whereas the other strand serves as mature miR (Bartel, 2004). In animals, single-stranded miRs bind through partial sequence homology to the 3' untranslated regions (3' UTRs) of target mRNAs, and cause either blockage of translation or mRNA degradation (Lytle *et al.*, 2007). Specific miRs are either upregulated or downregulated in cancer including breast cancer, depending on whether they are involved in apoptosis induction or cell proliferation. For example, it has been reported that miR-10b, miR-125b and miR-145 are downregulated in breast cancer suggesting that they may be playing a role of tumour suppressor genes, while miR-21 and miR-155 were upregulated suggesting that they can be oncogenes (Iorio *et al.*, 2005).

RNA polymerase II transcribes miRs genes found in animals, plants, and viruses, to a single stranded RNAs that fold because of sequence complementarity generating long primary transcripts called pri-miRs in the nucleus (Kim, 2005). Specific RNase III type of enzymes found in eukaryotes such as Drosha and DiGeorge critical region 8 (DGCR8) act on pri-miRs by cleaving them producing pre-miRs that are approximately 70 nucleotides in length (Yeom *et al.*, 2006). Pre-miRs are then exported from the nucleus to the cytoplasm by a protein called Exportin 5 (Bohnsack *et al.*, 2004). Once the pre-miRs are in the cytoplasm, an RNase III enzyme called Dicer processes the pre-miRs by cleaving out the hairpins, consequently, resulting in double stranded miRs without hairpins termed miRs duplexes (Sontheimer, 2005). The miRs duplex is loaded into RNA interference complex called RNA Interfering Silencing Complex (RISC). RISC consists of proteins such as *Argonaute* and Canonical Transient Receptor Potential Cation 6 (TRPC6). *Argonaute* protein is made of two domains, namely, P-element-induced wimpy testis (PIWI) domain and Piwi Argonaute Zwiille (PAZ) domain (Höck and Meister, 2008). PAZ domain functions to attach the chosen single stranded miRs to a sequence of interest

within the mRNA of interest. PIWI domain has an activity of RNase H that mainly breaks down the targeted single stranded messenger RNA (Höck and Meister, 2008; Song *et al.*, 2003). The miRs strand that binds the target mRNA is called the guide strand and the miRs strand that is released from the RISC complex because it does not form part of the RNA interference is called passenger strand (Khvorova *et al.*, 2003; Schwarz *et al.*, 2003). The guide strand binds to the mRNA of interest through few base complementarity and degrade the target mRNA through a process called nucleation (Long *et al.*, 2008). At present not much is known about the regulation of genes such as *RBBP6* by microRNAs. This study was also aimed at identifying microRNAs targeting *RBBP6* and relate their function in MCF-7 breast cancer cells.

2.7. Retinoblastoma Binding Protein 6

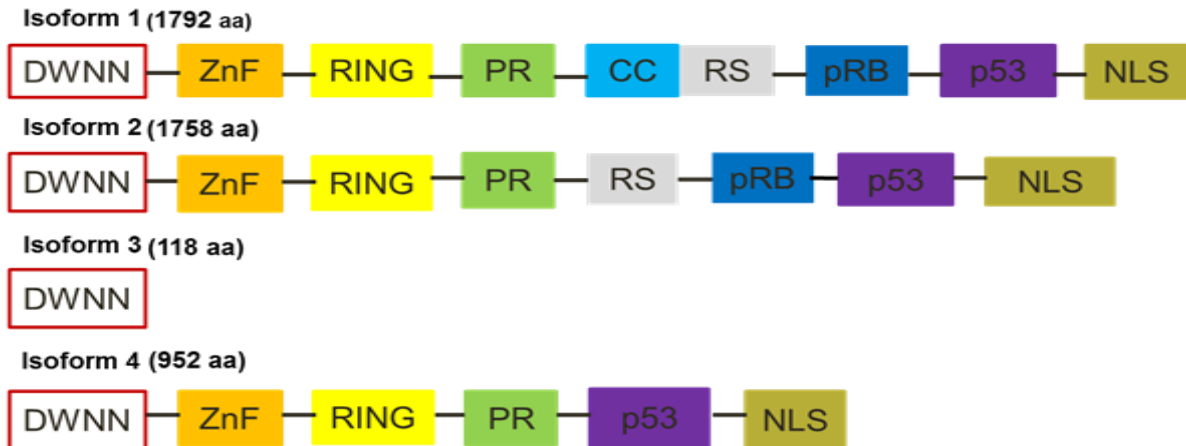
Gene therapy has attracted a lot of interest for the treatment of breast cancer. Research on finding regulatory biomolecules in the development of cancer has also intensified. *Retinoblastoma binding protein 6 (RBBP6)* is one of the genes that have shown potential as a therapeutic target (Mbita *et al.*, 2012; Motadi *et al.*, 2011; Li *et al.*, 2007). As already mentioned in chapter 1, the *RBBP6* gene is transcribed into three splice variants due to alternative splicing (Mbita *et al.*, 2012). These splice variants include a 6.1 kilobases (kb) variant and a 1.1 kilobases transcript (variant 3). The 6.1 kilobases transcript is alternatively spliced into 2 splice variants, one containing exon 16 (variant 1) while the other lacks exon 16 (variant 2), consequently, resulting in the three transcripts (Mbita *et al.*, 2012). Variant 3 is translated into RBBP6 Isoform 3, which only contains Domain With No Name (DWNN) while variant 1 and 2 are translated into isoform 1 and 2, respectively. Isoform 1 contains a DWNN domain, zinc finger, RING finger, Proline Rich (PR) domain, Coiled coil (CC) domain, Serine-arginine (RS), Rb-binding domain (pRB), p53-binding domain (p53) and Nuclear Localization Signal (NLS) [Fig. 2.3]. Isoform 2 contains all the domains found in isoform 1 but lacks the Coiled coil domain. Recently, Ntwasa (2016) reported that there are four isoforms, with isoform 4 containing a DWNN domain, a zinc finger, RING finger, Proline Rich domain (PR), p53-binding domain and Nuclear Localization Signal (NLS) (Fig.2.3A). Isoform 1 is made of 1792 amino acids, followed by isoform 2 with 1758 amino acids, isoform 3 with 118 amino acids (Mbita *et al.*, 2012) and

lastly, isoform 4 with 952 amino acids (Ntwasa, 2016). It is not clear how the fourth isoform is derived. Little is known about the expression and regulation of the human RBBP6 splice variants during cell cycle progression and breast cancer development.

Previously, Gao and Scott (2002) implicated the P2P-R, which is an RBBP6 rat homologue, in mitotic apoptosis but Mbita *et al.* (2012) and Motadi *et al.* (2011) implicated human RBBP6 in cell cycle regulation. Recently, Ntwasa (2016) reviewed the role of RBBP6 in carcinogenesis, implicating RBBP6 as a key role player in both carcinogenesis and cell cycle regulation. It remains a puzzle how RBBP6 is regulated during carcinogenesis and there is a growing interest in the role played by a novel group of regulatory biomolecules, microRNAs (miRs), in cell homeostasis and carcinogenesis.

RBBP6 proven and hypothetical isoforms

A



B

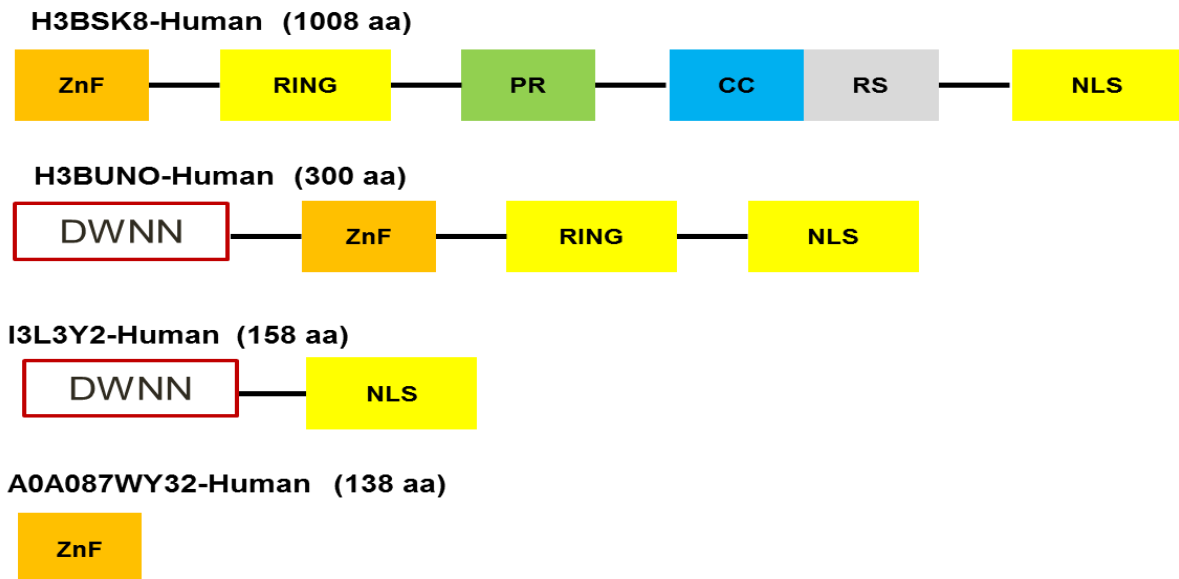


Figure 2.3: RBBP6 proven and hypothetical isoforms. (A) RBBP6 isoforms that are involved in cell cycle regulation and apoptosis (Ntwasa, 2016). (B) RBBP6 hypothetical variants adapted from:

http://www.ensembl.org/Human/Search/Results?q=rbbp6;facet_species=Human

2.7.1. Retinoblastoma binding protein 6 in carcinogenesis

RBBP6 was first identified as an interactor with the tumour suppressor proteins, pRb and p53 (Simons *et al.*, 1997). The tumour suppressor protein, p53, is a gene-specific transcription factor that regulates various genes involved in cell cycle arrest and apoptosis (Li and Prives, 2007). Following nuclear stress such as exposure to genotoxic chemicals and radiation, p53 activates *p21* gene, which is responsible for the induction of cell cycle arrest during which damaged DNA is allowed to undergo repair (Fig. 2.4). If the damage is irreversible, p53 induces the expression of pro-apoptotic proteins of the bcl-2 family, which includes Bax (Ghobrial *et al.*, 2005). *p53* and *pRB* are the most studied tumour suppressor genes and are often implicated in cancer progression.

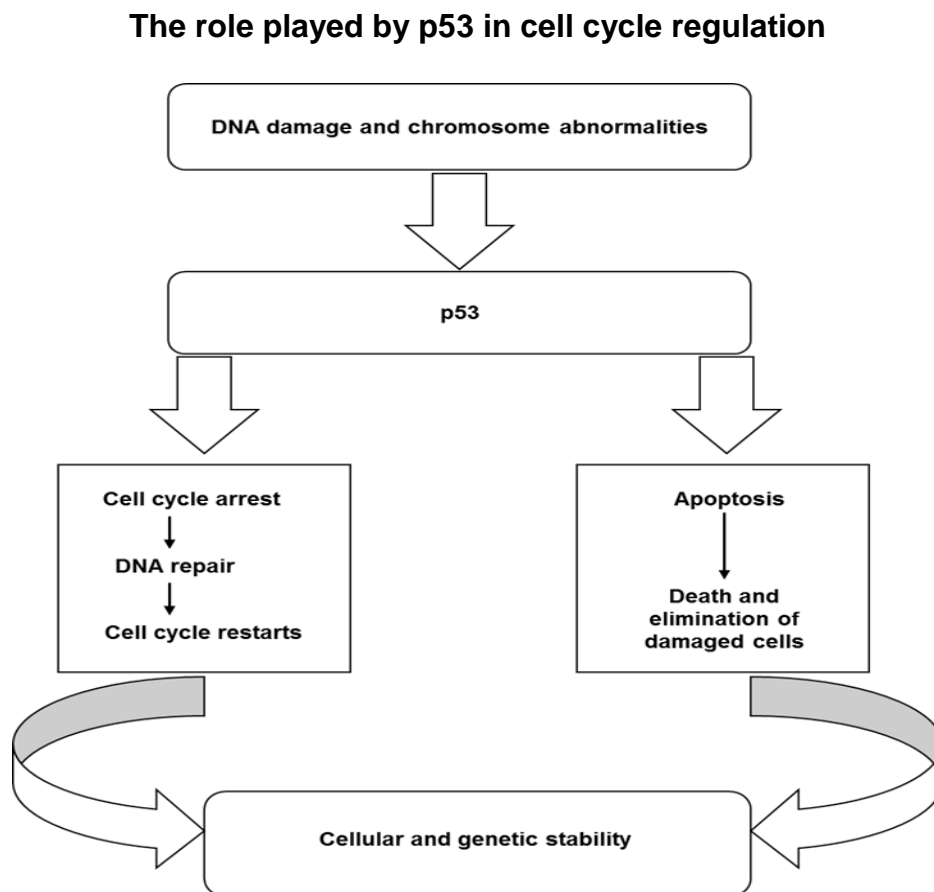


Figure 2.4: The role played by p53 in cell cycle regulation (Hanahan and Weinberg, 2000).

The locus of the *RB* gene, identified cytogenetically, is chromosome 13q14.1 (Rodríguez *et al.*, 2002). *pRB* is a tumour suppressor gene involved in the regulation G1 phase of the cell cycle. It mainly inhibits cells from exiting G1 phase by interacting with E2F involved in the transcription of genes required for cell division (Fig. 2.5). In quiescent cells, pRb is hypo-phosphorylated (active form), but its interaction with cyclin D/CDK 4 and 6, results in its hyper-phosphorylation. When pRB is hyper-phosphorylated by G1 cyclin-CDK complexes, it releases E2F allowing E2F to transcriptionally activates its target genes such as cyclin E. The E2F activates cyclin A and E/CDK2, which consequently allows cells to proceed from G1 phase to S-phase (Cobrinik, 2005). pRB is dysfunctional in several major cancers because it prevents excessive cell growth by inhibiting cell cycle progression until a cell is ready to divide. The relationship between RBBP6 and this tumour suppressor has not thus far been explored in human cells.

Regulation of pRB in coordination with the cell cycle

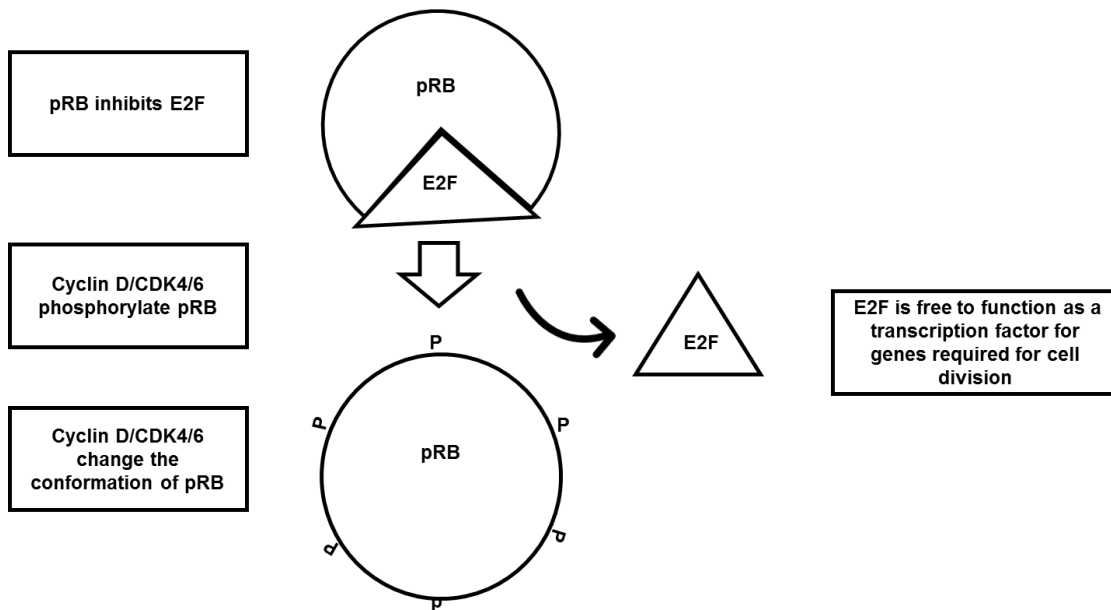


Figure 2.5: Regulation of pRB in coordination with the cell cycle. Adapted from Sachdeva and O'Brien (2012).

2.7.2. Involvement of RBBP6 in nucleic acid metabolism and embryonic development

Experimental evidence specifies that RBBP6 is involved in pre-mRNA processing, transcription, and replication (Di Giammartino *et al.*, 2014; Miotto *et al.*, 2014; Pugh *et al.*, 2006). Participation of RBBP6 in nucleic acid metabolism is evident from its domain configuration, which includes a zinc finger, a coiled coil, and a serine–arginine (RS) domain, since the former two motifs facilitate protein–nucleic acid interactions while the RS domain is found in pre-mRNA splicing factors (Di Giammartino *et al.*, 2014; Simons *et al.*, 1997). The importance of RNA-binding zinc knuckle motif in nucleic acid metabolism was also shown in yeast homologue, Mpe 1 (Minet *et al.*, 2001).

The exact mechanism by which RBBP6 influences splicing is presently unclear. Nevertheless, the mechanism by which it controls pre-mRNA cleavage and polyadenylation has been elucidated (Di Giammartino *et al.*, 2014). The full-length isoform 1 binds to the Cleavage stimulation Factor 64 kDa (CstF64), thus permitting proper pre-mRNA processing. Isoform 3 (DWNN) has been shown to hinder this binding competitively (Di Giammartino *et al.*, 2014).

In mouse embryonic development, RBBP6 is recognized as an ‘early riser’ present in the oocyte and extremely upregulated at 2–8-cell stages. In the absence of functional PACT, mouse embryos die at day 7.5 (E7.5) with widespread apoptosis. This lethality can be partially saved by concomitant deletion of p53 with defects in the anterior–posterior (A–P) axis suggesting that RBBP6 is important in A–P embryonic patterning (Li *et al.*, 2007).

2.8. Cell cycle

Cell division cycle (Fig. 2.6) is the time taken by a cell to grow and produce proteins required for DNA synthesis and cell division. There are four coordinated processes involved in the eukaryotic cell division cycle (Vermeulen *et al.*, 2003). The cell division cycle starts with gap 1 (G1), which is a phase where all the vital machinery for the DNA replication are synthesized. G1 phase is followed by the S phase, at which DNA is synthesized. Subsequent to S phase is the Gap 2 (G2) phase in which proteins required to proceed to mitosis phase (M) are synthesized. In the M phase, cells divide into two

daughter cells. The cell division cycle also consists of two check points (G1/S and G2/M) found at the boundaries between the G1/S and G2/M phases. A typical human cell divides roughly every 24 hours and even though mitosis is the most dramatic stage of the cell cycle, it only lasts about an hour while the interphase takes the 95% of the cell cycle duration (Harashima *et al.*, 2013).

Typical eukaryotic cell division cycle and CDKs that regulate each phase in the cycle

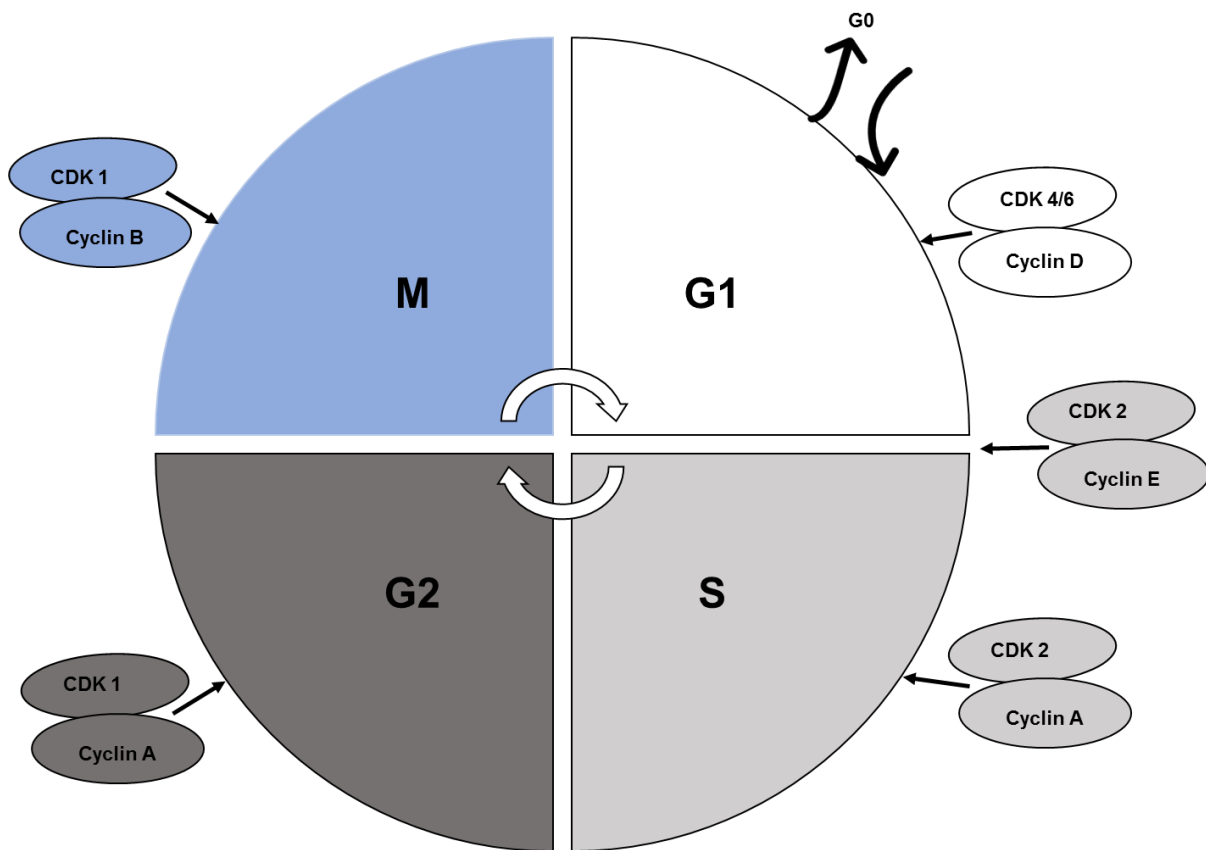


Figure 2.6: Typical eukaryotic cell division cycle and CDKs that regulate each phase in the cycle. Adapted from Moela (2014).

2.8.1. Regulation of the cell cycle

It is necessary for cell cycle control mechanisms to be precise in order to sense defects that can occur during cell division. In the heart of this control is the duty of a family of protein kinases that are called cyclin-dependent kinases (CDKs). The kinases are activated and deactivated as the cell progresses through phosphorylation and dephosphorylation mechanisms. There are four known cyclins that are involved in the progression of the cell division cycle and are expressed at different phases of the cycle. The cyclin D/cdk4/6 and cyclin E/cdk2 complexes are responsible for G1 phase entry and progression and for the transition from G1 to S phase, respectively. Cyclin A/cdk2 complex is required for S phase progression while G2/M transition and progression are characterised by the cyclin A/cdk1 complex (Fig. 2.6) [Harashima *et al.*, 2013; Suryadinata *et al.*, 2010; Vermeulen *et al.*, 2003]. Cyclin/cdk complexes (cyclin D/cdk4/6 and cyclin E/cdk2) promote cell division cycle entry and progression by phosphorylating the retinoblastoma protein (pRb) which functions as a negative regulator of cell division cycle.

2.9. Y-box binding protein 1 interaction with RBBP6

The localization of Y-box binding protein 1 (YB-1) is predominantly cytoplasmic, although it is known to shuttle back and forth between the cytoplasm and the nucleus, it localizes in the nuclear speckles, where RBBP6 has also been shown (Gao *et al.*, 2002). YB-1 performs a wide variety of cellular functions, including transcriptional and translational regulation and stress responses to extracellular signals (Kloks *et al.*, 2002). As a result of its interaction with RBBP6, YB-1 is ubiquitinated and degraded by the Ubiquitin Proteasome Pathway (UPP), leading to reduced levels of YB-1. Knockdown of YB-1 is mediated through the RING finger of the RBBP6 protein (Chibi *et al.*, 2008). YB-1 has been shown to repress levels of p53 and its transactivation of many apoptosis-inducing proteins (Okamoto *et al.*, 2000). The repressions of YB-1 levels by RBBP6 therefore established RBBP6 as a pro-apoptotic protein. On the other hand, RBBP6 has been reported to promote the repression of p53 by facilitating its ubiquitination by HDM2 (Li *et al.*, 2007), thus acting in an anti-apoptotic manner. Hence, it is possible that RBBP6 acts

on p53 by two independent pathways, one pro-apoptotic and one anti-apoptotic, with the final result depending on the relative weights of the two pathways.

Commonly, depletion of RBBP6 isoform 1 coincides with apoptosis, while depletion of RBBP6 isoform 3 is associated with carcinogenesis (Ntwasa, 2016). For example, isoform 1 is moderately expressed in the nuclei of poorly differentiated colon tumour cells and strongly expressed in colon cancer lymph node metastasis (Chen *et al.*, 2013). Isoform 3 has been shown to be downregulated in cancerous tissue but not in the nearby non-cancerous normal tissues (Mbita *et al.*, 2012). This suggests that different RBBP6 isoforms have different roles in apoptosis, cell cycle regulation and carcinogenesis. There is a possibility that some RBBP6 isoforms are pro-apoptotic while others are anti-apoptotic. This information is lacking, especially in breast cancer development.

2.10. Regulation of RBBP6 by microRNAs

Recently, Varghese *et al.* (2018) showed that RBBP6 may be under the regulation of miR-424, especially in cervical cancer. In their study, they showed that aberrant DNA promoter methylation of the miR-424 gene resulted in its inactivation. Most importantly, this study showed that the miR-424 interacts with RBBP6 3'-UTR and silences its activity in SiHa cells. According to this report, it is more likely that the low expression of miR-424 in cervical cancer due to its promoter silencing may support the high expression of RBBP6 that has been reported in cervical cancer cells (Teng *et al.*, 2018). Additionally, down-regulation of miR-424 has been reported to contribute to angiogenesis (Nakashima *et al.*, 2010) and inhibition of the proliferation of renal cancer cells (Chen *et al.*, 2013). The results of these studies suggest the regulation of RBBP6 by microRNAs in cervical cancer, but there is no report linking the regulation of RBBP6 variants by microRNAs in MCF-7 breast cancer cells. This suggests that targeting RBBP6 specific microRNAs for the treatment of breast cancer can be a promising strategy. Therefore, this study was aimed at determining the expression pattern of RBBP6 alternatively spliced variants during arsenic trioxide-induced cell cycle arrest and apoptosis in breast cancer MCF-7 cells. It was also aimed at determining RBBP6 specific microRNAs and how they are regulated in MCF-7 breast cancer cells.

CHAPTER THREE: MATERIALS AND METHODS

3.1. Introduction

This chapter describes all the materials and methods used in this study to achieve the objectives towards the aims of the study and the results that are discussed in subsequent chapters. To avoid repetition, all procedures that were conducted several times will only be described once but any adjustment made will be properly mentioned. The following techniques were used: 3-(4,5-dimethylthiazol-2-yl)-2,5 diphenyltetrazolium bromide (MTT) assay (section 3.3), apoptosis detection (section 3.5.1, 3.5.2, and 3.5.3), cell cycle analysis (section 3.5.4), Polymerase Chain Reaction (PCR) [section 3.9], Real-Time PCR [section 3.10], Immunocytochemistry (ICC) [section 3.11] and Web based bioinformatics tools for the prediction of RBBP6 specific microRNAs (3.12). Recipes for the solutions required for the methods are provided in Appendix A.

3.1.1. Cell lines

The breast cancer MCF-7 cells (ATCC-HTB-22, biosafety level 1) and non-cancerous cells (Hek-293, ATCC-CRL-1573, biosafety level 1) were kindly donated by Prof Mervin Meyer from the University of the Western Cape who had purchased the cells from the American Type Culture Collection (ATCC, Manassas, USA).

3.1.2. Chemicals and reagents

Curcumin, arsenic trioxide, cobalt chloride, and MTT [3-(4, 5-dimethylthiazol- 2-yl)-2, 5-diphenyltetrazolium bromide] were bought from Sigma-Aldrich (South-Africa).

3.1.3. Antibodies

The RBBP6 primary antibody was purchased from Novus Biologicals, USA (Cat: NBP1-49535). This antibody detects RBBP6 proteins and has been shown to have high affinity for the RBBP6 isoform 1, 2 and 4 (Appendix D). Alexa Fluor 488 secondary antibody was purchased from ThermoFischer Scientific, USA (Cat: A-11008). This secondary antibody fluoresces and detects live or fixed cells and generates a stable signal during imaging (Appendix E).

3.2. Cell culture maintenance and treatments

The MCF-7 cells were cultured in complete medium (Dulbecco's Modified Eagle's Medium [DMEM] supplemented with 10% Foetal bovine serum (FBS) and 1% Penicillin-Streptomycin-Neomycin) in a humidified atmosphere of 5% CO₂ at 37°C. The cells were nourished every day of the week by changing old growth medium with fresh growth medium after rinsing twice with 2 ml of 1X phosphate buffered saline (PBS). The cells were sub-cultured when they were at 80-90% confluent at least once per week and excess sub-cultures were preserved at -80°C in DMEM growth medium supplemented with 10% FBS and 5% dimethyl sulfoxide (DMSO).

For the treatment of MCF-7 cells, arsenic trioxide (As₂O₃) [1×10⁴ μM], Cobalt chloride (CoCl₂) [1×10⁶ μM] and curcumin (1×10⁴ μM) stock solution were diluted in complete medium to yield final required concentrations. For experimental set up, cells were seeded at a concentration of 1 × 10⁵ cells/ml and incubated at 37°C overnight. Thereafter, the cells were treated with arsenic trioxide concentrations (4-64 μM) for 24hrs. Cobalt chloride and curcumin were used as positive controls.

3.3. Cytotoxicity and cell viability analysis

The 3-(4,5-dimethylthiazol-2-yl)-2,5 diphenyltetrazolium bromide (MTT) assay was used to assess the effect of arsenic trioxide on cytotoxicity and cell viability against the MCF-7 cells. The MTT assay is a colorimetric assay that is used to measure cytotoxicity and cell proliferation. It involves the reaction of Nicotinamide Adenine Dinucleotide Phosphate Hydrogen (NADPH)-dependent cellular oxidoreductase enzymes that may, under defined conditions, reflect the number of viable cells present. These enzymes can reduce the tetrazolium dye MTT to its insoluble formazan form, which has a purple colour once solubilized for spectrophotometer measurement.

The effect of arsenic trioxide and the positive controls (curcumin and cobalt chloride) on the viability of MCF-7 cells was assessed using the MTT assay. Briefly, breast cancer cells (MCF-7) were seeded in a 96-well microtiter plate at 1 × 10⁵ cells/well and exposed to various concentrations of As₂O₃ (0-64 μM), cobalt chlorite (0-250 μM) and curcumin (0-100 μM) for 24 hours after allowing them to attach for overnight. After 24 hours, media

containing different concentrations of the treated compounds were removed followed by addition of 10 µl of MTT (5 mg/ml) into each well and the plates were incubated for an additional 4 hours at 37°C. After the MTT solution was aspirated off, to achieve solubilization of the formazan crystal formed in viable cells, 100 µl of DMSO was added in to each well before absorbance at 570nm could be measured using a GloMax-Multi+ (Promega, USA). Cell survival rate was calculated with the following formula:

$$\text{Survival rate (\%)} = \frac{\text{Average OD (experimental group)}}{\text{Average OD (experimental group)}} \times 100\%$$

To further confirm the MTT assay, cell viability was performed using the Muse™ Count & Viability Kit (Merck Millipore, Germany) following the manufacturer's instructions. Subsequent to exposure to different treatments, floating cells were collected by centrifugation, attached cells were washed with 1X PBS and trypsinized with 1X trypsin. Complete media was added to inactivate the trypsin followed by centrifugation at 3.500 x g for 3 minutes, after the pellet was resuspended in 20 µl of fresh complete media and mixed with 380 µl of Muse™ Count & Viability reagent followed by incubation for 5 minutes in the dark. The samples were then analysed using the Muse® Cell Analyzer (Merck-Millipore, Germany).

3.4. Morphological assessment of apoptosis using fluorescence and light microscopy

The 4',6-diamidino-2-phenylindole (DAPI) staining was used for morphological evaluation of the MCF-7 cells that had been treated with arsenic trioxide (11 and 32 µM) and the positive controls [cobalt chloride (100 µM) and curcumin (100 µM)]. Briefly, MCF-7 cells were plated at a density of 4 × 10³ cells per well in a six well plate in a complete medium (section 3.1) for 24 hours and starved for further 12 hours to synchronize all the cells into the same phase of the cell cycle. Following exposure of the cells to arsenic trioxide, cobalt chloride and curcumin the cells were washed with 1X PBS and stained for 15 minutes with 5µg/ml of DAPI for morphologic assessment of the cells using both fluorescence and normal light filters on the Nikon Eclipse TS100F Ti-E inverted microscope (Nikon Instruments, Japan).

3.5. Flow cytometry

3.5.1. Apoptosis analysis

To determine how arsenic trioxide (32 μM) reduces the viability of MCF-7 cells as determined using the cell viability assays, the Muse™ Annexin V & Dead Cell Kit (Merck Millipore, Germany) was used following the manufacturer's instructions. Briefly, the MCF-7 cells were cultured in 6-well plates at 1×10^5 cells/well overnight, synchronized for 12 hours and treated for 24 hours with curcumin (100 μM) and arsenic trioxide (32 μM). Following exposure to the different treatments, floating cells were collected by centrifugation and attached cells were washed with 1X PBS and trypsinized with 1X trypsin. Complete media was added to inactivate the trypsin. Cell suspension of 100 μl was then transferred to Eppendorf tubes and mixed with 100 μl of the Muse® apoptosis reagent, the samples were then incubated in the dark for 20 minutes. The percentage of apoptotic cells after treatment with the arsenic trioxide and the positive control (curcumin) was quantified and analysed using the Muse® Cell Analyzer (Merck-Millipore, Germany).

3.5.2. Multi-caspase analysis

To determine the mechanism of arsenic trioxide-induced apoptosis to assess whether the resultant apoptosis was caspase-dependent or independent, the Muse™ MultiCaspase Kit (Merck-Millipore, Germany) was used according to the manufacturer's instructions. Briefly, MCF-7 cells were seeded in a 6-well plate at 1×10^5 cells/well overnight. The cells were synchronised for 12 hours followed by treatment with arsenic trioxide (32 μM) and curcumin (100 μM) as a positive control for 24 hours. After 24 hr incubation, the floating cells were collected by centrifugation and the attached cells were washed with 1X PBS and trypsinized with 1X trypsin. Complete media was added to inactivate the trypsin followed by resuspension into a DMEM media supplemented with 10% FBS. A portion (50 μl) of each cell suspension was transferred to Eppendorf tubes, followed by addition of 5 μl of the Muse Multi-Caspase Reagent. The sample was vortexed at medium speed (3.500 $\times g$) for 3 to 5 seconds for mixing purposes. The tubes were then incubated for 30 minutes in the 37°C incubator containing 5% CO₂. After incubation, 150 μl of Muse Caspase7-ADD working solution was added into each tube and mixed by pipetting, and

the tubes were incubated for 5 minutes in the dark. Following staining, the cells were quantified and analysed using the Muse® Cell Analyzer (Merck-Millipore, Germany).

3.5.3. MitoPotential analysis

To determine the effect of arsenic trioxide on mitochondrial potential and cellular plasma membrane permeabilization in MCF-7 cells, the Muse™ MitoPotential Kit (Merck-Millipore, Germany) was used following the instructions. Briefly, MCF-7 cells were seeded in a 6-well plate at 1×10^5 cells/well overnight, after the cells were, synchronised for 12 hours followed by treatment with arsenic trioxide (32 μM) and curcumin (100 μM) as a positive control for 24 hours. After the treatments, the floating cells were collected by centrifugation, attached cells were washed with 1X PBS and trypsinized with 1X trypsin. Complete media was added to inactivate the trypsin followed by centrifugation at $3.500 \times g$ for 3 minutes. The pellets were resuspended in 100 μl of $1 \times$ Assay Buffer, the solutions were mixed by pipetting up and down followed by addition of 95 μl of MitoPotential working solution. The samples were mixed followed by incubation for 20 minutes inside a carbon dioxide incubator. Following incubation, 5 μl of the Muse® MitoPotential 7-AAD reagent was added in each of the samples, mixed by pipetting and incubated for 5 minutes at room temperature, and analysed using the Muse® Cell Analyzer (Merck-Millipore, Germany).

3.5.4. Cell cycle analysis

To evaluate the effect of 11 μM arsenic trioxide and 100 μM cobalt chloride (the positive control) on the cell cycle phases distribution, the Muse™ Cell Cycle Kit (Merck Millipore, Germany) was used according to the instructions. Briefly, MCF-7 cells were seeded in a 6-well plate at 1×10^5 cells/well overnight, the cells were further starved for 12 hours to be synchronized, followed by treatment with arsenic trioxide (11 μM) and cobalt chloride (100 μM) for 24 hours. Subsequent to exposure to different treatments, the cells were collected by centrifugation, washed with 1X PBS and trypsinized with 1X trypsin. Complete media was added to inactivate the trypsin followed by resuspension in 1 ml of 70% ethanol and the samples were stored in -20°C freezer for at least 3 hours for fixation, after fixation, 200 μl of cells were transferred to a new tube and centrifuged at $300 \times g$ for 5 minutes and the cells were washed once with 1X PBS. Lastly, 200 μl of muse cell cycle

reagent was added in the cells followed by incubation for 30 minutes at room temperature in the dark. The stained cells with the relative number of cells in the distinct phases after the treatment with the IC₅₀s of arsenic trioxide and cobalt chloride were analysed using the Muse® Cell Cycle Analyzer (Merck-Millipore, Germany).

3.6. Total RNA extraction

Total RNA is used as a starting point for downstream processes such as microarray analysis, Reverse Transcription Polymerase Chain Reaction, cDNA library construction, conventional PCR and quantitative Real-Time PCR. Total RNA was extracted from MCF-7 cells using the ZR RNA MiniPrep purchased from Zymo Research, USA. Briefly, MCF-7 cells were seeded in 10 × T75 flasks at 1 × 10⁵ cells/ml, followed by treatment with arsenic trioxide (32 μM and 11 μM), cobalt chloride (100 μM) and curcumin (100 μM) and incubation for 24 hours at 37°C. After treatments, the floating cells were collected by centrifugation, then the attached cells were washed with 1X PBS and trypsinized using 1X trypsin. Complete media was added to inactivate the trypsin and the cell suspension was centrifuged at 2000 × *g* for 5 minutes, after which the media was discarded followed by addition of 500 μl of Trizol reagent to each tube. The tubes were left at room temperature for 5 minutes. The cells were then centrifuged at 4300 × *g* for 15 minutes, resulting in three layers. The clear aqueous layer was transferred into a new labelled 1.5 ml centrifuge tube. After, 500 μl of ice cold 95% (v/v) ethanol was added into the 1.5 ml centrifuge tubes containing aqueous solution, mixed and left at room temperature for 5 minutes. The solutions were then transferred into a filter column that had been inserted into a collection tube and centrifuged for 5 minutes at 7500 × *g* at 4°C, and the flow throughs were discarded. Four hundred microlitre RNA wash buffer was added into each column and centrifuged at 7500 × *g* at 4°C for 5 minutes. In an RNase free tube, 5 μl of DNase 1 was mixed with 75 μl of DNA Digestion Buffer and directly transferred to each column matrix and incubated at room temperature for 15 minutes. Four hundred microlitre of Direct-zol RNA Prewash was added into the zymo-spin column and centrifuged for 5 minutes at 7500 × *g* at 6°C and the flow through was discarded. This step was repeated twice. RNA Wash Buffer of 700 μl was added to each column and centrifuged at 7500 × *g*, 2-8°C for 5 minutes to ensure complete removal of the wash buffer. The columns were

transferred into Eppendorf tubes, RNA Elution Buffer was added to this assembly to elute the total RNA, the elution was carried out by centrifugation at $7500 \times g$, 2-8°C for 5 minutes. The resulting RNA was quantified using a UV/VIS Spectrophotometer (Beckman Coulter, South Africa). RNA purity was confirmed by measuring absorbance and determining the A260/A280 with 1.8-2.0 showing good purity and quality. RNA integrity was confirmed by examination of the 18S and 28S RNA bands using agarose gel electrophoresis. The RNA was stored at -80 °C in aliquots of 10 µl for future use.

3.6.1. RNA Gel electrophoresis

3.6.1.1. Preparation of RNA agarose gel

Agarose gel (1.5%) was prepared in 1X MOPs [prepared in DEPC water, 0.6% (v/v) 37% formaldehyde]. When the solution was cooled to about 60°C, 0.0002 µg/µl ethidium bromide (EtBr) [Promega, USA] was added and the solution poured onto a casting tray containing the comb and left at room temperature to solidify. The RNA sample (500 ng) was heated at 65°C for five minutes, cooled on ice and mixed with an equal volume of the loading dye (BioLabs, USA). The mixture was then loaded onto a 1X MOPS agarose gel. The RNA was electrophoresed at 90 volts for one hour in 1X MOPS, viewed under ultraviolet (UV) and captured using MiniBIS DNR Bio Imaging Systems (Lasec, S.A).

3.7. cDNA synthesis

Complementary DNA (cDNA) was synthesized using the ImProm-II™ Reverse Transcription System (Promega, USA). One microgram (1 µg) of total RNA extracted from 11 µM As₂O₃ treated MCF-7 cells, 32 µM As₂O₃ treated MCF-7 cells and 100 µM cobalt and curcumin treated MCF-7 cells was added into a reverse transcription reaction mixture containing 5x Improm II reaction buffer, 25 mM magnesium chloride, 0.5 mM deoxy-nucleoside triphosphates (dNTPs) mix, recombinant RNAsin (40 u/µl), Improm II Reverse transcriptase (1 u/µl). The mixture was further diluted with nuclease free water to make the final volume of 20 µl as illustrated in table 3.1. Following this; the mixture was incubated at 25°C for five minutes to allow the primers to anneal at their sites. This was followed by incubation at 42°C for an hour to allow reverse transcription to occur. After this incubation, the reverse transcriptase was inactivated by incubation at 70°C for five

minutes and the samples were cooled on ice. The resulting cDNA was quantified using the UV/VIS Spectrophotometer (Beckman Coulter, South Africa). cDNA purity was confirmed by measuring absorbance and determining the A260/A280 with 1.6-1.8 showing good purity and quality. The cDNA was stored at -20 °C for future use.

Table 3.1: The cocktail for cDNA synthesis.

Components	Volume	Final Concentration
5x Improm II reaction buffer	4 µl	1x
Magnesium chloride (25 mM)	5 µl	5 mM
dNTP mix	1 µl	0.5 mM each dNTP
Recombinant RNAsin (40 u/µl)	0.5 µl	20 u
Nuclease free water	4.5 µl	-
Improm II Reverse transcriptase (1 u/µl)	1.0 µl	1 u
RNA	5 µl	500 ng
Final Volume	20 µl	

3.8. Primer design

Specific primers for the gene of interest, *RBBP6* and a housekeeping gene, *GAPDH* were designed using nucleotide sequences obtained from the NCBI database (www.ncbi.nlm.nih.gov), following primer design rules (Appendix B). The primer sequences were sent to Inqaba Biotech (SA) for primer synthesis. Primers were optimized using PCR to avoid or minimize nonspecific binding and formation of primer-primer dimers. Table 3.2 summarizes the designed primers that were used in this study. The specificity of primers was confirmed using the Web-based BLAST tool (blast.ncbi.nlm.nih.gov).

Table 3.2: Different primer sets, sequences and product sizes.

Gene name	Primer sequence (5'→3')	Amplicon size(bp)
GAPDH	Forward primer: AGCTGAACGGGAAGCTCACT Reverse primer: TGCTGTAGCCAAATTCGTTG	297
RBBP6 variant 1 and 2	Forward primer: GTA TAG TGT CCC TCC TCC AGG Reverse primer: GTA ATT GCG GCT CTT GCC TCT	Variant 1 = 445 Variant 2 = 343
<i>RBBP6</i> variant 3	Forward primer: GGA TAA TAT GTG GCA TCA CTT G Reverse primer: TCC CTG TAT GAC ACT GTG TTG	Variant 3 = 121

3.9. Polymerase chain reaction

Polymerase chain reaction (PCR) is a common laboratory technique used to amplify DNA molecules. In this study, PCR was used to amplify RBBP6 splice variants, in order to analyse their expressions during arsenic trioxide-induced cell cycle arrest and apoptosis. The PCR was performed using a 2X PCR Master Mix (Takara Bio Inc, China), following the manufacturer's protocol. As tabulated in table 3.3, briefly, in a microcentrifuge tube, to make a total of 25 μ l reaction, 12.5 μ l of 2X PCR Master Mix, 9.5 μ l of Nuclease free water, 1 μ l (500 ng) of cDNA, and 1 μ l (10 μ M) of both reverse and forward primers specific to each RBBP6 variants and GAPDH (positive control) were mixed. The reactions were subjected to 30 cycles (Table 3.4) consisting of the three PCR steps (denaturation, annealing and extension) in T100™ Thermal Cycler machine (Bio-Rad, USA). The products were electrophoresed on 1.5% agarose gel with 1000 bp DNA molecular weight marker (BioLabs, USA) to confirm the sizes of the PCR products. The PCR products were viewed under ultraviolet (UV) and captured using MiniBIS DNR Bio Imaging Systems (Lasec, S.A).

Table 3.3: The cocktail for Polymerase Chain Reaction.

Reagent	Volume (μ L)	Final Conc.
Master Mix (2X)	12.5	1X
Forward primer (10 μ M)	1.0	0.4 μ M
Reverse primer (10 μ M)	1.0	0.4 μ M
MgCl ₂ (25 mM)	2.0	2 mM
Nuclease free water	7.5	-
Template DNA (500 ng)	1.0	-
Total Volume	25.0	-

Table 3.4: Temperature profiles used for PCR.

Cycle	Temperature (°C)	Duration (sec)
Taq polymerase activation	98	30
Denaturation	95	30
Annealing	T _m -5	30
Extension	72	45
Holding step	72	60
Number of cycles (30)	-	-

3.9.1. Agarose gel electrophoresis of DNA

Agarose gel electrophoresis is a technique used to separate proteins and nucleic acids based on size. An agarose gel of 1.5% was prepared in 1X TBE buffer (prepared in deionised water) by weighing 1.5 g of agarose powder and dissolving it in 100 ml of 1X TBE buffer. The mixture was microwaved for 1-3 min until the agarose was completely dissolved. The solution was allowed to cool for 5 minutes, then 0.0002 µg/µl of EtBr (Promega, USA) was added, the gel solution was poured onto a casting tray containing the comb and left at room temperature to solidify. The PCR products were then loaded on the 1.5% agarose gel. The PCR products were electrophoresed at 90 volts for an hour and viewed under ultraviolet (UV). The images were captured using MiniBIS DNR Bio Imaging Systems (Lasec, S.A) and further analysed using Quantity One® 1-D analysis software.

3.10. Quantification of RBBP6 variant 3 mRNA using Real-Time PCR

To quantify the expression of RBBP6 variant 3 in MCF-7 and Hek-293 cells, Real Time PCR was performed. Real-time PCR differs from conventional PCR in that instead of detecting and quantifying amplified DNA at the end of the reaction, the amount of PCR product is measured at each cycle in real time. In this study, cDNAs synthesized from RNA extracted from untreated MCF-7 cells and Hek-293 cells were quantified using the UV/VIS Spectrophotometer (Beckman Coulter, South Africa). cDNAs of known concentration (500ng) were serially diluted by a dilution factor of 10 to 100 and subjected

to real-time reactions in Qiagen rotor-gene 6000 PCR machine (Bio-Rad, USA). The Real Time PCR was performed in a 20µl reaction mixture containing cDNA (500, 50 and 5 ng), Luna Universal qPCR master mix, forward and reverse primers and nuclease free water as shown in table 3.5, using the conditions shown in table 3.6. The expression of RBBP6 variant 3 and GAPDH as a housekeeping gene was quantified using comparative cycle number cross point (Ct) method (Livak and Schmittgen, 2001). This method uses the comparison of the Ct values of the samples of interest with a control sample and both the samples are normalised to an appropriate housekeeping gene.

Table 3.5: Real-Time PCR setup.

Component	20 µl Reaction	Final concentration
Luna Universal qPCR Master Mix	10 µl	1X
Forward primer (10 µM)	0.5 µl	0.25 µM
Reverse primer (10 µM)	0.5 µl	0.25 µM
Template DNA	Variable	-
Nuclease-free Water	to 20 µl	-

Table 3.6: Typical Real-Time conditions.

Cycle step	Temperature (°C)	Time (s)	Cycles
Initial Denaturation	95	60	1
Denaturation	95	15	30–45
Extension	60	30	
Melt Curve	60–95	Various	1

3.11. Immunocytochemistry

To evaluate the effect of arsenic trioxide on the expression and localization of RBBP6 isoforms 1, 2 and 4 in MCF-7 cells, ICC was performed. Breast cancer cells (MCF-7) were seeded on cover slips in a 6 well plate at 1×10^5 cells/well and exposed to various concentrations of As₂O₃ (11 and 32 µM), cobalt chlorite (100 µM) and curcumin (100 µM) for 24 hours after allowing them to attach for overnight. After the 24 hr incubation, the cells were washed twice with 1X PBS containing 0.5% BSA before fixing the cells in 4% (w/v) paraformaldehyde (PFA) in 1X PBS at room temperature for 15 min. The cells were then washed three times with 1X PBS before permeabilization in 1X PBS containing 0.1%

Triton X-100 for 10 min at room temperature. The cells were then washed twice in 1X PBS and antibody non-specific binding was blocked using 0.5% BSA for one hr at room temperature. The cells were then incubated with the [1:50 dilution in 1X PBS-BSA (0.5%)] for one hr. The protocol for RBBP6 primary antibody is shown in Appendix D. After primary antibody incubation, the cells were washed twice with 1X PBS-BSA. This was then followed by incubating the cells with the secondary antibody (Anti-rabbit Alexa Fluor 488) at 1:500 dilution for one hr in the dark (Appendix E). The cells were washed twice using 1X PBS, counter-stained with DAPI and examined under Nikon Eclipse TS100F Ti-E inverted microscope (Nikon Instruments, Japan) using the excitation at 590 nm and emission at 617 nm.

3.12. Prediction and validation of RBBP6 specific miRs

Bioinformatics tools TarBase v.8, miRDB.org and miRbase were used to search for the miRs targeting RBBP6 specific variants. The miRNA hits specific to RBBP6 transcripts that were predicted by all the three databases were analysed for their expressions in MCF-7 breast cancer cells using literature survey.

3.13. Statistical data analysis

The results of the different experiments (Cell viability assay, cell cycle phases analysis and apoptosis analysis) performed in triplicates were expressed as the mean \pm standard deviation (SD) using one way ANOVA employing the Tukey-Kramer Multiple Comparisons Test. Data was analysed to obtain statistical significant differences by comparing two sets of data. When the untreated samples were compared with the treated samples, the differences were considered significant when *P was ≤ 0.05 , **P ≤ 0.01 and ***P ≤ 0.0001 .

CHAPTER FOUR: RESULTS

4. Introduction

RBBP6 has a wide range of functions and these include a role in cell cycle regulation, apoptosis, protein stability, DNA replication and mRNA processing (Miotto *et al.*, 2014; Mbita *et al.*, 2012; Chibi *et al.*, 2008; Pugh *et al.*, 2006; Gao and Scott, 2002). Little is known about the expression and regulation of the human RBBP6 splice variants during cell cycle progression and breast cancer development. Therefore, this study was aimed at determining the expression pattern of RBBP6 alternatively spliced variants during arsenic trioxide-induced cell cycle arrest and apoptosis of breast cancer cells. It was also aimed at predicting and identifying RBBP6 specific-miRs. To achieve these aims, MTT assay, flow cytometry, PCR, Real-Time PCR, ICC as well as Web-based bioinformatics tools were employed.

4.1. *In vitro* reduction of the viability of MCF-7 cells by arsenic trioxide

Cell cytotoxicity was used to measure cell viability after treating the MCF-7 cells with arsenic trioxide, cobalt chloride (positive control for cell cycle arrest) and curcumin (positive control for apoptosis). The effect of arsenic trioxide on the growth and viability of MCF-7 cells was assessed using the MTT assay (section 3.3) and the kit assay (section 3.3).

As shown in figure 4.1A and table 4.1A, arsenic trioxide significantly inhibited the growth and viability of MCF-7 cells in a dose-dependent manner and its IC₅₀ was extrapolated to be 11 µM. Apoptosis-inducing concentration was found to be 32 µM (Fig. 4.1A) after 24 h treatment. Cobalt chloride as positive control for cell cycle analysis also inhibited the growth of MCF-7 cells at an IC₅₀ of 100 µM (Fig. 4.1B and table 4.1B) after 24 h treatment. Curcumin reduced the viability of MCF-7 cells at an apoptosis-inducing concentration of 100 µM (Fig. 4.1C and table 4.1C) after 24 h treatment. Using GraphPad Prism, the Tukey-Kramer Multiple Comparisons Test was performed and the results (Fig 4.1 A-C) were found to be statistically significant (*P < 0.05).

Table 4.1A: Cell viability average percentages \pm standard error of the mean (SEM) after the treatment of MCF-7 cells with various concentrations of arsenic trioxide (As_2O_3).

Arsenic trioxide treatments	Mean (%) \pm SEM
Control	100.00 \pm 0.000
4 μM	79.91 \pm 4.782 **
8 μM	55.43 \pm 4.201 ****
32 μM	28.73 \pm 2.134 ****
64 μM	24.64 \pm 2.665 ***

*** indicates $p \leq 0.001$ and ** indicates $p \leq 0.01$

Effect of arsenic trioxide on the viability of MCF-7 cells

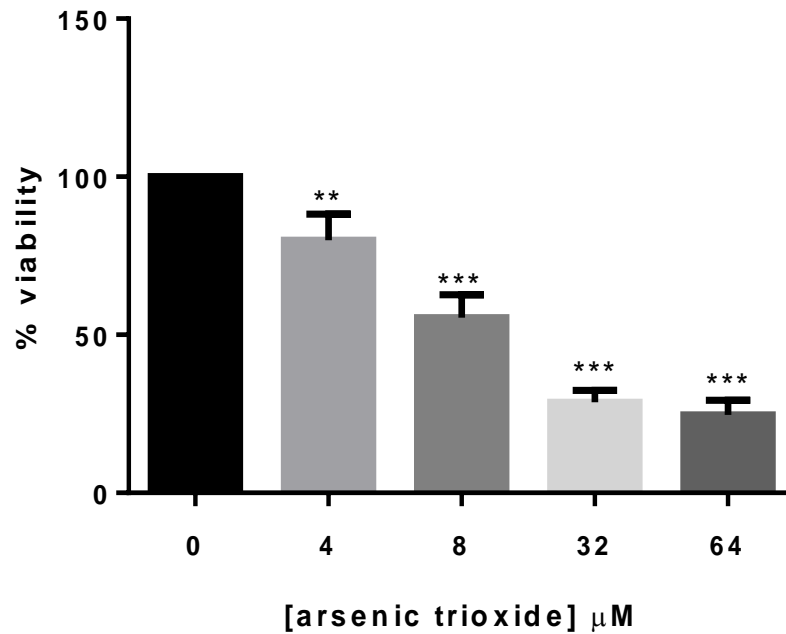


Figure 4.1A. Effect of arsenic trioxide on the viability of MCF-7 cells. The effect of arsenic trioxide significantly ($p \leq 0.01$ ** / $p \leq 0.001$ ***) reduced the viability of MCF-7 cells in a concentration-dependent manner.

Table 4.1B: Average percentages of cell viability \pm SEM after treating the MCF-7 cells with various concentrations of cobalt chloride (CoCl_2).

Cobalt chloride treatments	Mean (%) \pm SEM
Control	100.00 \pm 0.000
50 μM	60.98 \pm 4.128 ***
100 μM	51.60 \pm 1.570 ***
150 μM	46.99 \pm 1.026 ***
200 μM	39.95 \pm 2.200 ***
250 μM	33.10 \pm 5.321 ***

*** indicates $p \leq 0.001$

Effect of cobalt chloride on the viability of MCF-7 cells

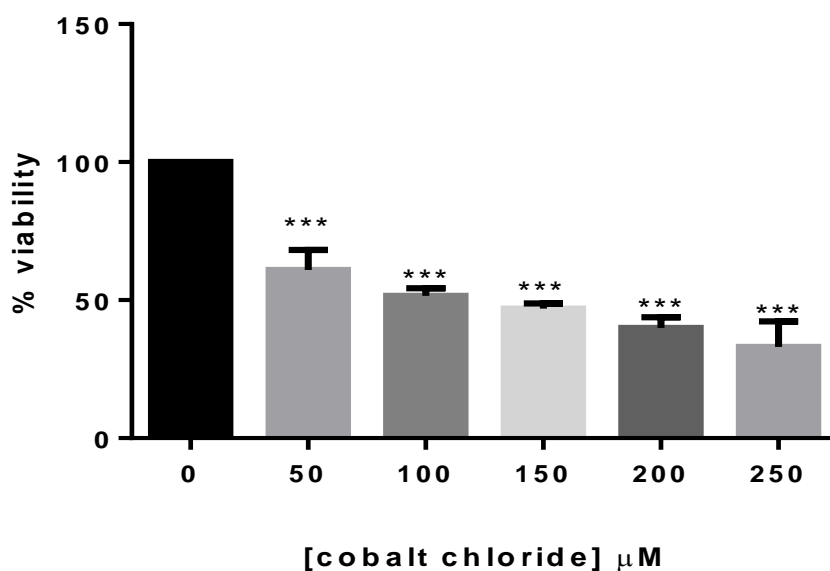


Figure 4.1B: Effect of cobalt chloride on the viability of MCF-7 cells. Cobalt chloride significantly ($p \leq 0.001$ ***) reduced the viability of the MCF-7 cells in a concentration-dependent manner.

Table 4.1C: Cell viability average percentages \pm SEM after treating MCF-7 cells with various concentrations of curcumin ($\text{C}_{21}\text{H}_{20}\text{O}_6$).

Curcumin treatments	Mean (%) ± SEM
Control	100.00 ± 0.000
25 µM	54.08 ± 4.441 ***
50 µM	48.28 ± 5.944 ***
75 µM	31.99 ± 3.947 ***
85 µM	24.80 ± 1.941 ***
100 µM	26.39 ± 1.630 ***

*** indicates $p \leq 0.001$

Effect of curcumin on the viability of MCF-7 cells

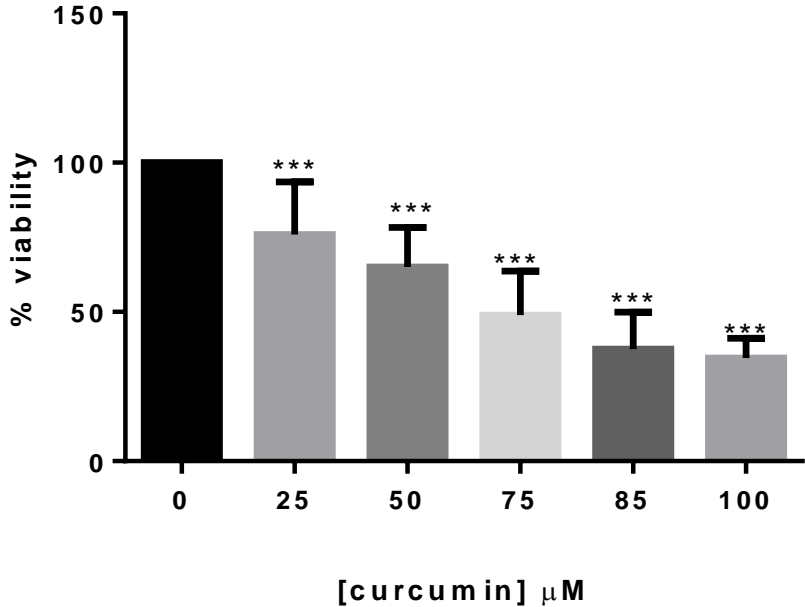


Figure 4.1C: Effect of curcumin on the viability of MCF-7 cells. Curcumin significantly ($p \leq 0.001$ ***) reduced the viability of the MCF-7 cells in a concentration-dependent manner.

4.1.1. Confirmation of arsenic trioxide-reduced cell viability in MCF-7 cells

MTT assay results (Fig. 4.1A-C) were further confirmed by the Muse® Cell Analyzer (Fig. 4.2A-F and Fig.4.3), which also showed that arsenic trioxide (11 μ M and 32 μ M) and the positive controls (cobalt chloride and curcumin) significantly inhibited the growth and viability of MCF-7 cells in a concentration dependent manner. Arsenic trioxide (11 μ M) and cobalt chloride (100 μ M) significantly (*P < 0.05) inhibited 51% cell viability in MCF-7 cells. Arsenic trioxide apoptosis-inducing concentration (32 μ M) also inhibited 66% cell viability, and the same trend was observed even in the positive control (curcumin). The same results from three independent experiments were represented graphically (Fig. 4.3) and summarised in table 4.3, to show that arsenic trioxide was potent in inhibiting the proliferation of MCF-7 cells *in vitro*.

Analysis of % cell viability in MCF-7 cells using the Muse™ Count & Viability Kit

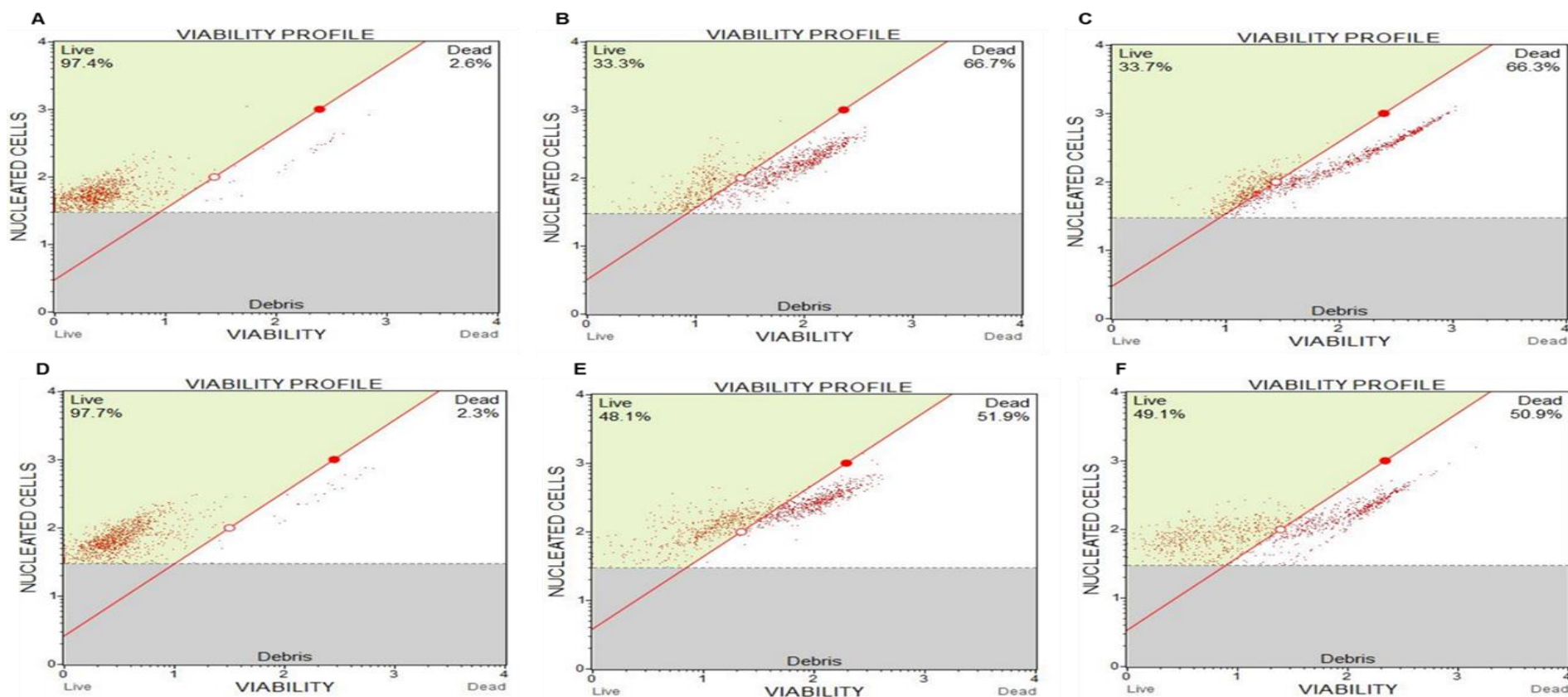


Figure 4.2 A-F: Analysis of % cell viability in MCF-7 cells using the Muse™ Count & Viability Kit. The untreated control (4.2A and D) was compared with the MCF-7 cells treated for 24 hours with 32 μM of arsenic trioxide (4.2B), 100 μM of curcumin (4.2C), 11 μM of arsenic trioxide (4.2E) and lastly, 100 μM cobalt chloride (4.2F). Arsenic trioxide reduced the viability of MCF-7 cells in a concentration-dependent manner.

Table 4.3: Cell viability average percentages \pm SEM after the treatment of MCF-7 cells with arsenic trioxide, cobalt chloride and curcumin.

Treatments	Mean (%) \pm SEM	
	Live	Dead
Control	95.08 \pm 0.858	4.94 \pm 0.850
Arsenic trioxide (11 μ M)	50.98 \pm 1.463 ***	49.78 \pm 1.969 ***
Arsenic trioxide (32 μ M)	29.44 \pm 2.563 ***	70.48 \pm 2.610 ***
Cobalt Chloride (100 μ M)	48.08 \pm 2.277 ***	48.56 \pm 2.345 ***
Curcumin (100 μ M)	28.76 \pm 2.386 ***	71.04 \pm 2.456 ***

*** indicates $p \leq 0.001$

Confirmation of percentage viability of MCF-7 cells in response to treatment with arsenic trioxide, cobalt chloride and curcumin

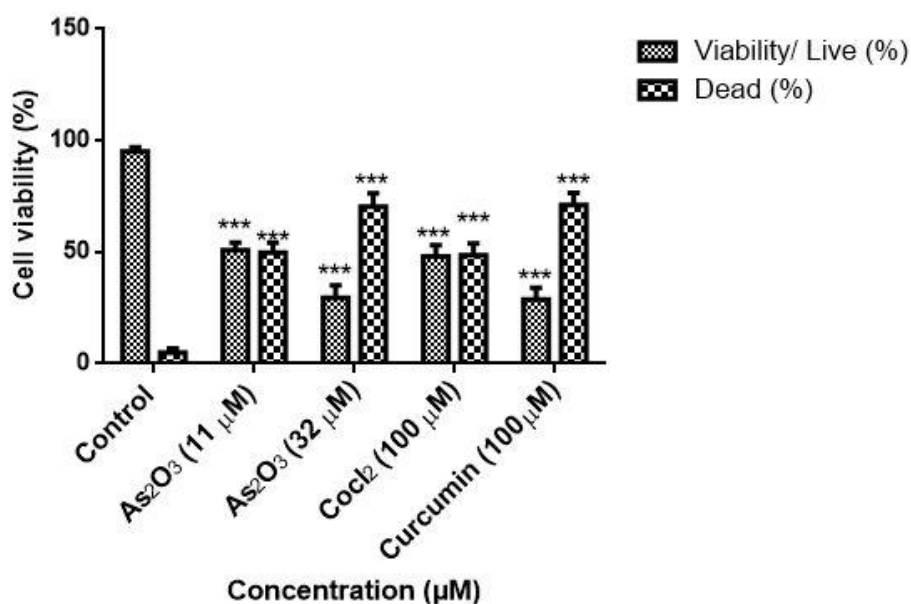


Figure 4.3: Confirmation of percentage viability of MCF-7 cells in response to treatment with arsenic trioxide, cobalt chloride and curcumin. Arsenic trioxide, cobalt chloride and curcumin significantly ($p \leq 0.001$ ***) inhibited the viability of MCF-7 cells *in vitro* when compared to the untreated control after 24 h treatment.

4.2. Morphological changes of arsenic trioxide, cobalt chloride and curcumin-treated MCF-7 cells

To investigate the mechanism of action on how arsenic trioxide, cobalt chloride and curcumin decreased the viability of MCF-7 cells, their morphology was examined (section 3.4). The treatment of the MCF-7 cells with arsenic trioxide, cobalt chloride and curcumin reduced their growth and this was evident with fewer cell numbers in treated cells compared to the untreated control. Using the inverted phase-contrast microscopy (Fig. 4.4), 11 μM arsenic trioxide (4.4b), 32 μM arsenic trioxide (4.4e), 100 μM curcumin (4.4f) and 100 μM cobalt chloride (4.4c) affected the morphology of the MCF-7 cells after 24-hour treatment with these compounds. Many cells showed typical morphological changes indicative of cells undergoing apoptosis and these include cell shrinkage (full arrow), membrane blebbing (broken arrow), formation of apoptotic bodies (broken arrow) [Fig. 4.4b, c, e and f]. There was a clear loss of the typical epithelial morphology (full arrow). On the other hand, the untreated control cells (Fig. 4.4a and d) showed intact and uniform epithelial morphology (arrow head).

Additionally, DAPI staining (section 3.4) was used to analyse and confirm morphological changes due to the exposure of the MCF-7 breast cancer cells to arsenic trioxide. Upon observation under the microscope, MCF-7 cells appeared to undergo apoptotic changes after treatment with 11 and 32 μM of arsenic trioxide as shown by nuclear condensation (broken arrow), apoptotic body formation and nuclear fragmentation (broken arrow) [Fig. 4.5b and e] but untreated cells maintained their epithelial morphology and remained attached on the culture flasks (Fig. 4.5a and d). The same trend was observed even in the positive controls (cobalt chloride and curcumin) which also reduced the number of MCF-7 cells and induced typical apoptotic morphological changes (Fig.4.5c and f). These changes suggested that arsenic trioxide is potent in inducing apoptosis in MCF-7 cells.

Light microscopic analysis of the effect of arsenic trioxide, cobalt chloride and curcumin on the morphology of MCF-7 cells

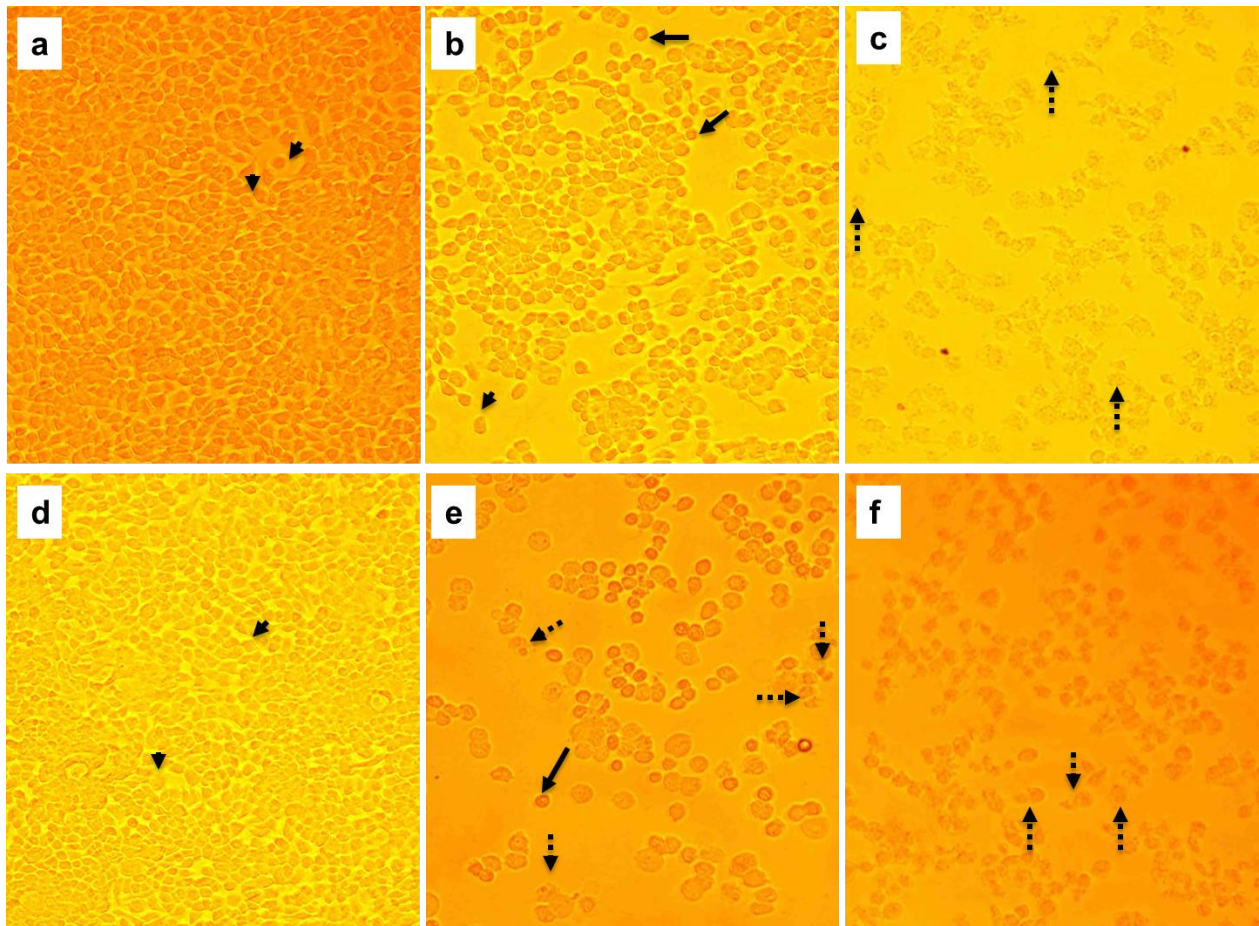


Figure 4.4 A-F Light microscopic analysis of the effect of arsenic trioxide, cobalt chloride and curcumin on the morphology of MCF-7 cells. Arsenic trioxide-induced visible apoptotic features on MCF-7 cells (4.4b and e) when compared with the untreated control cells (4.4a and d). The same trend was observed after treatment with 100 μ M of cobalt chloride (4.4c) and 100 μ M of curcumin (4.4f) as positive controls. Magnification: 20X

Fluorescence microscopic analysis of the effect of arsenic trioxide, cobalt chloride and curcumin on the morphology of MCF-7 cells

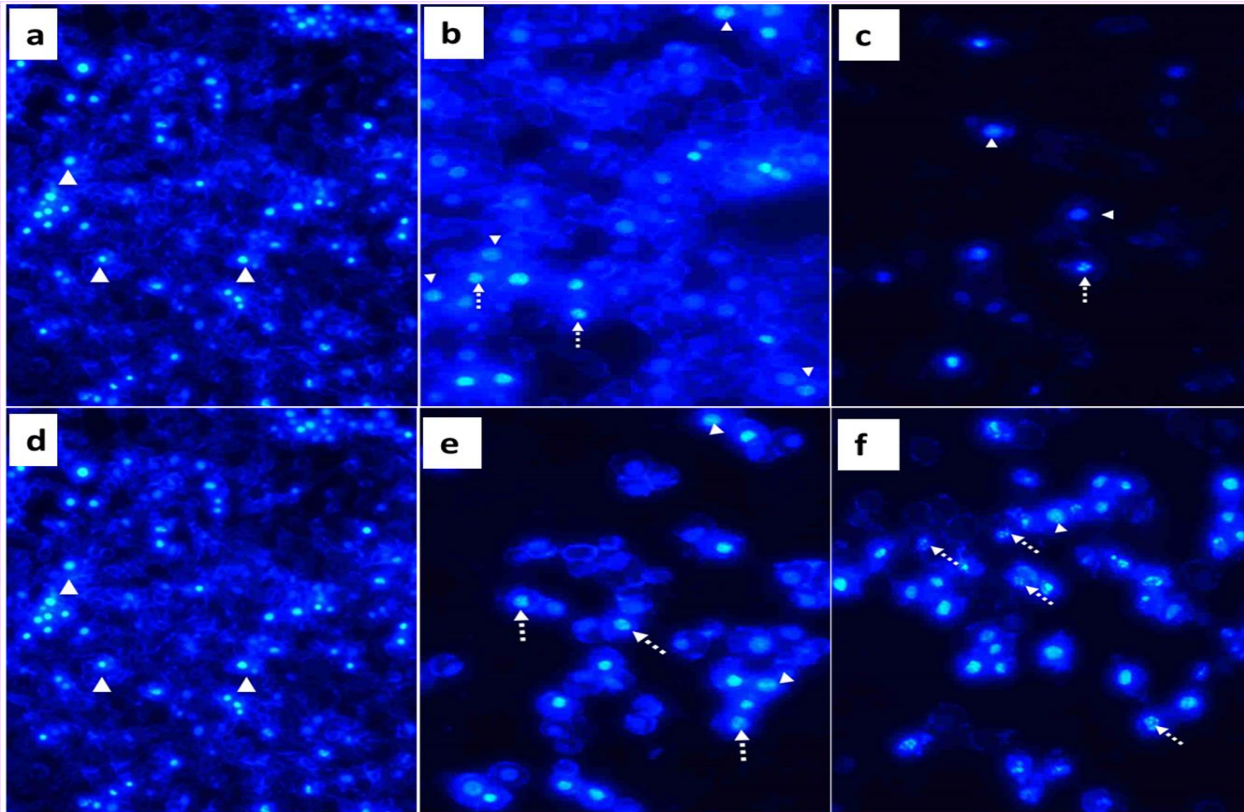


Figure 4.5. A-F: Fluorescence microscopic analysis of the effect of arsenic trioxide, cobalt chloride and curcumin on the morphology of MCF-7 cells. Arsenic trioxide (11 μM and 32 μM) induced evident apoptotic features on MCF-7 cells as shown by nuclear condensation and apoptotic body formation (4.5b and e, respectively). The same trend was observed after treatment with 100 μM of cobalt chloride (4.5c) and 100 μM of curcumin (4.5f) as positive controls. Magnification: 20X.

4.3. Arsenic trioxide induces apoptosis in MCF-7 cells

The objective of this section was to quantitatively analyse the percentage of MCF-7 cells undergoing apoptosis after arsenic trioxide treatment. The Muse™ Annexin V & Dead Cell analysis was used (section 3.5.1) and this technique substantiates results obtained from cytotoxicity assay (section 4.1) and morphology analysis (section 4.2). This assay denotes the viable cells with no apoptosis activity as “Live”, and cells with early apoptosis features as “Early Apop”, those cells that are dead and showing late apoptosis features are denoted by “Late Apop/Dead” and lastly, the cells that are dead without apoptosis activity are denoted as “Dead”. The Muse™ Annexin V & Dead Cell analysis showed that arsenic trioxide (32 μM) significantly ($*P < 0.05$) induced apoptosis in MCF-7 cells. As shown in figure 4.6, the average percentage of cells positive for apoptosis after treatment with 32 μM of arsenic trioxide was found to be 60% (Fig. 4.6B) relative to the untreated control (Fig. 4.6A). The same trend was observed in the positive control (100 μM of curcumin) cells that exhibited 61% positive cells for apoptosis (Fig. 4.6C). The same results from three independent experiments were represented graphically (Fig. 4.7) using the data summarized in table 4.7, to show that arsenic trioxide significantly ($*P < 0.05$) induced apoptosis in MCF-7 breast cancer cells.

Confirmation of arsenic trioxide induced apoptosis in MCF-7 cells

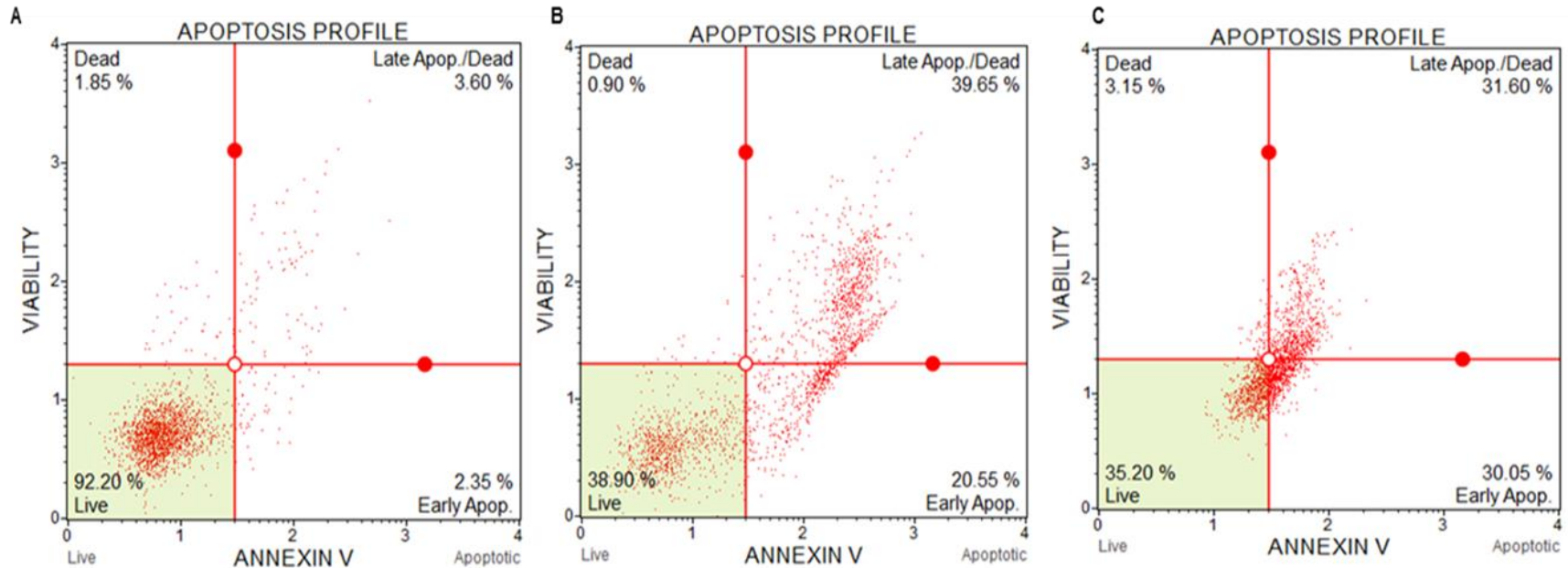


Figure 4.6 A-C: Confirmation of arsenic trioxide induced apoptosis in MCF-7 cells. The Muse™ Annexin V & Dead Cell apoptosis analysis confirmed that treatment with 32 μM of arsenic trioxide (Fig. 4.6B) and 100 μM of the positive control, curcumin (Fig. 4.6C) induced apoptosis in MCF-7 cells when compared with the untreated control (Fig. 4.6A).

Table 4.7: Apoptosis average percentages \pm SEM after the treatment of MCF-7 cells with arsenic trioxide and curcumin.

Treatments	Mean (%) \pm SEM			
	Live	Early apoptosis	Late apoptosis	Total apoptosis
Control	89.97 \pm 1.090	2.61 \pm 0.4675	4.54 \pm 0.5415	7.42 \pm 0.8845
Arsenic trioxide (32 μ M)	52.35 \pm 4.914 ^a	22.51 \pm 2.201 ^a	21.89 \pm 4.602 ^c	43.77 \pm 4.976 ^a
Curcumin (100 μ M)	48.66 \pm 7.322 ^a	18.85 \pm 3.079 ^b	34.16 \pm 6.709 ^b	50.75 \pm 7.210 ^a

a: ***($p \leq 0.001$); b: ** ($p \leq 0.01$) and c: * ($p \leq 0.05$)

Average % apoptosis in arsenic trioxide treated MCF-7 cells

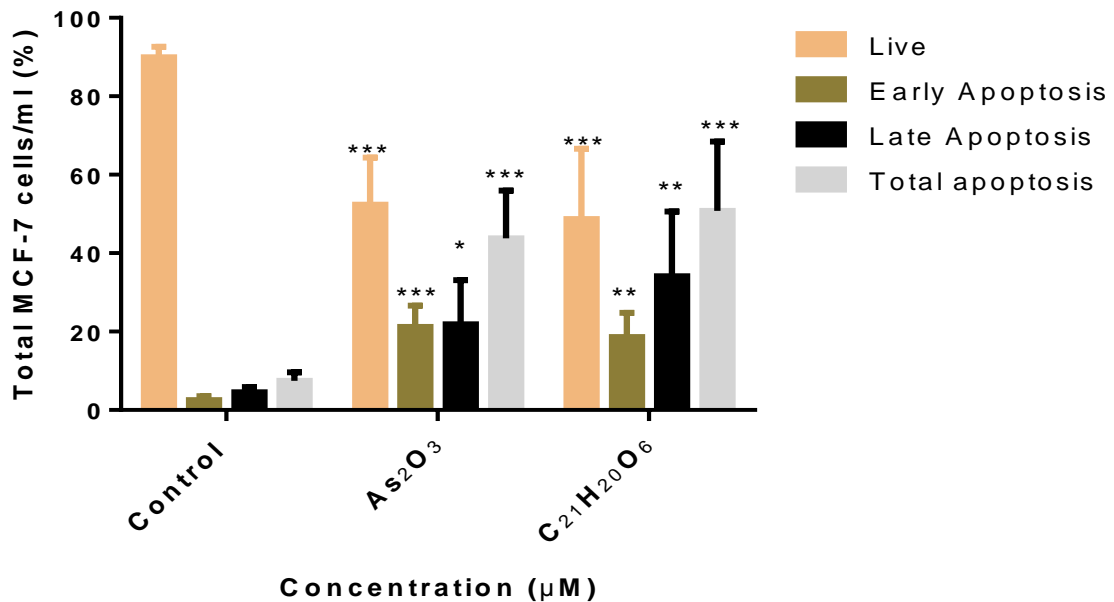


Figure 4.7: Average % apoptosis in arsenic trioxide-treated MCF-7 cells. Treatment with arsenic trioxide (32 μ M) and curcumin (100 μ M) for 24 hours significantly ($p \leq 0.05$ / $p \leq 0.01$ ** / $p \leq 0.001$ ***) induced apoptosis mode of death in MCF-7 cells relative to the untreated control.

4.4. Arsenic trioxide induces caspase-dependent apoptosis in MCF-7 cells

Several lines of evidence indicate that caspases are important for apoptosis (Zhou *et al.*, 2006). Caspase activation correlates with the onset of apoptosis and caspase inhibition attenuates apoptosis. Therefore, the involvement of caspases in arsenic trioxide-induced cell death in MCF-7 cells was investigated (section 3.5.2). This assay denotes the viable cells with no caspase activity as “Live”, and viable cells with caspase activity as “Caspase+”, those cells that are dead and still showing caspase activity are denoted as “Caspase+/Dead” and lastly, the cells that are dead without caspase activity are denoted as “Dead”. As shown in figure 4.8, the percentage of cells undergoing caspase-dependent mode of death after treatment with 32 μ M of arsenic trioxide was found to be 74% (Fig. 4.8B) compared to the untreated control (Fig. 4.8A). The same trend was observed in the positive control (100 μ M of curcumin) that showed 67% (Fig. 4.8C) of MCF-7 cells to undergo caspase dependent mode of death. The same results from three independent experiments were represented graphically (Fig. 4.9) using the data summarized in table 4.9, to show that arsenic trioxide significantly (* $P < 0.05$) induced caspase activation in MCF-7 breast cancer cells.

Confirmation of arsenic trioxide-induced caspase-dependent apoptosis in MCF-7 cells

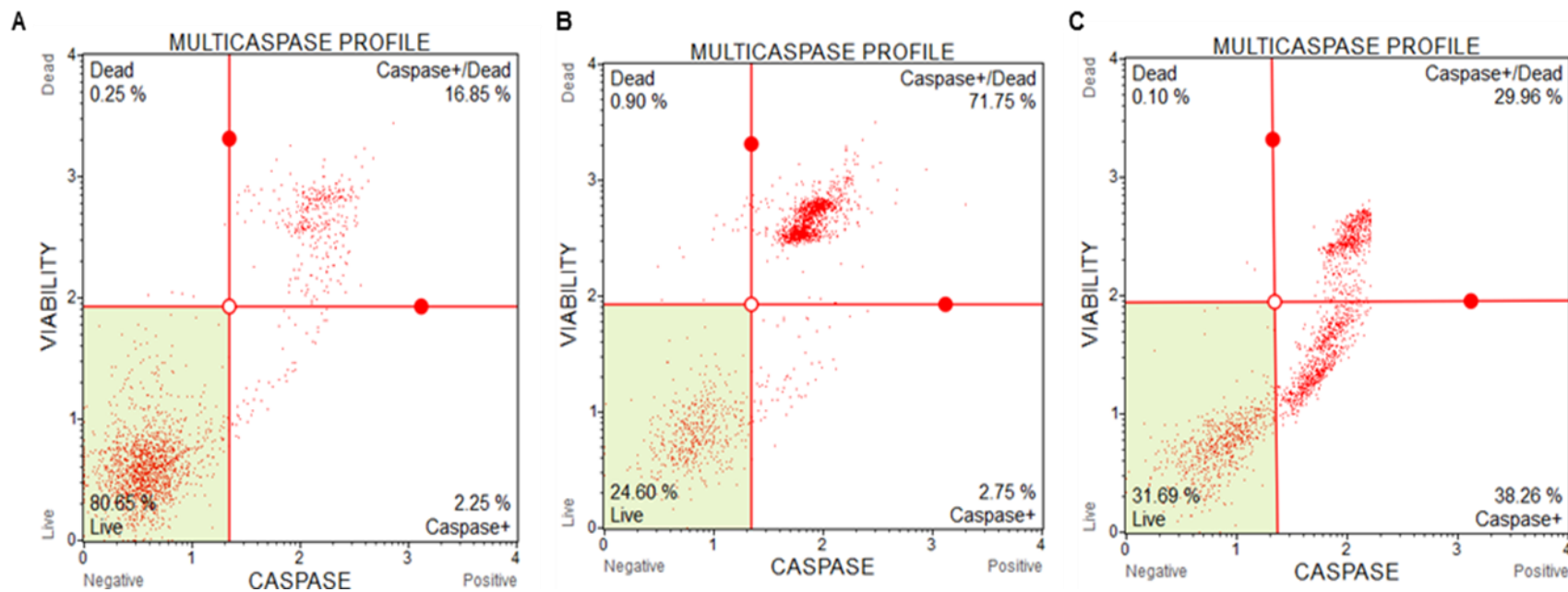


Figure 4.8 A-C: Confirmation of arsenic trioxide-induced caspase-dependent apoptosis in MCF-7 cells. The Muse™ MultiCaspase analysis confirmed that treatment with 32 μ M of arsenic trioxide (Fig. 4.8B) and 100 μ M of the positive control, curcumin (Fig. 4.8C) induced caspase-dependent mode of death in MCF-7 cells when compared with the untreated control cells (Fig.4.8A).

Table 4.9: Average percentages of caspase positive cells \pm SEM after treating the MCF-7 cells with various concentrations of arsenic trioxide and curcumin.

Mean (%) \pm SEM	Treatments		
	Control (%)	Arsenic trioxide (32 μ M) %	Curcumin (100 μ M) %
Live	81.18 \pm 5.102	37.73 \pm 5.791 ^a	23.40 \pm 6.509 ^a
Caspase+	3.15 \pm 1.120	17.42 \pm 5.143 ^c	32.96 \pm 2.091 ^b
Caspase+/Dead	21.12 \pm 7.500	44.02 \pm 4.603 ^c	43.34 \pm 5.608 ^c
Dead	0.54 \pm 0.187	0.11 \pm 0.049	0.11 \pm 0.039
Total caspase	17.48 \pm 5.401	61.44 \pm 5.911 ^a	75.96 \pm 6.491 ^a

a: ***($p \leq 0.001$); b: ** ($p \leq 0.01$) and c: * ($p \leq 0.05$)

Average % of caspase positive cells in arsenic trioxide treated MCF-7 cells

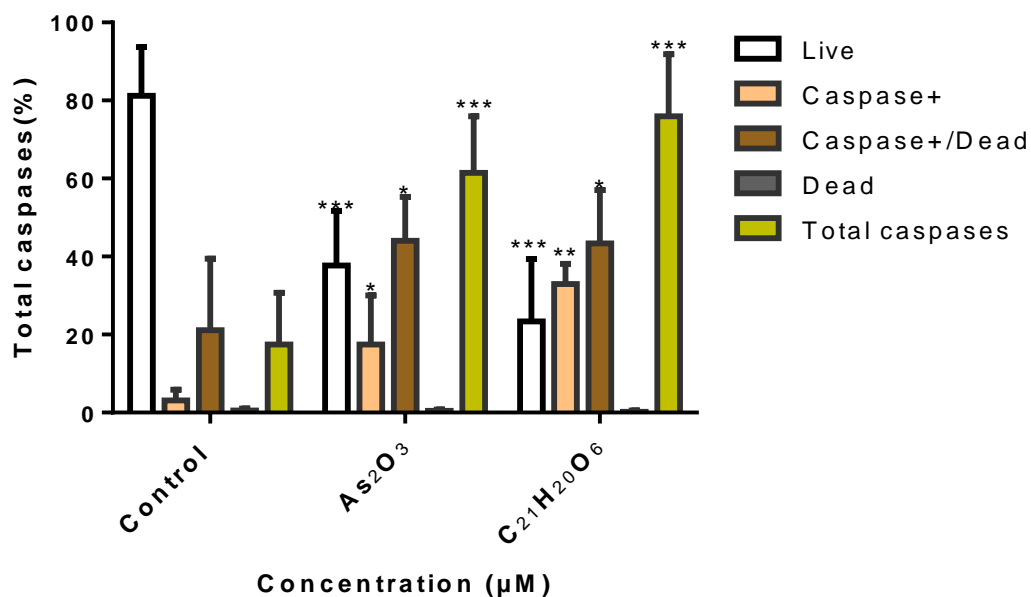


Figure 4.9: Average % of caspase positive cells in arsenic trioxide treated MCF-7 cells. Treatment with arsenic trioxide (32 μ M) and curcumin (100 μ M) for 24 hours significantly ($p \leq 0.05$ / $p \leq 0.01$ ** / $p \leq 0.001$ ***) induced caspase-dependent mode of death in MCF-7.

4.5. Arsenic trioxide induces the extrinsic apoptotic pathway in MCF-7 cells

The objective of this section was to confirm the apoptosis pathway (section 3.5.3) that is induced by arsenic trioxide in MCF-7 breast cancer cells. This technique substantiates results obtained from the apoptosis analysis (section 4.4) and caspase assay (section 4.5). The MitoPotential assay denotes the viable cells with no depolarized membrane as “Live”, and viable cells with depolarized membrane as “Depolarized/Live”, those cells that are dead and still showing depolarized membrane are denoted as “Depolarized/Dead” and lastly, the cells that are dead without depolarization are denoted “Dead”. Muse MitoPotential analysis revealed that there were undetectable percentage of cells with depolarized inner mitochondrial membrane following treatment with arsenic trioxide and the positive control (curcumin) in MCF-7 cells (Fig. 4.10 and 4.11). This suggests that arsenic trioxide induced death receptor-mediated apoptotic pathway in MCF-7 cells but not mitochondrial mediated pathway. As shown in figure 4.10, there were no MCF-7 cells dying through the intrinsic pathway after treatment with 32 μ M of arsenic trioxide (Fig.4.10B) and the same trend was observed in the untreated (Fig. 4.10A) and the positive control (curcumin) cells (Fig. 4.10C). The same results from three independent experiments were represented graphically (Fig. 4.11) using the data summarized in table 4.11, to show that arsenic trioxide significantly ($*P < 0.05$) induced extrinsic apoptotic pathway in MCF-7 breast cancer cells.

Confirmation of arsenic trioxide-induced extrinsic apoptosis pathway in MCF-7 cells

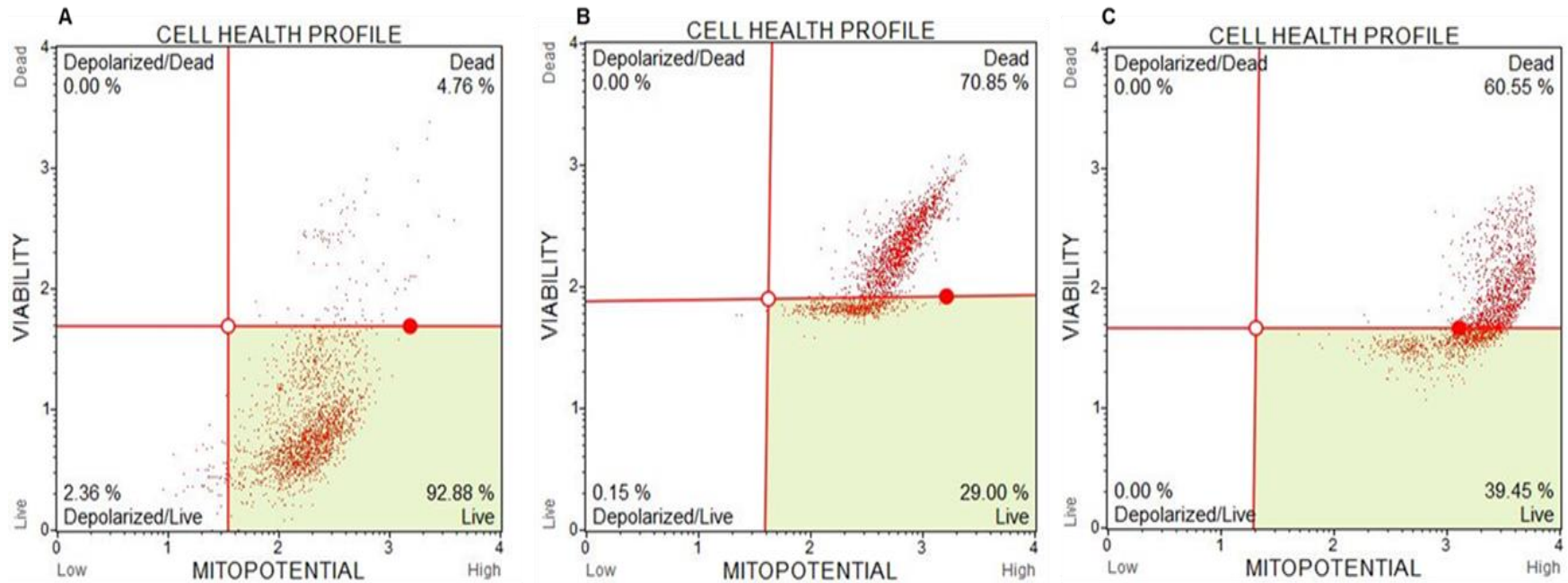


Figure 4.10 A-C: Confirmation of arsenic trioxide-induced extrinsic apoptosis pathway in MCF-7 cells. Treatment with 32 μ M of arsenic trioxide (4.10B) and 100 μ M of curcumin (4.10C) resulted in undetectable depolarization of the inner mitochondrial membrane potential and the same trend was observed even in the untreated control (4.10A).

Table 4.11: Extrinsic apoptosis average percentages \pm SEM after the treatment of MCF-7 cells with arsenic trioxide and curcumin.

Mean (%) \pm SEM	Treatments		
	Control (%)	Arsenic trioxide (32 μ M) %	Curcumin (100 μ M) %
Live	88.81 \pm 2.715	32.79 \pm 3.786 ^a	37.23 \pm 5.321 ^a
Depolarization/live	1.908 \pm 0.602	0.425 \pm 0.191 ^c	0.0600 \pm 0.0400 ^c
Depolarization/Dead	0.185 \pm 0.074	0.000 \pm 0.000 ^c	0.000 \pm 0.000 ^c
Dead	9.09 \pm 2.518	66.77 \pm 3.901 ^c	62.71 \pm 5.351 ^c
Total Depolarization	2.083 \pm 0.651	0.4250 \pm 0.191 ^a	0.060 \pm 0.040 ^a

a: ***($p \leq 0.001$) and c: * ($p \leq 0.05$)

Arsenic trioxide induced extrinsic apoptosis pathway in MCF-7 cells

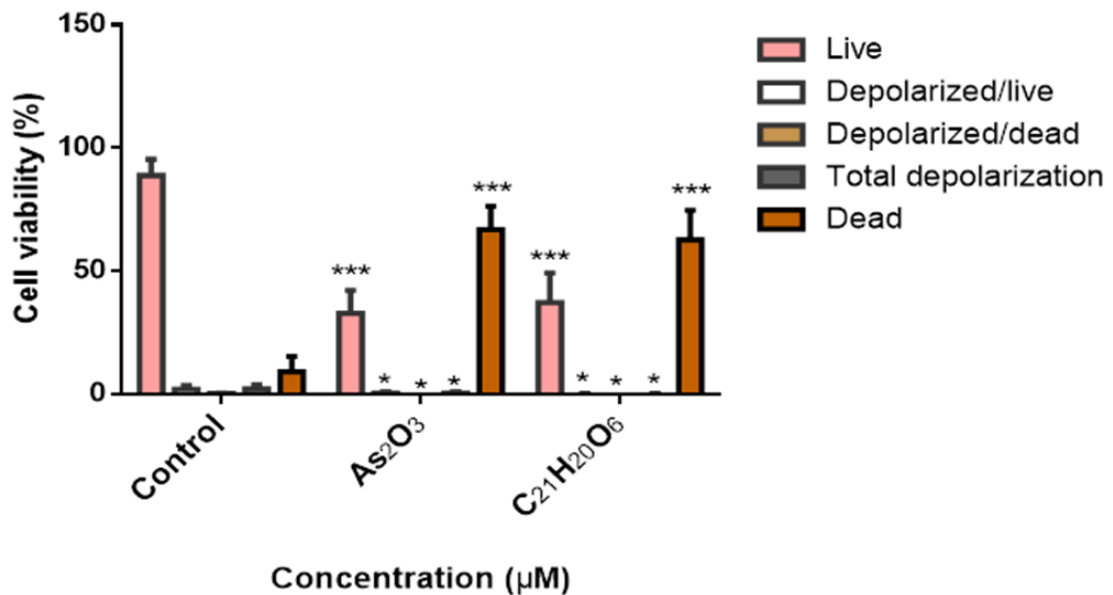


Figure 4.11: Arsenic trioxide induced extrinsic apoptosis pathway in MCF-7 cells. Treatment with arsenic trioxide (32 μ M) and curcumin (100 μ M) for 24 hours significantly ($p \leq 0.05$ / $p \leq 0.01$ ** / $p \leq 0.001$ ***) resulted in undetectable induction of mito-potential activity in MCF-7 cells relative to the untreated control. This suggests that arsenic trioxide induces extrinsic not the intrinsic apoptosis pathway in MCF-7 cells.

4.6. Arsenic trioxide induces G2/M cell cycle arrest in MCF-7 cells

To further understand how arsenic trioxide reduced the MCF-7 cell growth, cell-cycle analysis (section 3.5.4) was performed. This assay quantifies cell populations in different cell cycle phases and check points. The effect of As_2O_3 and the cell cycle arrest positive control, cobalt chloride, on MCF-7 cells was observed. Both inducers arrested the MCF-7 cells at G2/M cell cycle phase, the treatment with 11 μM of arsenic trioxide showed an increase in the population of cells at G2/M phase after 24 h and decreased the S phase population (Fig 4.12B) relative to the untreated control (Fig 4.12A). This trend was also observed for the treatment with the positive control, 100 μM cobalt chloride (Fig. 4.12C). The same results from three independent experiments were represented graphically (Fig. 4.13) using the data summarized in table 4.13, to show that arsenic trioxide significantly ($*P < 0.05$) induced G2/M cell cycle arrest in MCF-7 breast cancer cells.

Cell cycle analysis of arsenic trioxide treated in MCF-7 cells

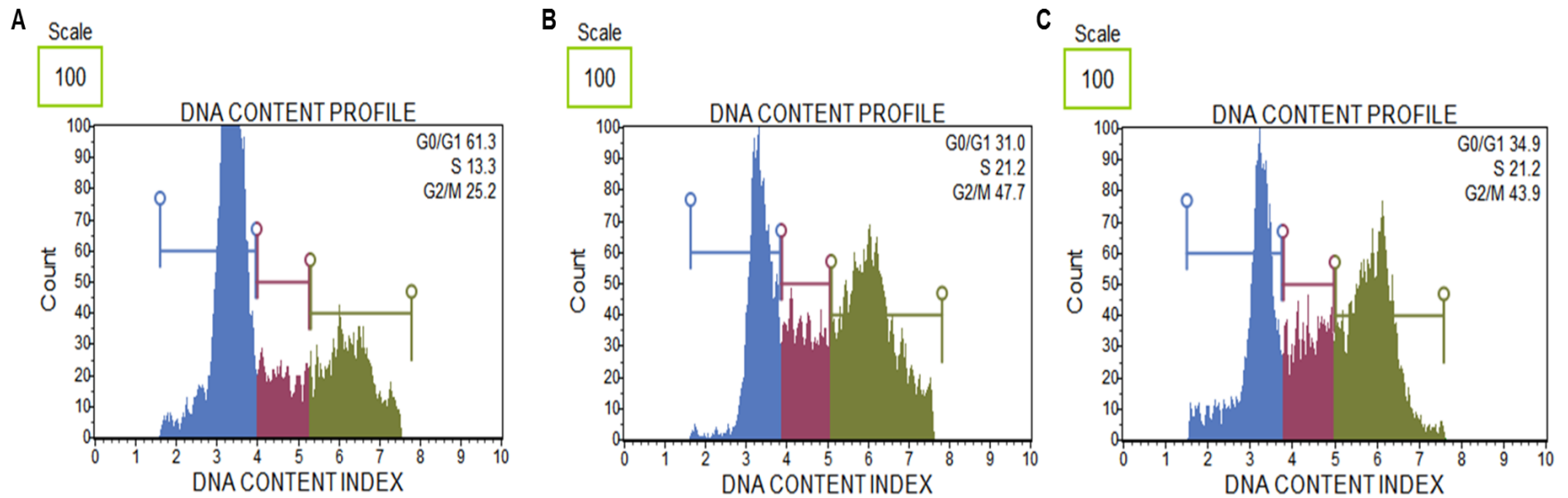


Figure 4.12 A-C: Cell cycle analysis of arsenic trioxide treated MCF-7 cells. The treatment with arsenic trioxide (4.12B) and cobalt chloride (4.12C) induced G2/M cell cycle arrest in MCF-7 breast cancer cells as compared with the untreated cells (4.12A).

Table 4.13: Average percentages of cell populations \pm SEM after treating the MCF-7 cells with arsenic trioxide and cobalt chloride.

Treatments	Mean (%) \pm SEM		
	G0/G1	S	G2/M
Control	56.23 \pm 2.531	14.13 \pm 0.938	26.75 \pm 2.057
Arsenic trioxide (11 μ M)	30.60 \pm 0.787 ^{***}	23.85 \pm 0.952 ^{***}	45.13 \pm 0.942 ^{***}
Cobalt chloride (100 μ M)	43.75 \pm 3.079 ^{**}	22.58 \pm 0.974 ^{***}	36.45 \pm 1.536 ^{**}

*** indicates $p \leq 0.001$ and ** indicates $p \leq 0.01$

Analysis of arsenic trioxide-induced G2/M cell cycle arrest in MCF-7 breast cancer cells

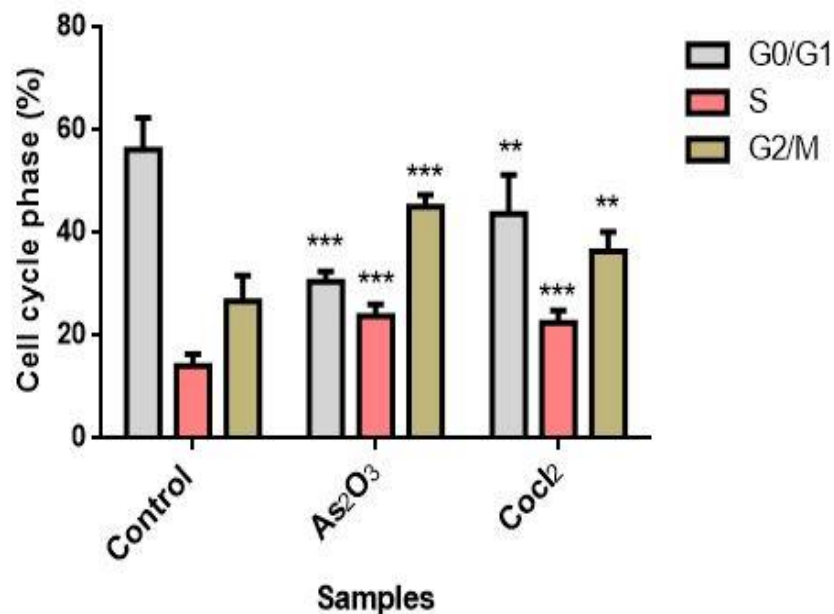


Figure 4.13: Analysis of arsenic trioxide-induced G2/M cell cycle arrest in MCF-7 breast cancer cells. The treatment with arsenic trioxide (11 μ M) and cobalt chloride (100 μ M) significantly ($p \leq 0.05$ / $p \leq 0.01$ ** / $p \leq 0.001$ ***) showed an increase in the number of cells found at the G2/M arrest relative to the untreated MCF-7 cells.

4.7. The effect of arsenic trioxide on the expression of RBBP6 splice transcripts

Genetic information is stored as deoxyribonucleic acid (DNA) within the nucleus of each cell. This genetic information is transcribed into mRNA and translated into functional proteins. Mutation of normal cellular genes plays a role in causing tumours. Regulation of genes such as RBBP6 in MCF-7 breast cancer cells is not fully understood, therefore this study was aimed at determining the expression patterns of RBBP6 alternatively spliced variants during arsenic trioxide-induced cell cycle arrest and apoptosis in breast cancer cells. Messenger RNA (mRNA) levels of RBBP6 transcripts in MCF-7 cells treated with arsenic trioxide (11 and 32 μM), curcumin (100 μM) and cobalt chloride (100 μM) for 24 hours were analysed using conventional PCR (section 3.9) to determine which RBBP6 variant can be implicated in the observed arsenic trioxide-induced cell cycle arrest and apoptosis. As shown in figure 4.14A (lane 1), untreated MCF-7 cells were observed to highly express the RBBP6 variant 1 when compared to the treated MCF-7 cells. Arsenic trioxide-, cobalt chloride-induced cell cycle arrest and arsenic trioxide- and curcumin-induced apoptosis downregulated the expression of RBBP6 variant 1. However, all these compounds did not induce detectable levels of variant 2 (lanes 2-5 in Fig. 4.14A). Glyceraldehyde 3-phosphate dehydrogenase (GAPDH) was used as a loading control to ascertain that equal amounts of the cDNAs from untreated and treated samples were used (Fig. 4.14B). Fig. 4.14C (lanes 1-3) showed that normal cells (Hek 293 cells) express both variant 1 and 2 with the later down-regulated in breast cancer MCF-7 cells. The PCR results quantified from three independent experiments using Quantity One® 1-D analysis software showed that the band density of RBBP6 variant 1 increased in untreated MCF-7 cells and downregulated by arsenic trioxide treatment (Fig. 4.15 and table 4.15). The results further show that RBBP6 variant 2 in both untreated and treated MCF-7 cells was undetectable.

Expression analysis of RBBP6 variant 1 and 2 in arsenic trioxide-treated MCF-7 cells and untreated Hek 293 cells

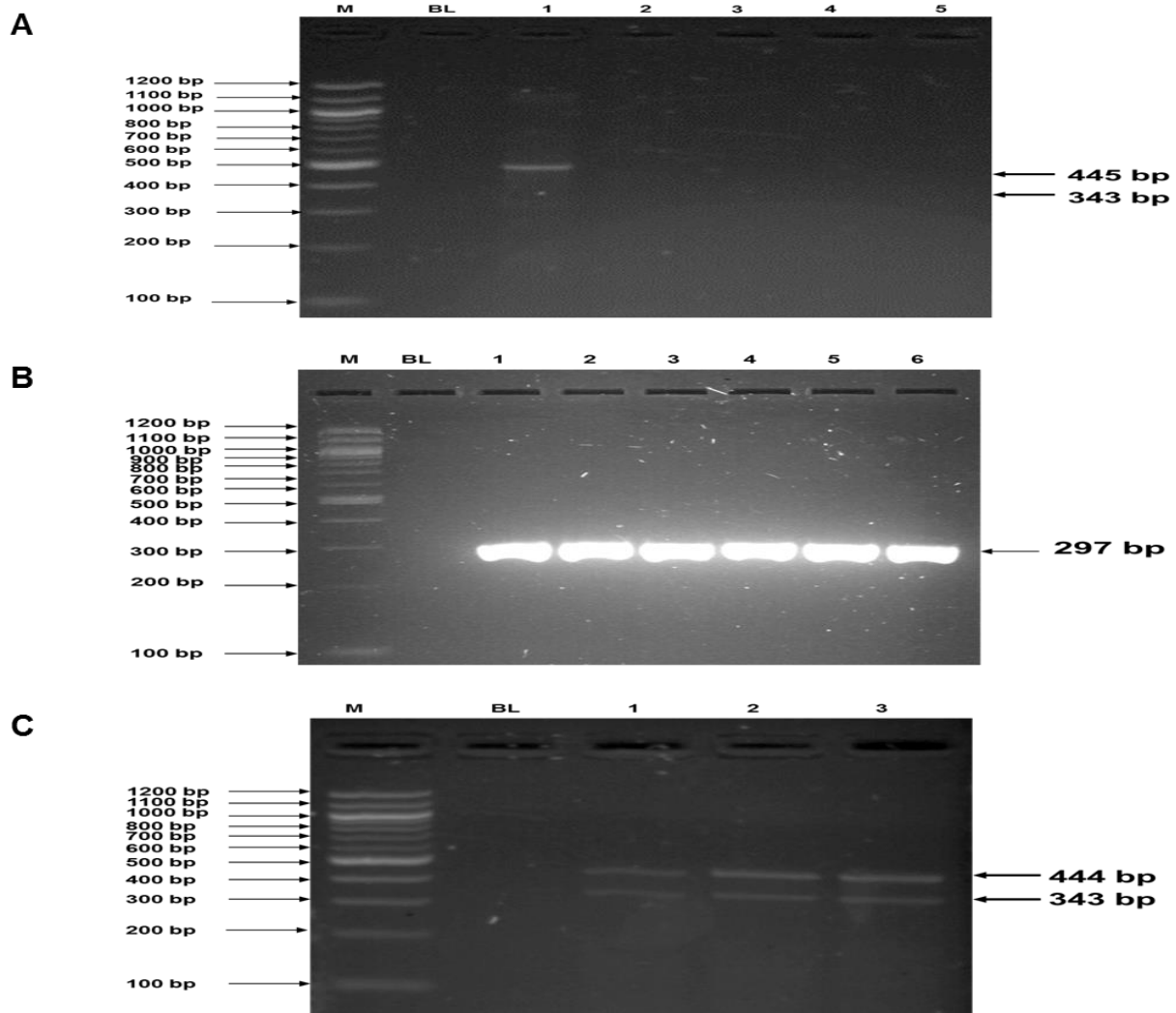


Figure 4.14 A-C: Expression analysis of RBBP6 variant 1 and 2 in arsenic trioxide-treated MCF-7 cells and untreated Hek 293 cells. Figure 4.14A shows the untreated MCF-7 cells (lane 1) expressing variant 1, treatment with 11 μM of As_2O_3 (lane 2), treatment with 32 μM of As_2O_3 (lane 3), treatment with 100 μM cobalt chloride (lane 4) and lastly, treatment with 100 μM curcumin (lane 5), all showing repressed expression of variant 1. Figure 4.14B (lanes 1-6) represents GAPDH that was used as a loading control. Lanes M stands for the molecular weight marker while lanes BL were blank controls. Fig. 4.14C (lanes 1-3) shows the expression of both variants 1 and 2 by the untreated Hek 293 cells.

Table 4.15: Average band densities of GAPDH and RBBP6 variant 1 and 2 \pm SEM for PCR analysis in MCF-7 and Hek 293 cells.

Treatments	Mean (%) \pm SEM		
	RBBP6 variant 1	RBBP6 variant 2	GAPDH
Control	244.67 \pm 16.45***	Undetectable	751.0 \pm 51.39
As ₂ O ₃ (11 μ M)	Undetectable	Undetectable	668.0 \pm 36.36
CoCl ₂ (100 μ M)	Undetectable	Undetectable	699.6 \pm 30.44
As ₂ O ₃ (32 μ M)	Undetectable	Undetectable	649.6 \pm 57.17
C ₂₁ H ₂₀ O ₆ (100 μ M)	Undetectable	Undetectable	699.6 \pm 49.67
Hek-293 cells	256.00 \pm 9.018***	210.33 \pm 11.865***	607.3.6 \pm 27.71

*** indicates $p \leq 0.001$

Analysis of RBBP6 variant 1 and 2 band densities in MCF-7 and Hek-293 cells

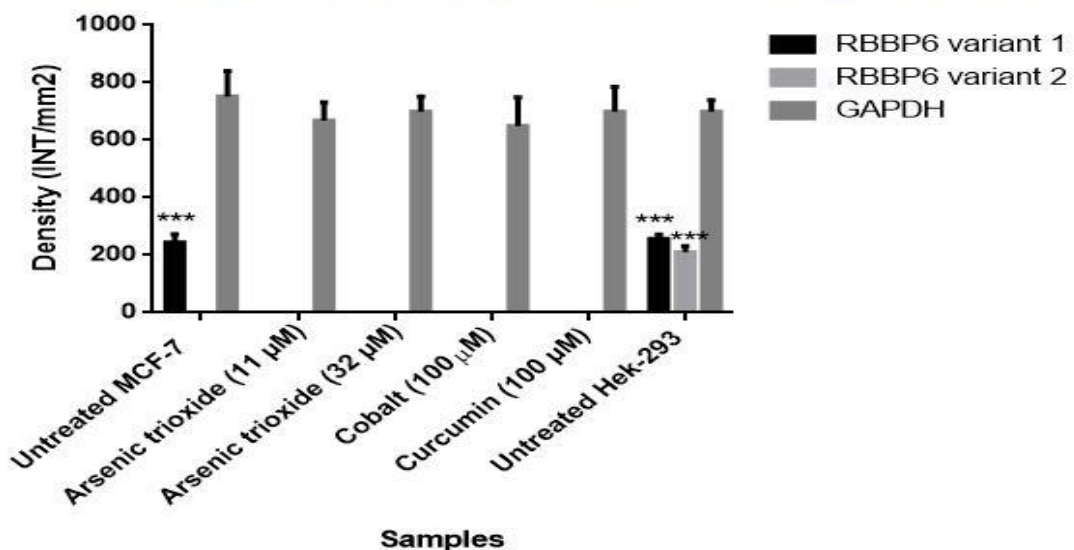


Figure 4.15: Analysis of RBBP6 variant 1 and variant 2 band densities in MCF-7 and Hek-293 cells. Untreated MCF-7 cells significantly ($p \leq 0.001$ ***) show increased band intensity of the RBBP6 variant 1 which diminished after treatment with arsenic trioxide, cobalt chloride and curcumin. Untreated MCF-7 cells didn't show any expression of RBBP6 variant 2, with only untreated Hek-293 cells showing detectable levels of both RBBP6 variant 1 and 2.

The mRNA levels of RBBP6 variant 3 in breast cancer MCF-7 cells and normal embryonic kidney, Hek 293 cells were also investigated using conventional PCR. Figure 4.16A shows that the RBBP6 variant 3 is expressed by normal embryonic kidney cells but not by the breast cancer cells. The blank controls (Fig. 4.16, lanes BL) showed no product as expected. The untreated Hek 293 cells (Fig. 4.16A, lane 3) showed expression of the RBBP6 variant 3 while RBBP6 variant 3 was undetectable in MCF-7 cells (Fig. 4.16A, lane 1) and in Caski cells (Fig. 4.16A, lane 2). The PCR results quantified from three independent experiments using Quantity One® 1-D analysis software showed that the band density of the RBBP6 variant 3 has increased in untreated Hek-293 cells and undetected in untreated MCF-7 and Caski cells (Fig. 17 and table 17). In summary, both RBBP6 variant 2 and 3 were undetectable in cancer cells, especially breast cancer MCF-7 cells. This suggests that both variants 2 and 3 may be crucial in maintaining cell homeostasis, which is lost during carcinogenesis while the expression of variant 1 may favour the carcinogenesis process.

Expression analysis of RBBP6 variant 3 in untreated MCF-7 cells, Caski cells and Hek 293 cells

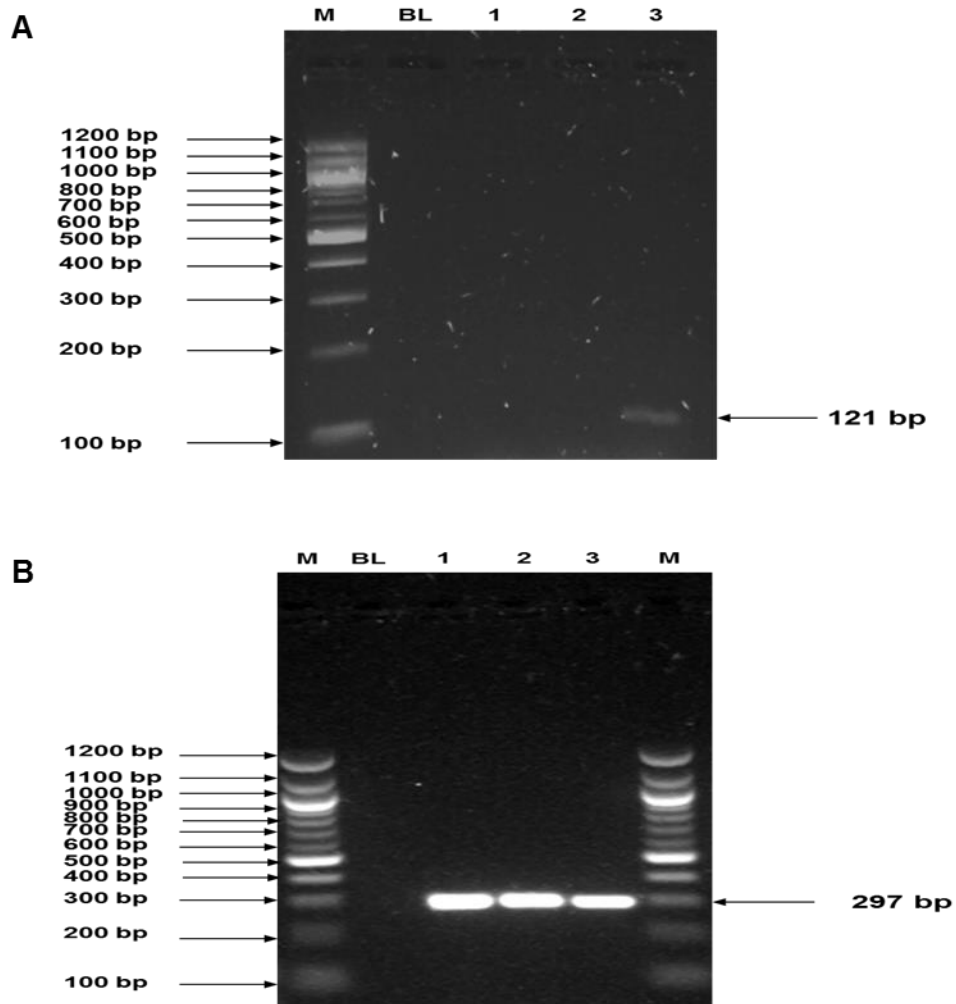


Figure 4.16 A-B: Expression analysis of RBBP6 variant 3 in untreated MCF-7 cells, Caski cells and Hek 293 cells. The results (Fig. 4.16A) show untreated MCF-7 cells (lane 1), untreated Caski cells (lane 2) both showing undetectable level of RBBP6 variant 3 respectively. Only untreated Hek-293 cells (lane 3) show amplification of RBBP6 variant 3. Figure 4.16B (lanes 1-3) represents GAPDH that was used as a loading control. Lanes M stand for the molecular weight marker while lanes BL were the blank controls, which showed no amplification as expected.

Table 4.17: Average band densities of RBBP6 variant 3 and GAPDH \pm SEM for PCR analysis in MCF-7 cells, Caski and Hek-293 cells.

Samples	Mean (%) \pm SEM	
	RBBP6 variant 3	GAPDH
Untreated MCF-7 cells	Undetectable	538.0 \pm 45.78
Untreated Caski cells	Undetectable	601.6 \pm 47.41
Untreated Hek-293 cells	305.3 \pm 22.10**	554.6 \pm 31.86

** indicates $p \leq 0.01$

Analysis of RBBP6 variant 3 band densities in MCF-7, Caski and Hek-293 cells

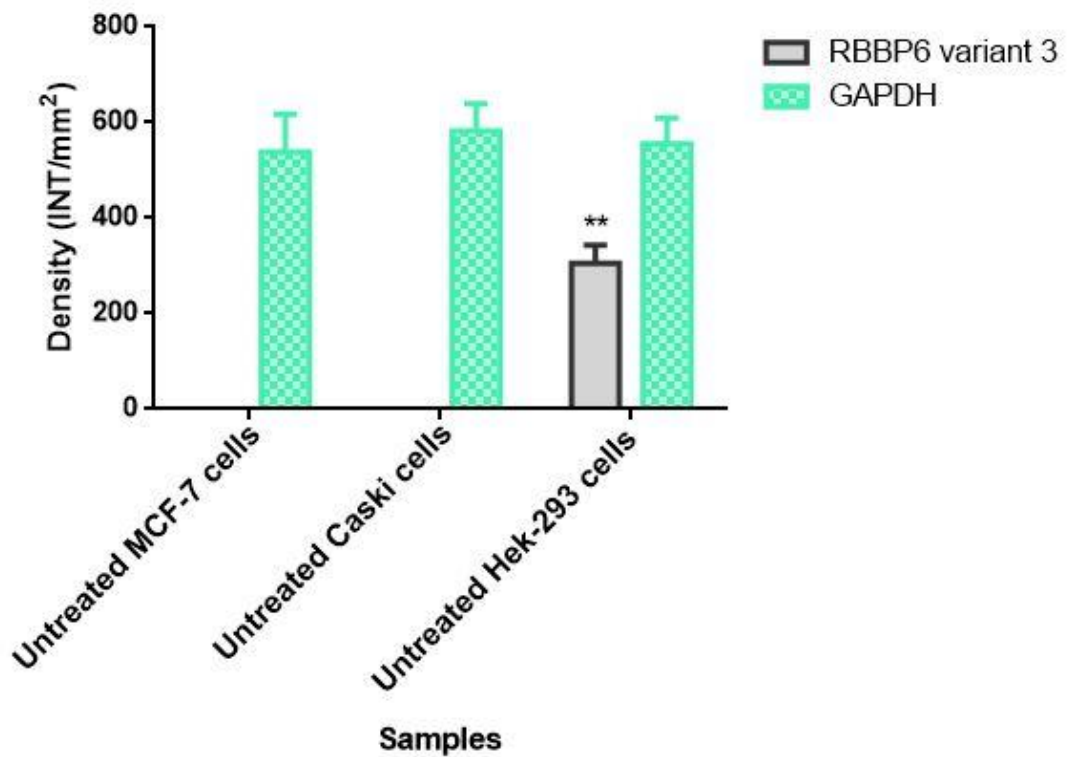


Figure 4.17: Analysis of RBBP6 variant 3 band densities in MCF-7, Caski and Hek-293 cells. Both untreated MCF-7 and Caski cells had undetectable expression of RBBP6 variant 3, only untreated Hek-293 cells show detectable levels of RBBP6 variant 3.

4.8. Quantitative Real-Time PCR analysis of RBBP6 variant 3 (DWNN) in MCF-7 and Hek-293 cells

Real Time PCR (section 3.10) was used to analyse the expression levels of RBBP6 variant 3 in untreated MCF-7 cells and Hek-293 cells. Relative real-time PCR using equal amounts of cDNA prepared from the two cell lines as a starting template showed that Hek 293 (non-cancerous kidney embryonic cells) had a higher expression of RBBP6 variant 3 than MCF-7 (breast cancer cells). The relative expression of RBBP6 variant 3 mRNA was calculated using the comparative threshold cycle (Ct) method, a variation of Livak and Schmittgen's (2001) method. The expression was normalized using GAPDH as a house keeping gene, using the relative expression formula:

$$\text{Ratio (reference/target)} = 2^{\text{Ct (Reference)} - \text{Ct (Target)}}$$

Table 4.18A shows the average RBBP6 variant 3 Ct values normalized with GAPDH and delta Ct values for Hek-293 cells and MCF-7 cells. This table further shows the calculated relative expression of RBBP6 variant 3 in Hek 293 and MCF-7 cells. The MCF-7 cells were found to have low expression of RBBP6 variant 3 (0.00017) as compared to Hek-293 cells (0.0039) [table 4.18A]. The results from three independent experiments were represented graphically (Fig. 4.18) using the data summarized in table 4.18B, to show that the expression of RBBP6 variant 3 is significantly (*P < 0.05) higher in Hek-293 cells than in MCF-7 cells. These results emphasize the important role of RBBP6 variant 3 in cell growth inhibition and cell cycle arrest as previously shown in Hek-293 cells (Mbita *et al.*, 2012).

Table 4.18A: Relative expression of RBBP6 variant 3 normalized using GAPDH.

Cell lines	RBBP6 variant 3 Av Ct	GAPDH Av Ct	Delta Ct	Relative expression
MCF-7	25.5	13	-12.5	0.00017
Hek-293	21.5	13.5	-8	0.0039

Table 4.18B: RBBP6 variant 3 relative expression average percentages \pm standard error of the mean (SEM) in MCF-7 and Hek-293 cells.

Treatments	Relative expression (%) \pm SEM
	RBBP6 variant 3
Untreated MCF-7 cells	0.000170 \pm 0.0000057
Untreated Hek-293 cells	0.003900 \pm 0.0005859**

** indicates $p \leq 0.01$

Quantitative analysis of the expression of RBBP6 variant 3 in untreated MCF-7 and Hek-293 cells

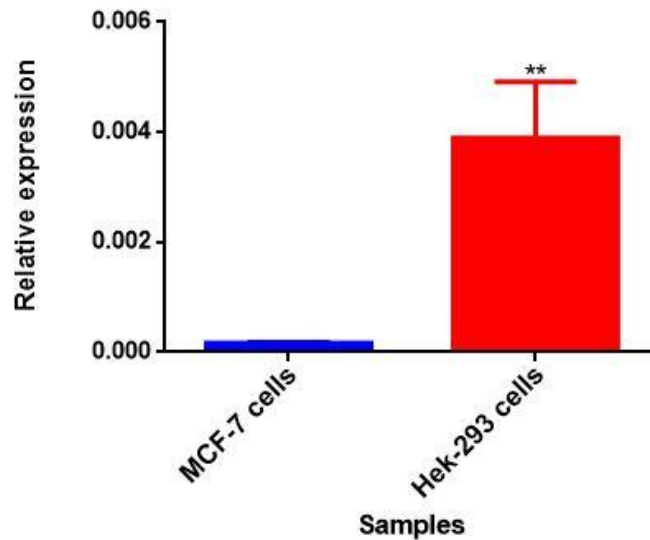


Figure 4.18: Quantitative analysis of the expression of RBBP6 variant 3 in untreated MCF-7 and Hek-293 cells. The results show the relative expression of the RBBP6 variant 3 using the optimised real-time PCR (Appendix C) in MCF-7 and Hek-293 cells. The RBBP6 variant 3 data was normalized to that of GAPDH as a house keeping gene. RBBP6 variant 3 is highly expressed in Hek-293 cells than in MCF-7 cells.

4.9. Immunocytochemistry analysis

In this section, RBBP6 protein localization and expression was investigated using immunocytochemistry (section 3.11). Immunocytochemistry is a technique used to assess the presence of a specific protein or proteins by the use of a specific antibody, which binds to it, thereby allowing visualization and examination under a microscope. In this study, RBBP6 antibody that detects the RBBP6 isoform 1, 2 and 4 was used. It is important to know the localization of the RBBP6 protein in order to be able to understand its cellular function. The results below as supported by PCR (Fig. 4.14A) reveal that RBBP6 isoform 1 but not isoform 2 is detected in untreated MCF-7 cells. The positive staining in the treatment samples is likely to show the detection of RBBP6 isoform 4 but not RBBP6 isoform 1 or 2, since PCR (Fig.4.14A) revealed that MCF-7 cells do not express isoform 2 and upon treatments, RBBP6 variant 1 becomes downregulated. Protein localization demonstrated that the RBBP6 protein is confined to the nucleus and cytoplasm of mitotic cells (Fig. 4.19). Untreated MCF-7 cells show the expression of RBBP6 isoform 1 (C and D), the treatments with 11 μ M of arsenic trioxide (E and F), 32 μ M of arsenic trioxide (I and J), 100 μ M of cobalt chloride (G and H) and 100 μ M of curcumin (K and L) are likely to show the detection of RBBP6 isoform 4. The ICC results quantified from three independent experiments using the ImageJ software were represented graphically (Fig. 4.20) using the data summarized in table 4.20, to show the localization of RBBP6 isoform 1 in untreated MCF-7 cells, and the localization of possible RBBP6 isoform 4 in treated MCF-7 cells.

Localization of RBBP6 isoform 1, 2 and 4 in MCF-7 cells

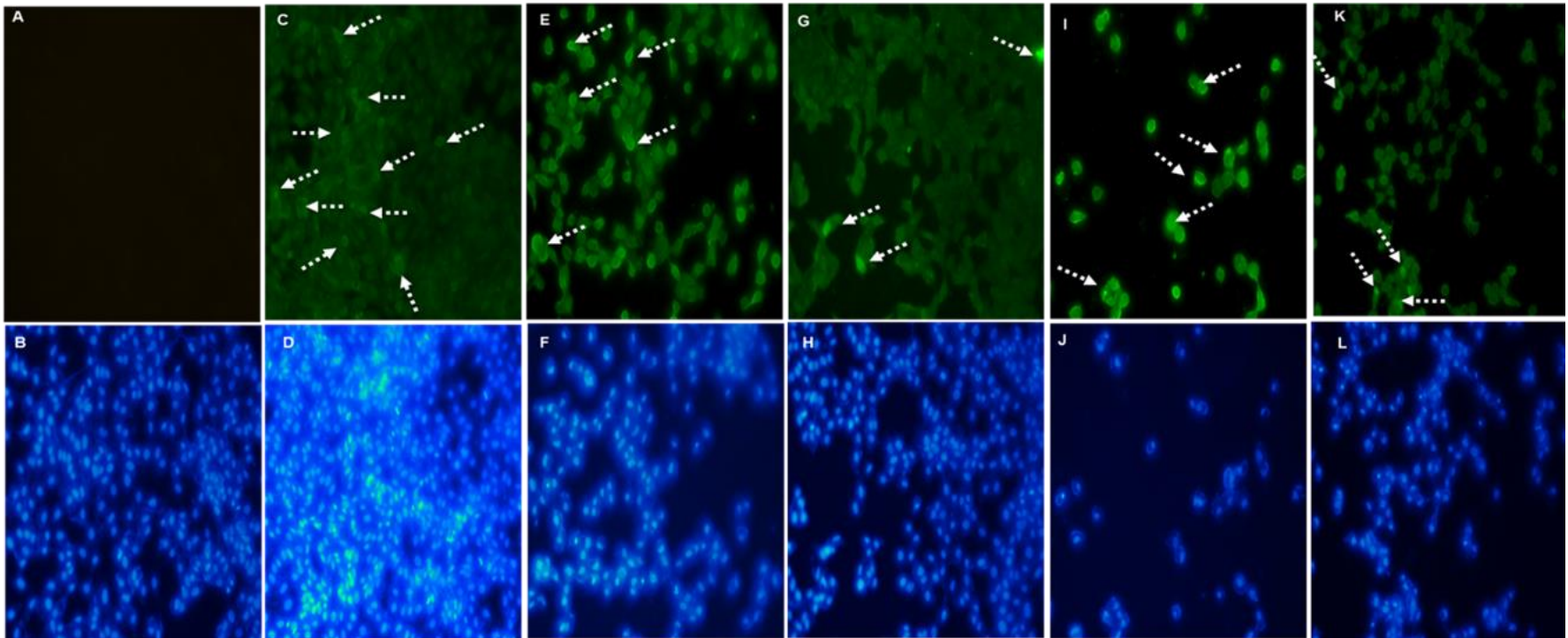


Figure 4.19 A-L: Localization of RBBP6 isoform 1, 2 and 4 in MCF-7 cells. The results show a negative control (A and B), no labelling is seen. Micrographs (C-L) show positive RBBP6 staining in the nucleus and cytoplasm. MCF-7 cells show the expression of RBBP6 isoform 1 in untreated cells (C and D) while RBBP6 isoform 4 expression may be detected upon treatment with 11 μM of arsenic trioxide (E and F), 32 μM of arsenic trioxide (I and J), 100 μM of cobalt chloride (G and H) and lastly 100, μM of curcumin (K and L). White dotted arrow points to mitotic cells with increased RBBP6 staining levels. Magnification: 20x

Table 4.20: Average fluorescence intensities \pm standard error of the mean (SEM) in MCF-7 cells for ICC analysis.

Treatments	Fluorescence intensity average (%) \pm SEM
	RBBP6
Control	21.24 \pm 1.705
Arsenic trioxide (11 μ M)	37.89 \pm 2.662**
Cobalt chloride (100 μ M)	8.85 \pm 0.998***
Arsenic trioxide (32 μ M)	41.00 \pm 3.512**
Curcumin (100 μ M)	34.05 \pm 2.515***

*** indicates $p \leq 0.001$ and ** indicates $p \leq 0.01$

Analysis of fluorescence intensities for the detection of RBBP6 isoform 1, 2 and 4 in MCF-7 cells

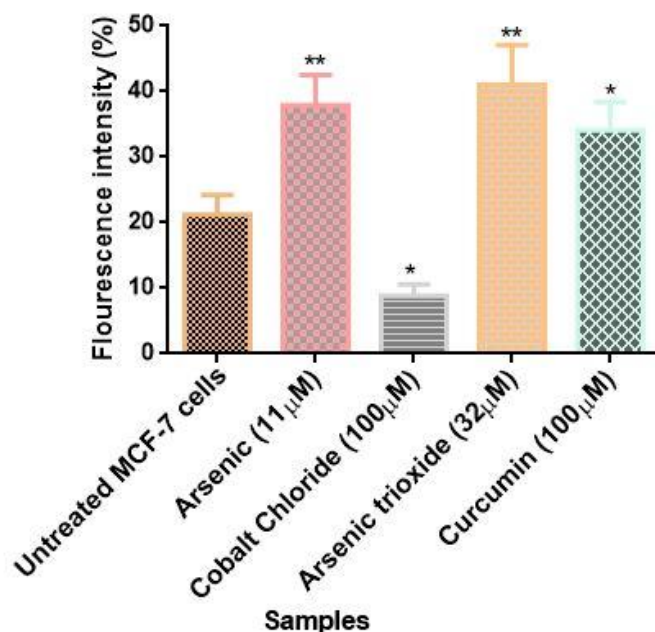


Figure 4.20: Analysis of fluorescence intensities for the detection of RBBP6 isoform 1, 2 and 4 in MCF-7 cells. The presence of fluorescence in untreated MCF-7 cells shows the localization of RBBP6 isoform 1, the increased fluorescence intensity in arsenic trioxide treated cells is likely to show the localization of RBBP6 isoform 4 but not RBBP6 isoforms 1 nor 2.

4.10. Predicted RBBP6 specific microRNAs analysis in MCF-7 breast cancer cells

Altered expression of different miRNAs has been demonstrated to play a key role in cancer development and progression (table 4.21), as well as in drug resistance (Yang *et al.*, 2013). Therefore, it was important to predict microRNAs targeting RBBP6, and also to check their expressions in MCF-7 breast cancer cells (section 3.12). The bioinformatics tools showed that Hsa-miR-195-5p and Hsa-miR-15a-5p microRNAs are specific to RBBP6 variant 1 (table 4.22). These microRNAs have been shown to be down regulated in MCF-7 breast cancer cells (table 4.23), allowing the enhanced expression of the RBBP6 variant 1 which will support the rapid growth of the breast cancer cells. At present, not much is known about the microRNAs targeting RBBP6 variant 2 and 3. The findings of this section suggest that Hsa-miR-195-5p and Hsa-miR-15a-5p microRNAs can be used as biomarkers for the detection of breast cancer.

Table 4.21: RBBP6 specific microRNAs regulated in cancer

Target gene	MicroRNA	Cancer type	Regulation	Reference
RBBP6	Hsa-miR-223	Cervical cancer	Up regulated	McBee <i>et al.</i> , 2011;
RBBP6	Has-miR-182-5p	Liver metastatic cancer	Up regulated	Huynh <i>et al.</i> , 2011
RBBP6	Hsa-miR-424	Cervical cancer	Down regulated	Varghese <i>et al.</i> , 2018

Table 4.22: Different bioinformatics tools predicting RBBP6 variant 1 specific miRNAs.

miRNA	TarBase v.8	miRDB.org	miRbase
Hsa-miR-15a-5p	√	√	√
Hsa-miR195-5p	√	√	√

√: Retrieved from

Table 4.23: The involvement of RBBP6 specific miRNAs in breast cancer.

Target gene	MicroRNA	Cell line	Regulation	Reference
RBBP6 (variant 1)	Hsa-miR-195-5p	MCF-7	Down regulated	Li <i>et al.</i> , 2011; Yang <i>et al.</i> , 2013
RBBP6 (variant 1)	Has-miR-15a-5p	MCF-7	Down regulated	Yang <i>et al.</i> , 2010; Luo <i>et al.</i> , 2013

CHAPTER FIVE: DISCUSSION AND CONCLUSION

5.0. Introduction

Apoptosis is the best studied mechanism by which many anticancer agents such as arsenic trioxide, cobalt chloride and curcumin induce cell death. These agents (arsenic trioxide, cobalt chloride and curcumin) may also induce cell cycle arrest (Li *et al.*, 2009). Therefore, it is important to understand the molecular and signalling pathways that are activated by arsenic trioxide which was reported to possess anti-proliferative effects and to induce G2/M arrest and enhances chk2/p53 mediated apoptosis in the study by Yoda *et al.* (2008). The regulation of apoptosis by genes such as RBBP6 is not fully understood in MCF-7 breast cancer cells. After many years subsequent to its discovery, RBBP6 has not been implicated in MCF-7 breast cancer development. Therefore, this study aimed at determining the expression patterns of RBBP6 alternatively spliced variants during arsenic trioxide-induced cell cycle arrest and apoptosis in MCF-7 breast cancer cells. This study showed that RBBP6 splice variants are regulated in arsenic trioxide treated MCF-7 breast cancer cells. It also showed that arsenic trioxide induces apoptosis and G2/M cell cycle arrest in MCF-7 cells.

Arsenic trioxide is a Food and Drug Administration (FDA) approved drug for the treatment of acute myeloid leukaemia called acute promyelocytic leukaemia (APL) [Sanz *et al.*, 2005]. It works by speeding up the death of leukemic cells and encouraging normal blood cells to develop properly (Lengfelder *et al.*, 2012). Arsenic trioxide hinders cancer development and progression through targeting cellular pathways, leading to inhibition of cell proliferation and invasion, and promoting apoptosis. The controlled release (CR) of arsenic trioxide to the specific site on the cancerous cells at the therapeutically optimal rate has been a major goal in minimizing side effects of many cancers such as breast cancer. Therefore, this study targeted arsenic trioxide to treat breast cancer by regulating RBBP6 splice variants.

5.1. Arsenic trioxide inhibits MCF-7 cell growth

The first objective of the study was to evaluate the effect of arsenic trioxide and the positive controls (cobalt chloride and curcumin) on the growth of the MCF-7 cells. The results showed a dose- and time- dependent inhibition of cell growth and decrease in cell viability (Fig. 4.1A-C; 4.2 and 4.3). These results support the previous studies that showed the cytotoxic effect of arsenic trioxide on lung cancer (Zheng *et al.*, 2015), prostate and ovarian carcinoma (Uslu *et al.*, 2000) and myeloma (Gartenhaus *et al.*, 2002).

5.2. Arsenic trioxide induces features of apoptosis in MCF-7 cells

Cell death is known to occur in two distinct modes, namely apoptosis, a controlled biological event leading to characteristic cell changes and death (Kanduc *et al.*, 2002) and necrosis, which is a series of morphological changes in a lethally injured cell (Fink and Cookson, 2005). Apoptotic cells are characterized by several cellular and nuclear morphological features such as cell shrinkage, nuclear fragmentation and DNA fragmentation.

Therefore, to characterize the mode of cell death associated with arsenic trioxide-induced growth inhibition of MCF-7 cells, the morphological changes were assessed. These results (Fig. 4.4 and 4.5) indicate that the growth inhibitory activity of arsenic trioxide in MCF-7 cells is associated with the induction of apoptosis. To further support these results arsenic trioxide induced apoptosis was analysed in MCF-7 breast cancer cells.

5.2.1. Arsenic trioxide induces apoptosis in MCF-7 cells

Apoptosis is the type of cell death involving caspase enzymes, that are either activated by intrinsic pathway that is initiated by DNA damage leading to the release of cytochrome *c* and activation of caspase cascade reaction or extrinsic pathway that is initiated by the binding of the ligand to the receptor on the surface of the target cell, therefore triggering caspase cascade reaction (Ghobrial *et al.*, 2005).

To confirm apoptosis induction in MCF-7 cells by arsenic trioxide and the positive control (curcumin), the MUSE[®] Cell Analyzer was used. The results showed that arsenic trioxide and the positive control (curcumin) remarkably increased apoptosis in MCF-7 cells (Fig.

4.6B and C) compared to the untreated control (Fig. 4.6A). These results support studies done by Zhang *et al.* (2016) and Wang *et al.* (2011), where it was demonstrated that arsenic trioxide induced apoptosis in MCF-7 breast cancer cells. Apoptosis is a better pathway to eliminate the cancer cells relative to necrosis that leads to inflammation, which is characterized by redness, swelling, heat, pain, and loss of cell function (Ouyang *et al.*, 2012).

5.2.2. Arsenic trioxide induces caspase-dependent apoptosis in MCF-7 cells

To further confirm whether the mode of MCF-7 cell death was caspase-dependent, multi-caspase analysis was performed which revealed that the percentage of cells that underwent caspase-dependent arsenic trioxide apoptosis was higher (Fig. 4.8B) compared to the untreated control cells (Fig. 4.8A). This trend was also observed in the positive control (100 μ M of curcumin) that also induced caspase-dependent apoptosis in MCF-7 cells (Fig. 4.8C). These results support studies done by Zhang *et al.* (2016) and Wang *et al.* (2011), who also implicated arsenic trioxide in caspase-dependent cell death in solid tumours. The involvement of arsenic trioxide in caspases activation was also shown in T-cell leukaemia–lymphoma (Mahieux *et al.*, 2001). Yedjou *et al.* (2010) supported this by showing similar results in APL.

5.2.3. Arsenic trioxide induces death receptor-mediated apoptotic pathway in MCF-7 cells

Depolarization of the inner mitochondrial membrane potential is a reliable indicator of mitochondrial dysfunction and cellular health, which has become increasingly important in the study of intrinsic apoptotic pathway. Therefore, MitoPotential Assay was performed to determine the apoptotic pathway that the MCF-7 cells underwent during the arsenic trioxide-induced cell demise. The results showed that the percentage of cells with depolarized inner mitochondrial membrane potential following treatment with arsenic trioxide and its positive control (curcumin) was significantly low in MCF-7 cells and the same trend was observed even in the untreated control cells (Fig. 4.10.). Many studies revealed that arsenic trioxide can induce intrinsic apoptosis in tumours (Gao *et al.*, 2014; Jiang *et al.*, 2015). But Gatti *et al.* (2014) contradicted by implicating arsenic trioxide in

extrinsic pathway of apoptosis. This suggests that arsenic trioxide can induce either extrinsic or intrinsic apoptosis pathway in cancerous cells depending on the cell type. This study showed that arsenic trioxide-induced apoptotic pathway is independent of the mitochondria in MCF-7 cells. This was supported by two assays, namely, the Muse™ Annexin V & Dead Cell Assay (Fig. 4.6 and 4.7) and Muse™ MitoPotential Assay (Fig. 4.10 and 4.11). Arsenic trioxide also induced caspase-dependent apoptosis (Fig. 4.8 and 4.9) in MCF-7 cells.

5.3. Arsenic trioxide induces G2/M cell cycle arrest in MCF-7 cells

In most cases, the advent of apoptosis is reported to be associated with the cell cycle arrest. Therefore, it was relevant to investigate the effect of arsenic trioxide and the positive control (cobalt chloride) on cell cycle progression of MCF-7 cells. Clearly, this study demonstrated that treatment of the MCF-7 cells with arsenic trioxide and cobalt chloride (positive control) led to the arrest of the cell cycle at G2/M phase (Fig. 4.12 and 4.13). Since cell proliferation is tightly linked to the cell cycle, these results suggest that the observed arsenic trioxide-induced anti-proliferative activity is associated with cell cycle arrest at G2/M phase in MCF-7 breast cancer cells. Arsenic trioxide induced G2/M arrest was also reported in hepatocellular carcinoma (Zhang *et al.*, 2012) and promyelocytic leukaemia (Park *et al.*, 2001).

5.4. Arsenic trioxide regulates the expression of RBBP6 variants during cell cycle arrest and apoptosis

RBBP6 is a 250kDa splicing associated protein that is found in all eukaryotes but has not been found in prokaryotes. RBBP6 has a wide range of functions and these include a role in cell cycle regulation, apoptosis, protein stability and mRNA processing (Chibi *et al.*, 2008; Pugh *et al.*, 2006; Gao and Scott, 2002). RBBP6 has been shown to induce cell cycle progression by ubiquitinating p53 through Murine Double Minute 2 (MDM2), therefore, promoting carcinogenesis (Li *et al.*, 2007). RBBP6 variant 1 has ubiquitin ligase activity and this activity leads to enhanced degradation of p53, the cell guardian, which is crucial for antitumour formation (Li *et al.*, 2007). Furthermore, RBBP6 isoform 3 is involved in G2/M arrest, but its absence triggers cell cycle progression and high

proliferation rates in normal kidney cells (Mbita *et al.*, 2012). Consequently, it would be advantageous for cancer cells to regulate or not to express this isoform to support their rapid growth. Some lines of evidence showed that enhanced expression of different RBBP6 variants correlate with poor clinical prognosis in colon, prostate and oesophageal cancers (Chen *et al.*, 2013; Singh *et al.*, 2006; Yoshitake *et al.*, 2004). Breast cancer treatment remains a challenge and therefore, there is a need for more specific and effective therapeutic tools. RBBP6 is a promising therapeutic target and there are a lot of promising drug development targets, such arsenic trioxide (As_2O_3).

This study showed that arsenic trioxide (Fig. 4.14) regulates the expression of RBBP6 variants, especially the two big transcripts; variant 1 and 2. Figure 4.14A (lane 1) demonstrates that breast cancer cells express RBBP6 variant 1 and lack the expression of variant 2. Treatment of these cells with arsenic trioxide, cobalt chloride and curcumin diminished the expression of RBBP6 variant 1 but did not restore the expression of variant 2. RBBP6 variant 1 may be involved in breast cancer development and its expression in breast cancer cells may promote cell survival. It is no surprise that upon treatment with arsenic trioxide, this variant is down-regulated.

It was previously suggested that RBBP6 variants and isoforms may have opposing cellular functions (Mbita *et al.*, 2012). In this study, we showed that RBBP6 variant 3 is expressed in non-cancerous cells, Hek 293s but undetectable in MCF-7 breast cancer cells (Fig. 4.16A). RBBP6 variant 3 might be involved in the regulation of cell cycle arrest, especially in G2/M cell cycle arrest as previously shown in kidney embryonic cells (Mbita *et al.*, 2012). It is also fitting that gene products that are crucial in cell cycle control to be down-regulated during carcinogenesis. This study showed that non-cancer cells, at least, the Hek 293 cells, express both variants 1 and 2 (Fig. 4.14C). These results together showed that As_2O_3 is effective against MCF-7 cells and also regulate the expression of RBBP6 variants.

5.4.1. Quantitative analysis of the expression of RBBP6 variant 3

RBBP6 isoform 3 has been reported as a cell cycle regulator with anticancer potential (Mbita *et al.*, 2012). The RBBP6 variant 3 was undetectable in MCF-7 cells but detectable in Hek-293 cells (Fig.4.16A lane 3), this led to quantitative analysis of this variant using real time PCR. Real time PCR also confirmed that the expression of RBBP6 variant 3 is higher in Hek-293 cells than in MCF-7 cells (Fig. 4.18). Up-regulation of this variant in non-cancerous cells (Hek-293) and down-regulation in cancer (MCF-7) implies that RBBP6 variant 3 is involved in cell cycle arrest (Mbita *et al.*, 2012). This finding adds to the sufficient evidence that RBBP6 multiple splice variants are involved in different cellular mechanisms and may have opposing functions depending on the cells they are expressed in.

5.4.2. Analysis of RBBP6 protein localization

Immunocytochemistry was performed to locate RBBP6 proteins in MCF-7 cells (Fig. 4.19). This study found that *RBBP6* gene products accumulate in the nucleus and cytoplasm of breast cancer cells (Fig. 4.19). Based on these results, a positive staining was also observed even in the treatment samples, but the RT-PCR (Fig. 4.14) confirmed that the positive staining observed in treatment samples is likely to be due to the detection of RBBP6 isoform 4 but neither isoform1 nor isoform 2. It remains a matter of debate how RBBP6 isoform 4 is derived. In summary, the findings of this section showed that the diversity in *RBBP6* gene products may be critical in understanding how this gene influences the carcinogenesis process.

5.5. Analysis of predicted RBBP6 specific microRNAs in MCF-7 cells

Altered expression of miRNAs plays an important role in regulating cell activities, including proliferation, apoptosis, morphogenesis, differentiation as well as cancer development (Calin and Croce, 2006). Dysregulated expression of miRNA was also reported to play a role in resistance to cancer therapy (Hannafon *et al.*, 2011). The findings of this study showed that both Hsa-miR-195-5p and Hsa-miR-15a-5p microRNAs are down regulated in MCF-7 breast cancer cells (table 4.22 and 4.23). This suggests that Hsa-miR-195-5p and Hsa-miR-15a-5p microRNAs might play tumour-suppressor

roles in MCF-7 breast cancer cells as previously shown in human cancers (Calin and Croce, 2006). Our data also imply that both miR-195 and miR-497 might play important inhibitory roles in breast cancer malignancy, by regulating the expression of RBBP6 variant 1 that is highly expressed in MCF-7 breast cancer cells. This suggest that microRNAs targeting RBBP6 can be potential therapeutic and diagnostic targets.

5.6. Conclusion

Cancer is characterized by the loss of cell cycle control and resistance to apoptosis. Several genes that regulate apoptosis are inappropriately expressed or mutated in breast cancer. The present study showed the ability of arsenic trioxide to induce G2/M cell cycle arrest and extrinsic apoptosis in MCF-7 breast cancer cells. This study also showed that there are RBBP6 variants that are pro-carcinogenic and there are those that are anti-carcinogenic. It was found that breast cancer cells express RBBP6 variant 1 and lack the expression of RBBP6 variant 2. Treatment of these cells with arsenic trioxide diminished the expression of RBBP6 variant 1 but did not restore the expression of RBBP6 variant 2. MCF-7 breast cancer cells also showed low expression of RBBP6 variant 3. In conclusion, different RBBP6 variants can be targeted for breast cancer therapeutic development. In conjunction with RBBP6 expression, arsenic trioxide should be further explored as possible breast cancer drug.

5.7. Future work

This study showed the possibly roles of RBBP6 variant 1 and variant 3, but the role of RBBP6 variant 2 remains unknown because this variant is not expressed in MCF-7 breast cancer cells but expressed in normal embryonic Hek-293 cells. Therefore, it will be of interest to upregulate this variant in MCF-7 cells in order to check how this expression will affect apoptosis and cell cycle.

CHAPTER SIX: REFERENCES

Abdollahi, A., Ali-Bakhshi, A. and Farahani, Z. 2015. Concentration study of high sensitive C-reactive protein and some serum trace elements in patients with benign and malignant breast tumour. *International Journal of Hematology-oncology and Stem Cell Research* 9 (4): 180.

Abud, H.E. 2004. Shaping developing tissues by apoptosis. *Cell Death and Differentiation* 11 (8): 797.

Allred, D.C., Wu, Y., Mao, S., Nagtegaal, I.D., Lee, S., Perou, C.M., Mohsin, S.K., O'Connell, P., Tsimelzon, A. and Medina, D. 2008. Ductal carcinoma in situ and the emergence of diversity during breast cancer evolution. *Clinical Cancer Research* 14 (2): 370-378.

Anderson, K.N., Schwab, R.B. and Martinez, M.E. 2014. Reproductive risk factors and breast cancer subtypes: a review of the literature. *Breast Cancer Research and Treatment* 144 (1):1-10.

Arpino, G., Milano, M. and De Placido, S. 2015. Features of aggressive breast cancer. *The Breast* 24 (5): 594-600.

Ashkenazi, A. 2002. Targeting death and decoy receptors of the tumour-necrosis factor superfamily. *Nature Reviews Cancer* 2 (6): 420-430.

Baatjes, K.J., Apffelstaedt, J.P., Kotze, M.J. and Conradie, M. 2016. Postmenopausal Breast Cancer, Aromatase Inhibitors, and Bone Health: What the Surgeon Should Know. *World Journal of Surgery* 40 (9): 2149-2156.

Bahrami, A., Aledavood, A., Anvari, K., Hassanian, S.M., Maftouh, M., Yaghobzade, A., Salarzaee, O., ShahidSales, S. and Avan, A. 2018. The prognostic and therapeutic application of microRNAs in breast cancer: tissue and circulating microRNAs. *Journal of Cellular Physiology* 233 (2): 774-786.

- Baj, G., Arnulfo, A., Deaglio, S., Mallone, R., Vigone, A., De Cesaris, M.G., Surico, N., Malavasi, F. and Ferrero, E. 2002. Arsenic trioxide and breast cancer: analysis of the apoptotic, differentiative and immunomodulatory effects. *Breast Cancer Research and Treatment* 73 (1): 61-73.
- Bartel, D.P. 2004. MicroRNAs: genomics, biogenesis, mechanism, and function. *Cell* 116 (2): 281-297.
- Bembenek, A. and Schlag, P.M. 2000. Lymph-node dissection in breast cancer. *Langenbeck's Archives of Surgery* 385 (4): 236-245.
- Berenson, J.R. and Yeh, H.S. 2006. Arsenic compounds in the treatment of multiple myeloma: a new role for a historical remedy. *Clinical Lymphoma and Myeloma* 7 (3): 192-198.
- Bickel, H., Pinker-Domenig, K., Bogner, W., Spick, C., Bagó-Horváth, Z., Weber, M., Helbich, T. and Baltzer, P. 2015. Quantitative apparent diffusion coefficient as a noninvasive imaging biomarker for the differentiation of invasive breast cancer and ductal carcinoma in situ. *Investigative Radiology* 50 (2): 95-100.
- Bohnsack, M.T., Czaplinski, K. and GÖRLICH, D. 2004. Exportin 5 is a RanGTP-dependent dsRNA-binding protein that mediates nuclear export of pre-miRNAs. *RNA* 10 (2): 185-191.
- Calin, G.A. and Croce, C.M. 2006. MicroRNA signatures in human cancers. *Nature Reviews Cancer* 6 (11): 857.
- Calin, G.A., Sevignani, C., Dumitru, C.D., Hyslop, T., Noch, E., Yendamuri, S., Shimizu, M., Rattan, S., Bullrich, F., Negrini, M. and Croce, C.M. 2004. Human microRNA genes are frequently located at fragile sites and genomic regions involved in cancers. *Proceedings of the National Academy of Sciences of the United States of America* 101 (9): 2999-3004.

- Carruthers, K.H., Metzger, G., Choi, E., During, M.J. and Kocak, E. 2016. A Therapeutic Role for Survivin in Mitigating the Harmful Effects of Ionizing Radiation. *Sarcoma* 2016: 8.
- Chen, G. and Goeddel, D.V. 2002. TNF-R1 signaling: a beautiful pathway. *Science* 296 (5573): 1634-1635.
- Chen, J., Tang, H., Wu, Z., Zhou, C., Jiang, T., Xue, Y., Huang, G., Yan, D. and Peng, Z. 2013. Overexpression of RBBP6, alone or combined with mutant TP53, is predictive of poor prognosis in colon cancer. *Public Library of Science One* 8 (6): 66524.
- Chen, Z., Chen, G.Q., Shen, Z.X., Sun, G.L., Tong, J.H., Wang, Z.Y. and Chen, S.J. 2002. Expanding the use of arsenic trioxide: leukemias and beyond. *In Seminars in Hematology* 39 (2): 22-26).
- Cheraghi, Z., Poorolajal, J., Hashem, T., Esmailnasab, N. and Irani, A.D. 2012. Effect of body mass index on breast cancer during premenopausal and postmenopausal periods: a meta-analysis. *Public Library of Science One* 7 (12): e51446.
- Chibi, M., Meyer, M., Skepu, A., Rees, D.J.G., Moolman-Smook, J.C. and Pugh, D.J. 2008. RBBP6 interacts with multifunctional protein YB-1 through its RING finger domain, leading to ubiquitination and proteosomal degradation of YB-1. *Journal of Molecular Biology* 384 (4): 908-916.
- Cobrinik, D. 2005. Pocket proteins and cell cycle control. *Oncogene* 24 (17): 2796-2809.
- Czabotar, P.E., Lessene, G., Strasser, A. and Adams, J.M. 2014. Control of apoptosis by the BCL-2 protein family: implications for physiology and therapy. *Nature Reviews Molecular Cell Biology* 15 (1): 49.
- Di Giammartino, D.C., Li, W., Ogami, K., Yashinskie, J.J., Hoque, M., Tian, B. and Manley, J.L. 2014. RBBP6 isoforms regulate the human polyadenylation machinery and modulate expression of mRNAs with AU-rich 3' UTRs. *Genes and Development* 28 (20): 2248-2260.

Di Leo, A., Curigliano, G., Diéras, V., Malorni, L., Sotiriou, C., Swanton, C., Thompson, A., Tutt, A. and Piccart, M. 2015. New approaches for improving outcomes in breast cancer in Europe. *The Breast* 24 (4): 321-330.

Dilda, P.J. and Hogg, P.J. 2007. Arsenical-based cancer drugs. *Cancer Treatment Reviews* 33 (6): 542-564.

Early Breast Cancer Trialists' Collaborative Group. 2005. Effects of radiotherapy and of differences in the extent of surgery for early breast cancer on local recurrence and 15-year survival: an overview of the randomised trials. *The Lancet* 366 (9503): 2087-2106.

Eroles, P., Bosch, A., Pérez-Fidalgo, J.A. and Lluch, A. 2012. Molecular biology in breast cancer: intrinsic subtypes and signaling pathways. *Cancer Treatment Reviews* 38 (6): 698-707.

Eyvani, H., Moghaddaskho, F., Kabuli, M., Zekri, A., Momeny, M., Tavakkoly-Bazzaz, J., Alimoghaddam, K., Ghavamzadeh, A. and Ghaffari, S.H. 2016. Arsenic trioxide induces cell cycle arrest and alters DNA methylation patterns of cell cycle regulatory genes in colorectal cancer cells. *Life Sciences* 167: 67-77.

Fan, T.J., Han, L.H., Cong, R.S. and Liang, J. 2005. Caspase family proteases and apoptosis. *Acta Biochimica et Biophysica Sinica* 37 (11): 719-727.

Fink, S.L. and Cookson, B.T. 2005. Apoptosis, pyroptosis, and necrosis: mechanistic description of dead and dying eukaryotic cells. *Infection and Immunity* 73 (4): 1907-1916.

Foghsgaard, L., Wissing, D., Mauch, D., Lademann, U., Bastholm, L., Boes, M., Elling, F., Leist, M. and Jäättelä, M. 2001. Cathepsin B acts as a dominant execution protease in tumour cell apoptosis induced by tumour necrosis factor. *The Journal of Cell Biology* 153 (5): 999-1010.

Francken, A.B., Schouten, P.C., Bleiker, E.M., Linn, S.C. and Emiel, J.T. 2013. Breast cancer in women at high risk: the role of rapid genetic testing for BRCA1 and-2 mutations and the consequences for treatment strategies. *The Breast* 22 (5): 561-568.

- Gao, S. and Scott, R.E. 2002. P2P-R protein overexpression restricts mitotic progression at prometaphase and promotes mitotic apoptosis. *Journal of Cellular Physiology* 193 (2): 199-207.
- Gao, S., Witte, M.M. and Scott, R.E. 2002. P2P-R protein localizes to the nucleolus of interphase cells and the periphery of chromosomes in mitotic cells which show maximum P2P-R immunoreactivity. *Journal of Cellular Physiology* 191 (2): 145-154.
- Gao, Y.H., Zhang, H.P., Yang, S.M., Yang, Y., Ma, Y.Y., Zhang, X.Y. and Yang, Y.M. 2014. Inactivation of Akt by arsenic trioxide induces cell death via mitochondrial-mediated apoptotic signaling in SGC-7901 human gastric cancer cells. *Oncology Reports* 31 (4): 1645-1652.
- Gartenhaus, R.B., Prachand, S.N., Paniaqua, M., Li, Y. and Gordon, L.I. 2002. Arsenic trioxide cytotoxicity in steroid and chemotherapy-resistant myeloma cell lines: enhancement of apoptosis by manipulation of cellular redox state. *Clinical Cancer Research* 8 (2): 566-572.
- Garzon, R., Marcucci, G. and Croce, C.M. 2010. Targeting microRNAs in cancer: rationale, strategies and challenges. *Nature Reviews Drug Discovery* 9 (10): 775.
- Gatti, L., Cossa, G., Tinelli, S., Carenini, N., Arrighetti, N., Pennati, M., Cominetti, D., De Cesare, M., Zunino, F., Zaffaroni, N. and Perego, P. 2014. Improved Apoptotic Cell Death in Drug-Resistant Non-Small-Cell Lung Cancer Cells by Tumour Necrosis Factor-Related Apoptosis-Inducing Ligand-Based Treatment. *Journal of Pharmacology and Experimental Therapeutics* 348 (3): 360-371.
- Gatza, M.L., Lucas, J.E., Barry, W.T., Kim, J.W., Wang, Q., Crawford, M.D., Datto, M.B., Kelley, M., Mathey-Prevot, B., Potti, A. and Nevins, J.R. 2010. A pathway-based classification of human breast cancer. *Proceedings of the National Academy of Sciences* 107 (15): 6994-6999.
- Germain, M. and Shore, G.C. 2003. Cellular distribution of Bcl-2 family proteins. *Science. Signal Transduction Knowledge Environment* 2003 (173): 10-10.

Ghavami, S., Hashemi, M., Ande, S.R., Yeganeh, B., Xiao, W., Eshraghi, M., Bus, C.J., Kadkhoda, K., Wiechec, E., Halayko, A.J. and Los, M. 2009. Apoptosis and cancer: mutations within caspase genes. *Journal of Medical Genetics* 46 (8): 497-510.

Ghobrial, I.M., Witzig, T.E. and Adjei, A.A. 2005. Targeting apoptosis pathways in cancer therapy. *Cancer Journal for Clinicians* 55 (3): 178-194.

Goldhirsch, A., Winer, E.P., Coates, A.S., Gelber, R.D., Piccart-Gebhart, M., Thürlimann, B., Senn, H.J., Albain, K.S., André, F., Bergh, J. and Bonnefoi, H. 2013. Personalizing the treatment of women with early breast cancer: highlights of the St Gallen International Expert Consensus on the Primary Therapy of Early Breast Cancer 2013. *Annals of Oncology* 24 (9): 2206-2223.

Götte, M., Mohr, C., Koo, C.Y., Stock, C., Vaske, A.K., Viola, M., Ibrahim, S.A., Peddibhotla, S., Teng, Y.H., Low, J.Y. and Ebnet, K. 2010. miR-145-dependent targeting of junctional adhesion molecule A and modulation of fascin expression are associated with reduced breast cancer cell motility and invasiveness. *Oncogene* 29 (50): 6569-6580.

Hanahan, D. and Weinberg, R.A. 2000. The hallmarks of cancer. *Cell* 100 (1): 57-70.

Hannafon, B.N., Sebastiani, P., de las Morenas, A., Lu, J. and Rosenberg, C.L. 2011. Expression of microRNA and their gene targets are dysregulated in preinvasive breast cancer. *Breast Cancer Research* 13 (2): R24.

Harashima, H., Dissmeyer, N. and Schnittger, A. 2013. Cell cycle control across the eukaryotic kingdom. *Trends in Cell Biology* 23 (7): 345-356.

Hengartner, M.O. and Horvitz, H.R. 1994. C. elegans cell survival gene ced-9 encodes a functional homolog of the mammalian proto-oncogene bcl-2. *Cell* 76 (4): 665-676.

Höck, J. and Meister, G. 2008. The Argonaute protein family. *Genome Biology* 9 (2): 210.

Homer, C., Knight, D.A., Hananeia, L., Sheard, P., Risk, J., Lasham, A., Royds, J.A. and Braithwaite, A.W. 2005. Y-box factor YB1 controls p53 apoptotic function. *Oncogene* 24 (56): 8314-8325.

Hortobagyi, G.N. 1998. Treatment of breast cancer. *New England Journal of Medicine* 339 (14): 974-984.

Huynh, C., Segura, M.F., Gaziel-Sovran, A., Menendez, S., Darvishian, F., Chiriboga, L., Levin, B., Meruelo, D., Osman, I., Zavadil, J. and Marcusson, E.G. 2011. Efficient in vivo microRNA targeting of liver metastasis. *Oncogene* 30 (12): 1481.

Iorio, M.V., Ferracin, M., Liu, C.G., Veronese, A., Spizzo, R., Sabbioni, S., Magri, E., Pedriali, M., Fabbri, M., Campiglio, M. and Ménard, S. 2005. MicroRNA gene expression deregulation in human breast cancer. *Cancer Research* 65 (16): 7065-7070.

Jiang, J., Lee, E.J., Gusev, Y. and Schmittgen, T.D. 2005. Real-time expression profiling of microRNA precursors in human cancer cell lines. *Nucleic acids research*, 33 (17): 5394-5403.

Jiang, L., Wang, L., Chen, L., Cai, G.H., Ren, Q.Y., Chen, J.Z., Shi, H.J. and Xie, Y.H. 2015. As₂O₃ induces apoptosis in human hepatocellular carcinoma HepG2 cells through a ROS-mediated mitochondrial pathway and activation of caspases. *International Journal of Clinical and Experimental Medicine* 8 (2): 2190.

Jiao, G., Ren, T., Guo, W., Ren, C. and Yang, K. 2015. Arsenic trioxide inhibits growth of human chondrosarcoma cells through G2/M arrest and apoptosis as well as autophagy. *Tumour Biology* 36 (5): 3969-3977.

Kamińska, M., Ciszewski, T., Łopacka-Szatan, K., Miotła, P. and Starosławska, E. 2015. Breast cancer risk factors. *Przegląd Menopauzalny= Menopause Review* 14 (3): 196.

Kanduc, D., Mittelman, A., Serpico, R.O.S.A.R.I.O., Sinigaglia, E.B.E.R.T.A., Sinha, A.A., Natale, C., Santacroce, R., Di Corcia, M.G., Lucchese, A.L.B.E.R.T.A., Dini, L.U.C.I.A.N.A. and Pani, P.A.O.L.O. 2002. Cell death: apoptosis versus necrosis. *International Journal of Oncology* 21 (1): 165-170.

Kaufmann, S.H. and Earnshaw, W.C. 2000. Induction of apoptosis by cancer chemotherapy. *Experimental Cell Research* 256 (1): 42-49

Khvorova, A., Reynolds, A. and Jayasena, S.D. 2003. Functional siRNAs and miRNAs exhibit strand bias. *Cell* 115 (2): 209-216.

Kim, V.N. 2005. MicroRNA biogenesis: coordinated cropping and dicing. *Nature Reviews Molecular Cell Biology* 6 (5): 376.

Kloks, C.P., Spronk, C.A., Lasonder, E., Hoffmann, A., Vuister, G.W., Grzesiek, S. and Hilbers, C.W. 2002. The solution structure and DNA-binding properties of the cold-shock domain of the human Y-box protein YB-1. *Journal of Molecular Biology* 316 (2): 317-326.

Korsmeyer, S.J., Wei, M.C., Saito, M.T., Weiler, S., Oh, K.J. and Schlesinger, P.H. 2000. Pro-apoptotic cascade activates BID, which oligomerizes BAK or BAX into pores that result in the release of cytochrome c. *Cell Death and Differentiation* 7 (12): 1166.

Kourinou, K.M., Mazonakis, M., Lyraraki, E., Stratakis, J. and Damilakis, J. 2013. Scattered dose to radiosensitive organs and associated risk for cancer development from head and neck radiotherapy in pediatric patients. *Physica Medica* 29 (6): 650-655.

La Vecchia, C., Giordano, S.H., Hortobagyi, G.N. and Chabner, B. 2011. Overweight, obesity, diabetes, and risk of breast cancer: interlocking pieces of the puzzle. *The Oncologist* 16 (6): 726-729.

Lee, R.C., Feinbaum, R.L. and Ambros, V. 1993. The *C. elegans* heterochronic gene *lin-4* encodes small RNAs with antisense complementarity to *lin-14*. *Cell* 75 (5): 843-854.

Lee, Y.S., Kim, H.K., Chung, S., Kim, K.S. and Dutta, A. 2005. Depletion of human micro-RNA miR-125b reveals that it is critical for the proliferation of differentiated cells but not for the down-regulation of putative targets during differentiation. *Journal of Biological Chemistry* 280 (17): 16635-16641.

Lengfelder, E., Hofmann, W.K. and Nowak, D. 2012. Impact of arsenic trioxide in the treatment of acute promyelocytic leukemia. *Leukemia* 26 (3): 433.

Li, D., Zhao, Y., Liu, C., Chen, X., Qi, Y., Jiang, Y., Zou, C., Zhang, X., Liu, S., Wang, X. and Zhao, D. 2011. Analysis of MiR-195 and MiR-497 expression, regulation and role in breast cancer. *Clinical Cancer Research: clincanres-1800*.

- Li, L., Deng, B., Xing, G., Teng, Y., Tian, C., Cheng, X., Yin, X., Yang, J., Gao, X., Zhu, Y. and Sun, Q. 2007. PACT is a negative regulator of p53 and essential for cell growth and embryonic development. *Proceedings of the National Academy of Sciences* 104 (19): 7951-7956.
- Li, P., Nijhawan, D., Budihardjo, I., Srinivasula, S.M., Ahmad, M., Alnemri, E.S. and Wang, X. 1997. Cytochrome c and dATP-dependent formation of Apaf-1/caspase-9 complex initiates an apoptotic protease cascade. *Cell* 91 (4): 479-489.
- Li, Y. and Prives, C. 2007. Are interactions with p63 and p73 involved in mutant p53 gain of oncogenic function?. *Oncogene* 26 (15): 2220.
- Li, Y., Qu, X., Qu, J., Zhang, Y., Liu, J., Teng, Y., Hu, X., Hou, K. and Liu, Y. 2009. Arsenic trioxide induces apoptosis and G2/M phase arrest by inducing Cbl to inhibit PI3K/Akt signaling and thereby regulate p53 activation. *Cancer Letters* 284 (2): 208-215.
- Liu, Q., Hilsenbeck, S. and Gazitt, Y. 2003. Arsenic trioxide–induced apoptosis in myeloma cells: p53-dependent G1 or G2/M cell cycle arrest, activation of caspase-8 or caspase-9, and synergy with APO2/TRAIL. *Blood* 101 (10): 4078-4087.
- Livak, K.J. and Schmittgen, T.D. 2001. Analysis of relative gene expression data using real-time quantitative PCR and the 2⁻ ΔΔCT method. *Methods* 25 (4): 402-408.
- Locksley, R.M., Killeen, N. and Lenardo, M.J. 2001. The TNF and TNF receptor superfamilies: integrating mammalian biology. *Cell* 104 (4): 487-501.
- Long, D., Chan, C.Y. and Ding, Y. 2008. Analysis of microRNA-target interactions by a target structure based hybridization model. In *Biocomputing 2008*: 64-74.
- Lu, J., Chew, E.H. and Holmgren, A. 2007. Targeting thioredoxin reductase is a basis for cancer therapy by arsenic trioxide. *Proceedings of the National Academy of Sciences* 104 (30): 12288-12293.
- Luo, Q., Li, X., Li, J., Kong, X., Zhang, J., Chen, L., Huang, Y. and Fang, L. 2013. MiR-15a is underexpressed and inhibits the cell cycle by targeting CCNE1 in breast cancer. *International Journal of Oncology* 43 (4): 1212-1218.

Ly, D., Forman, D., Ferlay, J., Brinton, L.A. and Cook, M.B. 2013. An international comparison of male and female breast cancer incidence rates. *International Journal of Cancer* 132 (8): 1918-1926.

Lytle, J.R., Yario, T.A. and Steitz, J.A. 2007. Target mRNAs are repressed as efficiently by microRNA-binding sites in the 5' UTR as in the 3' UTR. *Proceedings of the National Academy of Sciences* 104 (23): 9667-9672.

Mahieux, R., Pise-Masison, C., Gessain, A., Brady, J.N., Olivier, R., Perret, E., Misteli, T. and Nicot, C. 2001. Arsenic trioxide induces apoptosis in human T-cell leukemia virus type 1–and type 2–infected cells by a caspase-3–dependent mechanism involving Bcl-2 cleavage. *Blood* 98 (13): 3762-3769.

Martinon, F. and Tschopp, J. 2004. Inflammatory caspases: linking an intracellular innate immune system to autoinflammatory diseases. *Cell* 117 (5): 561-574.

Mbita, Z., Meyer, M., Skepu, A., Hosie, M., Rees, J. and Dlamini, Z. 2012. De-regulation of the RBBP6 isoform 3/DWNN in human cancers. *Molecular and Cellular Biochemistry* 362 (1-2): 249-262.

McBee Jr, W.C., Gardiner, A.S., Edwards, R.P., Lesnock, J.L. and Bhargava, R. 2011. MicroRNA analysis in human papillomavirus (HPV)-associated cervical neoplasia and cancer. *J Carcinogene Mutagene* 1(1).

McPherson, K., Steel, C. and Dixon, J.M. 2000. Breast cancer-epidemiology, risk factors, and genetics. *British Medical Journal* 321 (7261): 624.

Miller, W.H., Schipper, H.M., Lee, J.S., Singer, J. and Waxman, S. 2002. Mechanisms of action of arsenic trioxide. *Cancer Research* 62 (14): 3893-3903.

Minet, M., Schmitter, J.M., Lacroute, F. and Wyers, F. 2001. Mpe1, a zinc knuckle protein, is an essential component of yeast cleavage and polyadenylation factor required for the cleavage and polyadenylation of mRNA. *Molecular and Cellular Biology* 21 (24): 8346-8356.

Ministry of Health Malaysia. Clinical practice guidelines. Management of breast cancer (2nd edition). November 2010. MOH/P/PAK/ 212.10(GU). <http://www.moh.gov.my>.

Miotto, B., Chibi, M., Xie, P., Koundrioukoff, S., Moolman-Smook, H., Pugh, D., Debatisse, M., He, F., Zhang, L. and Defossez, P.A. 2014. The RBBP6/ZBTB38/MCM10 axis regulates DNA replication and common fragile site stability. *Cell Reports* 7 (2): 575-587.

Moela, P. 2014. Silencing RBBP6 (retinoblastoma binding protein 6) sensitizes breast cancer cells to staurosporine and camptothecin-induced cell death (Doctoral dissertation).

Moela, P., Choene, M.M. and Motadi, L.R. 2014. Silencing RBBP6 (Retinoblastoma Binding Protein 6) sensitises breast cancer cells MCF7 to staurosporine and camptothecin-induced cell death. *Immunobiology* 219 (8): 593-601.

Motadi, L.R., Bhoola, K.D. and Dlamini, Z. 2011. Expression and function of retinoblastoma binding protein 6 (RBBP6) in human lung cancer. *Immunobiology* 216 (10): 1065-1073.

Nakashima, T., Jinnin, M., Etoh, T., Fukushima, S., Masuguchi, S., Maruo, K., Inoue, Y., Ishihara, T. and Ihn, H. 2010. Down-regulation of mir-424 contributes to the abnormal angiogenesis via MEK1 and cyclin E1 in senile hemangioma: its implications to therapy. *PLoS One* 5 (12): 14334.

Ntwasa, M. 2016. Retinoblastoma Binding Protein 6, Another p53 Monitor. *Trends in Cancer* 2 (11): 635-637.

Okamoto, T., Izumi, H., Imamura, T., Takano, H., Ise, T., Uchiumi, T., Kuwano, M. and Kohno, K. 2000. Direct interaction of p53 with the Y-box binding protein, YB-1: a mechanism for regulation of human gene expression. *Oncogene* 19 (54): 6194.

Ola, M.S., Nawaz, M. and Ahsan, H. 2011. Role of Bcl-2 family proteins and caspases in the regulation of apoptosis. *Molecular and Cellular Biochemistry* 351 (1-2): 41-58.

Oosthuysen, B. 2015. Biochemical analysis of RBBP6 proteins and their impact on tumour suppressors (Doctoral dissertation).

Ouyang, L., Shi, Z., Zhao, S., Wang, F.T., Zhou, T.T., Liu, B. and Bao, J.K. 2012. Programmed cell death pathways in cancer: a review of apoptosis, autophagy and programmed necrosis. *Cell Proliferation* 45 (6): 487-498.

Park, J.W., Choi, Y.J., Jang, M.A., Baek, S.H., Lim, J.H., Passaniti, T. and Kwon, T.K. 2001. Arsenic trioxide induces G2/M growth arrest and apoptosis after caspase-3 activation and bcl-2 phosphorylation in promonocytic U937 cells. *Biochemical and Biophysical Research Communications* 286 (4): 726-734.

Parkin, D.M. and Fernández, L.M. 2006. Use of statistics to assess the global burden of breast cancer. *The Breast Journal* 12 (1): 70-80.

Pugh, D.J., Eiso, A.B., Faro, A., Lutya, P.T., Hoffmann, E. and Rees, D.J.G. 2006. DWNN, a novel ubiquitin-like domain, implicates RBBP6 in mRNA processing and ubiquitin-like pathways. *BioMed Central Structural Biology* 6 (1): 1.

Rathmell, J.C. and Thompson, C.B. 2002. Pathways of apoptosis in lymphocyte development, homeostasis, and disease. *Cell* 109 (2): 97-107.

Riedl, S.J. and Salvesen, G.S. 2007. The apoptosome: signalling platform of cell death. *Nature Reviews Molecular Cell Biology* 8 (5): 405-413.

Rippy, E.E., Ainsworth, R., Sathananthan, D., Kollias, J., Bochner, M. and Whitfield, R. 2014. Influences on decision for mastectomy in patients eligible for breast conserving surgery. *The Breast* 23 (3): 273-278.

Rock, C.L., Flatt, S.W., Byers, T.E., Colditz, G.A., Demark-Wahnefried, W., Ganz, P.A., Wolin, K.Y., Elias, A., Krontiras, H., Liu, J. and Naughton, M. 2015. Results of the exercise and nutrition to enhance recovery and good health for you (ENERGY) trial: a behavioral weight loss intervention in overweight or obese breast cancer survivors. *Journal of Clinical Oncology* 33 (28): 3169-3176.

Rodríguez, M., Salcedo, M., González, M., Coral-Vazquez, R., Salamanca, F. and Arenas, D. 2002. Identification of novel mutations in the RB1 gene in Mexican patients with retinoblastoma. *Cancer Genetics and Cytogenetics* 138 (1): 27-31.

Sachdeva, U.M. and O'Brien, J.M. 2012. Understanding pRb: toward the necessary development of targeted treatments for retinoblastoma. *The Journal of Clinical Investigation* 122 (2): 425-434.

Sanz, M.A., Fenaux, P. and Coco, F.L. 2005. Arsenic trioxide in the treatment of acute promyelocytic leukemia. A review of current evidence. *Haematologica* 90 (9): 1231-1235.

Schwarz, D.S., Hutvagner, G., Du, T., Xu, Z., Aronin, N. and Zamore, P.D. 2003. Asymmetry in the assembly of the RNAi enzyme complex. *Cell* 115 (2): 199-208.

Shalini, G., Remya, R.S., Gayathri, G., Vishalakshi, V. and Phaneendra, M. 2011. Organ specific cancers—recent advances in diagnosis and treatment. *Cancer Sci therapy*: S17.

Shalini, S., Dorstyn, L., Dawar, S. and Kumar, S., 2015. Old, new and emerging functions of caspases. *Cell Death and Differentiation* 22 (4): 526.

Shenouda, S.K. and Alahari, S.K. 2009. MicroRNA function in cancer: oncogene or a tumour suppressor?. *Cancer and Metastasis Reviews* 28 (3-4): 369.

Simons, A., Melamed-Bessudo, C., Wolkowicz, R., Sperling, J., Sperling, R., Eisenbach, L. and Rotter, V. 1997. PACT: cloning and characterization of a cellular p53 binding protein that interacts with Rb. *Oncogene* 14 (2):145.

Singh, E., Underwood, J.M., Nuttey, C., Babb, C., Sengayi, M. and Kellett, P. 2015. South African National Cancer Registry: Effect of withheld data from private health systems on cancer incidence estimates. *South African Medical Journal* 105 (2).

Singh, J., Manickam, P., Shmoish, M., Natic, S., Denyer, G., Handelsman, D., Gong, D.W. and Dong, Q. 2006. Annotation of androgen dependence to human prostate cancer-associated genes by microarray analysis of mouse prostate. *Cancer Letters* 237 (2): 298-304.

Song, J.J., Liu, J., Tolia, N.H., Schneiderman, J., Smith, S.K., Martienssen, R.A., Hannon, G.J. and Joshua-Tor, L. 2003. The crystal structure of the Argonaute2 PAZ domain reveals an RNA binding motif in RNAi effector complexes. *Nature Structural and Molecular Biology* 10 (12): 1026.

- Sontheimer, E.J. 2005. Assembly and function of RNA silencing complexes. *Nature Reviews Molecular Cell Biology* 6 (2): 127.
- Suryadinata, R., Sadowski, M. and Sarcevic, B. 2010. Control of cell cycle progression by phosphorylation of cyclin-dependent kinase (CDK) substrates. *Bioscience Reports*: 30 (4): 243-255.
- Tartter, P.I., Kaplan, J., Bleiweiss, I., Gajdos, C., Kong, A., Ahmed, S. and Zapetti, D. 2000. Lumpectomy margins, reexcision, and local recurrence of breast cancer. *The American Journal of Surgery* 179 (2): 81-85.
- Taylor, C.W. and Kirby, A.M. 2015. Cardiac side-effects from breast cancer radiotherapy. *Clinical Oncology* 27 (11): 621-629.
- Teng, F., Ruan, H.J., Xu, J., Ni, J., Qian, B., Shen, R. and Gao, L.J. 2018. RBBP6 promotes human cervical carcinoma malignancy via JNK signaling pathway. *Biomedicine & Pharmacotherapy* 101: 399-405.
- Timmer, J.C. and Salvesen, G.S. 2007. Caspase substrates. *Cell Death and Differentiation*, 14 (1): 66.
- Tomasetti, C. and Vogelstein, B. 2015. Variation in cancer risk among tissues can be explained by the number of stem cell divisions. *Science* 347 (6217): 78-81.
- Torre, L.A., Bray, F., Siegel, R.L., Ferlay, J., Lortet-Tieulent, J. and Jemal, A. 2015. Global cancer statistics, 2012. *Cancer Journal for Clinicians* 65 (2): 87-108.
- Uslu, R., Sanli, U.A., Sezgin, C., Karabulut, B., Terzioglu, E., Omay, S.B. and Goker, E. 2000. Arsenic trioxide-mediated cytotoxicity and apoptosis in prostate and ovarian carcinoma cell lines. *Clinical Cancer Research* 6 (12): 4957-4964.
- Varghese, V.K., Shukla, V., Kabekkodu, S.P., Pandey, D. and Satyamoorthy, K. 2018. DNA methylation regulated microRNAs in human cervical cancer. *Molecular Carcinogenesis* 57 (3): 370-382.

Varghese, V.K., Shukla, V., Kabekkodu, S.P., Pandey, D. and Satyamoorthy, K. 2018. DNA methylation regulated microRNAs in human cervical cancer. *Molecular Carcinogenesis* 57 (3): 370-382.

Vasudevan, S., Tong, Y. and Steitz, J.A. 2008. Cell cycle control of microRNA-mediated translation regulation. *Cell Cycle* 7 (11): 1545-1549.

Vermeulen, K., Van Bockstaele, D.R. and Berneman, Z.N. 2003. The cell cycle: a review of regulation, deregulation and therapeutic targets in cancer. *Cell Proliferation* 36 (3): 131-149.

Wagland, R., Richardson, A., Ewings, S., Armes, J., Lennan, E., Hankins, M. and Griffiths, P. 2016. Prevalence of cancer chemotherapy-related problems, their relation to health-related quality of life and associated supportive care: a cross-sectional survey. *Supportive Care in Cancer* 24 (12): 4901-4911.

Wajant, H. 2002. The Fas signaling pathway: more than a paradigm. *Science* 296 (5573): 1635-1636.

Walker, A.R., Adam, F.I. and Walker, B.F. 2004. Breast cancer in black African women: a changing situation. *The Journal of the Royal Society for the Promotion of Health* 124 (2): 81-85.

Wang, S., Liu, Q., Zhang, Y., Liu, K., Yu, P., Liu, K., Luan, J., Duan, H., Lu, Z., Wang, F. and Wu, E. 2009. Suppression of growth, migration and invasion of highly-metastatic human breast cancer cells by berbamine and its molecular mechanisms of action. *Molecular Cancer* (1): 81.

Wang, X. 2001. The expanding role of mitochondria in apoptosis. *Genes and Development* 15 (22): 2922-2933.

Wang, Y., Zhang, Y., Yang, L., Cai, B., Li, J., Zhou, Y., Yin, L., Yang, L., Yang, B. and Lu, Y. 2011. Arsenic trioxide induces the apoptosis of human breast cancer MCF-7 cells through activation of caspase-3 and inhibition of HERG channels. *Experimental and Therapeutic Medicine* 2 (3): 481-486.

WHO (2015). Breast cancer: prevention and control [Online]. Available: <http://www.who.int/cancer/detection/breastcancer/en/index1.html# 4/1/2015>].

Wu, S., Powers, S., Zhu, W. and Hannun, Y.A. 2016. Substantial contribution of extrinsic risk factors to cancer development. *Nature* 529 (7584): 43.

Yan, L.X., Huang, X.F., Shao, Q., Huang, M.Y., Deng, L., Wu, Q.L., Zeng, Y.X. and Shao, J.Y. 2008. MicroRNA miR-21 overexpression in human breast cancer is associated with advanced clinical stage, lymph node metastasis and patient poor prognosis. *Rna* 14 (11): 2348-2360.

Yang, G., Wu, D., Zhu, J., Jiang, O., Shi, Q., Tian, J. and Weng, Y. 2013. Upregulation of miR-195 increases the sensitivity of breast cancer cells to Adriamycin treatment through inhibition of Raf-1. *Oncology Reports* 30 (2): 877-889.

Yang, J., Cao, Y., Sun, J. and Zhang, Y. 2010. Curcumin reduces the expression of Bcl-2 by upregulating miR-15a and miR-16 in MCF-7 cells. *Medical Oncology* 27(4): 1114-1118.

Yang, J.K., Wang, L., Zheng, L., Wan, F., Ahmed, M., Lenardo, M.J. and Wu, H. 2005. Crystal structure of MC159 reveals molecular mechanism of DISC assembly and FLIP inhibition. *Molecular Cell* 20 (6): 939-949.

Yedjou, C., Tchounwou, P., Jenkins, J. and McMurray, R. 2010. Basic mechanisms of arsenic trioxide (ATO)-induced apoptosis in human leukemia (HL-60) cells. *Journal of Hematology and Oncology* 3 (1): 28.

Yeom, K.H., Lee, Y., Han, J., Suh, M.R. and Kim, V.N. 2006. Characterization of DGCR8/Pasha, the essential cofactor for Drosha in primary miRNA processing. *Nucleic Acids Research* 34 (16): 4622-4629.

Yoda, A., Toyoshima, K., Watanabe, Y., Onishi, N., Hazaka, Y., Tsukuda, Y., Tsukada, J., Kondo, T., Tanaka, Y. and Minami, Y. 2008. Arsenic trioxide augments Chk2/p53-mediated apoptosis by inhibiting oncogenic Wip1 phosphatase. *Journal of Biological Chemistry* 283 (27): 18969-18979.

Yoshitake, Y., Nakatsura, T., Monji, M., Senju, S., Matsuyoshi, H., Tsukamoto, H., Hosaka, S., Komori, H., Fukuma, D., Ikuta, Y. and Katagiri, T. 2004. Proliferation potential-related protein, an ideal esophageal cancer antigen for immunotherapy, identified using complementary DNA microarray analysis. *Clinical Cancer Research* 10 (19): 6437-6448.

Young, E.W. 2013. Cells, tissues, and organs on chips: challenges and opportunities for the cancer tumour microenvironment. *Integrative Biology* 5 (9): 1096-1109.

Yu, J., Qian, H., Li, Y., Wang, Y., Zhang, X., Liang, X., Fu, M. and Lin, C. 2007. Arsenic trioxide (As_2O_3) reduces the invasive and metastatic properties of cervical cancer cells in vitro and in vivo. *Gynecologic Oncology* 106 (2): 400-406.

Yun, S.M., Woo, S.H., Oh, S.T., Hong, S.E., Choe, T.B., Ye, S.K., Kim, E.K., Seong, M.K., Kim, H.A., Noh, W.C. and Lee, J.K. 2016. Melatonin enhances arsenic trioxide-induced cell death via sustained upregulation of Redd1 expression in breast cancer cells. *Molecular and Cellular Endocrinology* 422: 64-73.

Zhang, J. and Wang, B. 2006. Arsenic trioxide (As_2O_3) inhibits peritoneal invasion of ovarian carcinoma cells in vitro and in vivo. *Gynecologic Oncology* 103 (1): 199-206.

Zhang, S., Ma, C., Pang, H., Zeng, F., Cheng, L., Fang, B., Ma, J., Shi, Y., Hong, H., Chen, J. and Wang, Z. 2016. Arsenic trioxide suppresses cell growth and migration via inhibition of miR-27a in breast cancer cells. *Biochemical and Biophysical Research Communications* 469 (1): 55-61.

Zhang, X., Jia, S., Yang, S., Yang, Y., Yang, T. and Yang, Y. 2012. Arsenic trioxide induces G2/M arrest in hepatocellular carcinoma cells by increasing the tumour suppressor PTEN expression. *Journal of Cellular Biochemistry* 113 (11): 3528-3535.

Zhang, Y.F., Zhang, M., Huang, X.L., Fu, Y.J., Jiang, Y.H., Bao, L.L., Maimaitiyiming, Y., Zhang, G.J., Wang, Q.Q. and Naranmandura, H. 2015. The combination of arsenic and cryptotanshinone induces apoptosis through induction of endoplasmic reticulum stress-reactive oxygen species in breast cancer cells. *Metallomics* 7 (1): 165-173.

Zheng, C.Y., Lam, S.K., Li, Y.Y. and Ho, J.C.M. 2015. Arsenic trioxide-induced cytotoxicity in small cell lung cancer via altered redox homeostasis and mitochondrial integrity. *International Journal of Oncology* 46 (3): 1067-1078.

Zhou, D., Chu, W., Rothfuss, J., Zeng, C., Xu, J., Jones, L., Welch, M.J. and Mach, R.H. 2006. Synthesis, radiolabeling, and in vivo evaluation of an 18 F-labeled isatin analog for imaging caspase-3 activation in apoptosis. *Bioorganic and Medicinal Chemistry Letters* 16(19): 5041-5046.

Zhou, J., Ye, J., Zhao, X., Li, A. and Zhou, J. 2008. JWA is required for arsenic trioxide induced apoptosis in HeLa and MCF-7 cells via reactive oxygen species and mitochondria linked signal pathway. *Toxicology and Applied Pharmacology* 230 (1): 33-40.

CHAPTER SEVEN: APPENDIX

Appendix A: Stock solutions recipes

Note: The working solutions were diluted down to the desired concentrations with DEPC-treated water or sterile distilled water.

10x TBE: 0.9 M Tris, 0.89 M boric acid and 25 mM EDTA, pH 8.3. This stock solution was diluted 1X for the electrophoresis of agarose

10x MOPS: 200 mM 3-[N-mophonolino] propane sulphuric acid (MOPS), 50 mM sodium acetate, 10 mM EDTA.

0.1%v/v DEPC treated water: Diethylpyrocarbonate (DEPC) was diluted in a litre of deionised H₂O and incubated at 37°C with shaking and then autoclaved

Appendix B: PCR primer design guidelines

Polymerase Chain Reaction is widely held as one of the most important inventions of the 20th century in molecular biology. Small amounts of the genetic material can now be amplified to be able to identify, manipulate DNA, detect infectious organisms, including the viruses that cause AIDS, hepatitis, tuberculosis, detect genetic variations, including mutations, in human genes and numerous other tasks.

PCR involves the following three steps: Denaturation, Annealing and Extension. First, the genetic material is denatured, converting the double stranded DNA molecules to single strands. The primers are then annealed to the complementary regions of the single stranded molecules. In the third step, they are extended by the action of the DNA polymerase. All these steps are temperature sensitive and the common choice of temperatures is 94°C, 60°C and 70°C respectively. Good primer design is essential for successful reactions. The important design considerations described below are a key to specific amplification with high yield. The preferred values indicated are built into all our products by default.

1. Primer Length: It is generally accepted that the optimal length of PCR primers is 18-22 bp. This length is long enough for adequate specificity and short enough for primers to bind easily to the template at the annealing temperature.

2. Primer Melting Temperature: Primer Melting Temperature (T_m) by definition is the temperature at which one half of the DNA duplex will dissociate to become single stranded and indicates the duplex stability. Primers with melting temperatures in the range of 52-58 °C generally produce the best results. Primers with melting temperatures above 65°C have a tendency for secondary annealing. The GC content of the sequence gives a fair indication of the primer T_m . All our products calculate it using the nearest neighbor thermodynamic theory, accepted as a much superior method for estimating it, which is considered the most recent and best available.

Formula for primer T_m calculation:

Melting Temperature $T_m(K) = \{\Delta H / \Delta S + R \ln(C)\}$, Or Melting Temperature $T_m(^{\circ}C) = \{\Delta H / \Delta S + R \ln(C)\} - 273.15$ where

ΔH (kcal/mole) : H is the Enthalpy. Enthalpy is the amount of heat energy possessed by substances. ΔH is the change in Enthalpy. In the above formula the ΔH is obtained by adding up all the di-nucleotide pairs enthalpy values of each nearest neighbor base pair.

ΔS (kcal/mole) : S is the amount of disorder a system exhibits is called entropy. ΔS is change in Entropy. Here it is obtained by adding up all the di-nucleotide pairs entropy values of each nearest neighbor base pair. An additional salt correction is added as the Nearest Neighbor parameters were obtained from DNA melting studies conducted in 1M Na⁺ buffer and this is the default condition used for all calculations.

$$\Delta S (\text{salt correction}) = \Delta S (1M \text{ NaCl}) + 0.368 \times N \times \ln([Na^+])$$

Where

N is the number of nucleotide pairs in the primer (primer length -1).
[Na⁺] is salt equivalent in mM.

[Na⁺] calculation:

$$[Na^+] = \text{Monovalent ion concentration} + 4 \times \text{free Mg}^{2+}.$$

3. Primer Annealing Temperature: The primer melting temperature is the estimate of the DNA-DNA hybrid stability and critical in determining the annealing temperature. Too high T_a will produce insufficient primer-template hybridization resulting in low PCR product yield. Too low T_a may possibly lead to non-specific products caused by a high number of base pair mismatches,. Mismatch tolerance is found to have the strongest influence on PCR specificity.

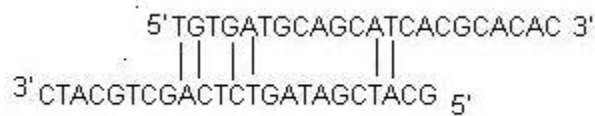
$$T_a = 0.3 \times T_m(\text{primer}) + 0.7 T_m (\text{product}) - 14.9$$

where,

$T_m(\text{primer})$ = Melting Temperature of the primers

primers form intermolecular dimers much more readily than hybridizing to target DNA, they reduce the product yield. Optimally a 3' end self dimer with a ΔG of -5 kcal/mol and an internal self dimer with a ΔG of -6 kcal/mol is tolerated generally.

iii) Cross Dimer: Primer cross dimers are formed by intermolecular interaction between sense and antisense primers, where they are homologous. Optimally a 3' end cross dimer with a ΔG of -5 kcal/mol and an internal cross dimer with a ΔG of -6 kcal/mol is tolerated generally.



7. Repeats: A repeat is a di-nucleotide occurring many times consecutively and should be avoided because they can misprime. For example: ATATATAT. A maximum number of di-nucleotide repeats acceptable in an oligo is 4 di-nucleotides.

8. Runs: Primers with long runs of a single base should generally be avoided as they can misprime. For example, AGCGGGGGATGGGG has runs of base 'G' of value 5 and 4. A maximum number of runs accepted is 4bp.

9. 3' End Stability: It is the maximum ΔG value of the five bases from the 3' end. An unstable 3' end (less negative ΔG) will result in less false priming.

10. Avoid Template Secondary Structure: A single stranded Nucleic acid sequences is highly unstable and fold into conformations (secondary structures). The stability of these template secondary structures depends largely on their free energy and melting temperatures(T_m). Consideration of template secondary structures is important in designing primers, especially in qPCR. If primers are designed on a secondary structures which is stable even above the annealing temperatures, the primers are unable to bind to the template and the yield of PCR product is significantly affected. Hence, it is important to design primers in the regions of the templates that do not form

stable secondary structures during the PCR reaction. Our products determine the secondary structures of the template and design primers avoiding them.

11. Avoid Cross Homology: To improve specificity of the primers it is necessary to avoid regions of homology. Primers designed for a sequence must not amplify other genes in the mixture. Commonly, primers are designed and then BLASTed to test the specificity. Our products offer a better alternative. You can avoid regions of cross homology while designing primers. You can BLAST the templates against the appropriate non-redundant database and the software will interpret the results. It will identify regions significant cross homologies in each template and avoid them during primer search.

Parameters for Primer Pair Design

1. Amplicon Length: The amplicon length is dictated by the experimental goals. For qPCR, the target length is closer to 100 bp and for standard PCR, it is near 500 bp. If you know the positions of each primer with respect to the template, the product is calculated as: Product length = (Position of antisense primer-Position of sense primer) + 1.

2. Product Position: Primer can be located near the 5' end, the 3' end or any where within specified length. Generally, the sequence close to the 3' end is known with greater confidence and hence preferred most frequently.

3. T_m of Product: Melting Temperature (T_m) is the temperature at which one half of the DNA duplex will dissociate and become single stranded. The stability of the primer-template DNA duplex can be measured by the melting temperature (T_m).

4. Optimum Annealing Temperature (T_a Opt): The formula of Rychlik is most respected. Our products use this formula to calculate it and thousands of our customers have reported good results using it for the annealing step of the PCR cycle. It usually results in good PCR product yield with minimum false product production.

$$T_a \text{ Opt} = 0.3 \times (T_m \text{ of primer}) + 0.7 \times (T_m \text{ of product}) - 14.9$$

where

T_m of primer is the melting temperature of the less stable primer-template pair
 T_m of product is the melting temperature of the PCR product.

5. Primer Pair T_m Mismatch Calculation: The two primers of a primer pair should have closely matched melting temperatures for maximizing PCR product yield. The difference of 5°C or more can lead no amplification.

Primer Design using Software

A number of primer design tools are available that can assist in PCR primer design for new and experienced users alike. These tools may reduce the cost and time involved in experimentation by lowering the chances of failed experimentation.

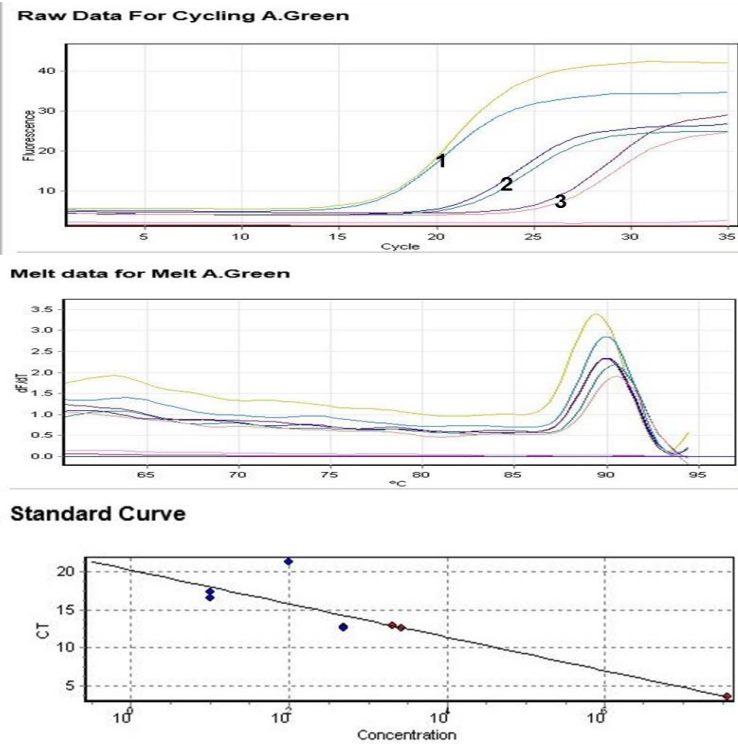
Primer Premier follows all the guidelines specified for PCR primer design. Primer Premier can be used to design primers for single templates, alignments, degenerate primer design, restriction enzyme analysis. contig analysis and design of sequencing primers.

The guidelines for qPCR primer design vary slightly. Software such as AlleleID and Beacon Designer can design primers and oligonucleotide probes for complex detection assays such as multiplex assays, cross species primer design, species specific primer design and primer design to reduce the cost of experimentation.

PrimerPlex is a software that can design primers for Multiplex PCR and multiplex SNP genotyping assays.

Appendix C: GAPDH and RBBP6 variant 3 standard curves constructed with dilutions made from Hek 293 cDNA

A



B

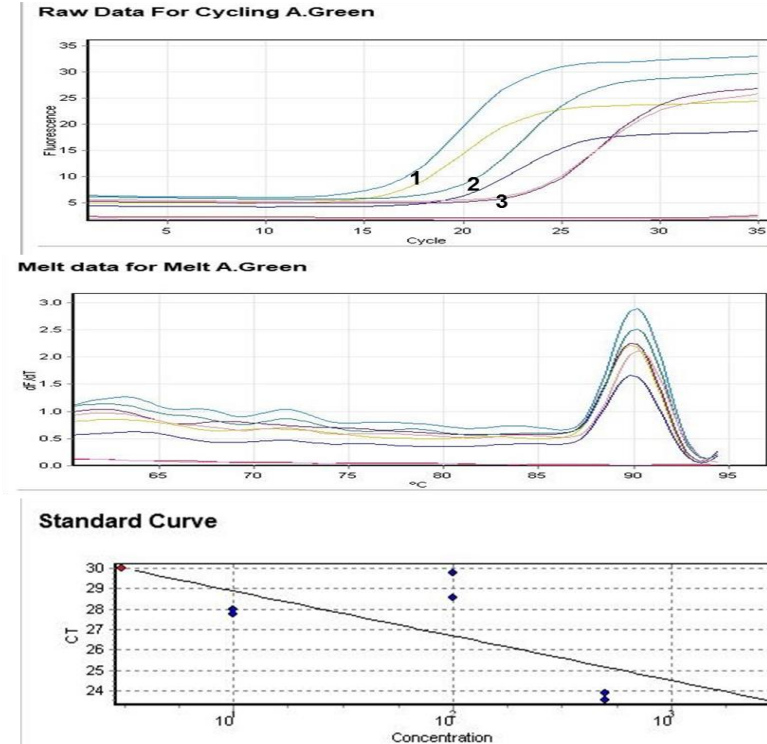


Figure 11 A-B: GAPDH and DWNN standard curve constructed with dilutions made from a Hek 293 cDNA: Appendix C demonstrates a good PCR amplification by RBBP6 variant 3 and GAPDH house-keeping genes. The Hek-293 cDNA was diluted (1 is 1:0, 2 is 1:10, 3 is 1:100) to construct the GAPDH and RBBP6 variant 3 standard curve. The melting curves for both GAPDH (A) and RBBP6 variant 3 (B) show that only one product was amplified.

Appendix D: RBBP6 primary antibody

Protocol specific for RBBP6 Antibody (NBP1-49535)

orders@novusbio.com

Protocols, Publications, Related Products, Reviews and more:

www.novusbio.com/NBP1-49535

Orders:

NBP1-49535

Support: technical@novusbio.com

Web: www.novusbio.com

NBP1-49535 Protocol

Western Blot Protocol

1. Perform SDS-PAGE (4-12% MOPS) on samples to be analyzed, loading 40 ug of total protein per lane.
2. Transfer proteins to Nitrocellulose according to the instructions provided by the manufacturer of the transfer apparatus.
3. Rinse membrane with dH₂O and then stain the blot using Ponceau S for 1-2 minutes to access the transfer of proteins onto the nitrocellulose membrane. Rinse the blot in water to remove excess stain and mark the lane locations and locations of molecular weight markers using a pencil.
4. Rinse the blot in TBS for approximately 5 minutes.
5. Block the membrane using 5% NFDM + 1% BSA in TBS + Tween, 1 hour at RT.
6. Rinse the membrane in dH₂O and then wash the membrane in wash buffer [TBS + 0.1% Tween] 3 times for 10 minutes each.
7. Dilute the rabbit anti-RBBP6 primary antibody (NBP1-49535) in blocking buffer and incubate 1 hour at room temperature.
8. Rinse the membrane in dH₂O and then wash the membrane in wash buffer [TBS + 0.1% Tween] 3 times for 10 minutes each.
9. Apply the diluted rabbit-IgG HRP-conjugated secondary antibody in blocking buffer (as per manufacturers instructions) and incubate 1 hour at room temperature.
10. Wash the blot in wash buffer [TBS + 0.1% Tween] 3 times for 10 minutes each (this step can be repeated as required to reduce background).
11. Apply the detection reagent of choice in accordance with the manufacturers instructions (Pierce ECL).

Note: Tween-20 can be added to the blocking or antibody dilution buffer at a final concentration of 0.05-0.2%, provided it does not interfere with antibody-antigen binding.

Protocol specific for RBBP6 Antibody (NBP1-49535) Page 1 of 1

Appendix E: RBBP6 secondary antibody

Goat anti-Rabbit IgG (H+L) Cross-Adsorbed
Secondary Antibody, Alexa Fluor 488
Catalog Number A-11008 Product data sheet
Details

Size 500 μ L

Host/Isotope Goat / IgG

Class Polyclonal

Type Secondary Antibody

Immunogen

Gamma Immunoglobins Heavy and
Light chains

Target Class IgG

Cross Adsorption

Against human IgG, human serum,
mouse IgG, mouse serum and
bovine serum

Antibody Form Whole Antibody

Conjugate Alexa Fluor® 488

Form liquid

Concentration 2 mg/mL

Purification purified

Storage buffer PBS, pH 7.5

Contains 5mM sodium azide

Storage Conditions 4° C, store in dark

Species Reactivity

Species reactivity Rabbit

Tested Applications Dilution *

Flow Cytometry (Flow) 1-10 μ g/mL

Immunocytochemistry (ICC) 4 μ g/mL

Immunofluorescence (IF) 4 μ g/mL